



TECHNISCHE  
UNIVERSITÄT  
WIEN

VIENNA  
UNIVERSITY OF  
TECHNOLOGY

DIPLOMARBEIT

# Development of a Temperature Monitoring System for the ATLAS Muon Spectrometer

Ausgeführt am Institut für  
Atomphysik  
der Österreichischen Hochschulen

Unter der Anleitung von  
Univ.Doiz. Univ.Prof. Dr. Christian Fabjan  
und Dr. Jörg Wotschack

durch  
Hermann Fuchs  
Franz - Resch - Gasse 5  
3200 Ober - Grafendorf

Dezember 2010

# Acknowledgements

I would like to thank the ATLAS MDT group for their hospitality, feedback and support while developing the MTM system described here. I am especially grateful to my CERN supervisor Dr. J. Wotschack for his efforts and help to complete this work and also for the many detailed discussions related to Monitored Drift Tube chambers and temperature sensors. I also would like to thank my Austrian supervisor Dr. C. Fabjan for his help, guidance and the possibility of conducting my diploma thesis at CERN during which the MTM system was developed. I am also grateful to Dr. R. Voss, who supported that this work could be done as a part of the stimulating research activities of his group.

# Abstract

The ATLAS detector featuring a diameter of 22 m and a length of 44 m is the largest particle detector ever built. It is controlled by the ATLAS Detector Control System (DCS) to ensure a safe and coherent operation of the experiment.

This thesis describes the Muon Temperature Monitoring (MTM) project and its development at CERN, for which I was completely responsible, from the conception until the final implementation into the ATLAS DCS. Its scope is to provide an efficient temperature monitoring of the ATLAS Monitored Drift Tube (MDT) chambers accessible from the ATLAS control room.

The MTM project takes advantage of common ATLAS DCS development tools and development strategies. It is written in PVSS, with the majority of the user interface implemented in the ATLAS Finite State Machine (FSM) interface. The operator can choose between various panels, providing an overview of the state of the MDT chamber temperature monitoring and of the respective chamber temperatures themselves. In addition, a temperature overview panel is available, which provides a quick overview of the temperature distribution within the MDT system. Specialised expert panels can be used by trained detector experts to quickly pinpoint faulty devices and debug the MDT system. The MTM project uses a PVSS distributed system to collect the temperature data. After sorting and analysing the data, temperature gradients are exported to COOL and the temperatures of the MDT chambers are displayed.

For every temperature sensor mounted on all the MDT chambers a number of configuration parameters have been collected. This included coordinates, location, calibration constants, readout channels, alarm levels... This data was stored in a way which enables other ATLAS DCS projects and even off-line analysis tools to access this data.

Furthermore, during this thesis a flagging system has been designed not only to keep track, but also to deal with faulty temperature sensors. A database based approach ensures coherent and centrally managed flag information at all times, while providing maximum flexibility. Emphasis has been put on the flexibility of the system to make it easily adaptable to all other kinds of devices. Currently three other MDT DCS projects are using this flagging system. Feedback from this systems and the flexibility makes it a good candidate for further enrolment.

After extensive tests and reviews, the MTM project has been integrated into the ATLAS DCS and is available in the ATLAS control room.

# Zusammenfassung

Der ATLAS Detektor ist mit einem Durchmesser von 22 m und einer Länge von 44 m der größte Teilchendetektor. Er wird durch das ATLAS Detector Control System (DCS) kontrolliert um einen sicheren und konsistenten Betrieb zu gewährleisten.

Diese Diplomarbeit beschreibt das Muon Temperature Monitoring (MTM) Projekt und seine Entwicklung am CERN, für welches ich von der Planung bis zur abschließenden Implementierung in das ATLAS DCS verantwortlich war. Dieses gewährleistet eine effiziente Temperaturüberwachung der ATLAS Monitored Drift Tubes (MDT) Kammern.

Das MTM Projekt verwendet gemeinsame ATLAS DCS Entwicklungswerkzeuge und Strategien. Es wurde mit Hilfe der Programmierumgebung PVSS erstellt, wobei der Großteil des User Interfaces in das ATLAS Finite State Machine (FSM) Interface integriert wurde. Der Anwender hat die Möglichkeit aus verschiedenen Ansichten auszuwählen, welche einen Überblick über den Zustand der Temperaturüberwachung, sowie den entsprechenden Temperaturen der MDT Kammern bieten. Spezielle Ansichten können von ausgebildeten Detektorexperten verwendet werden um defekte Komponenten aufzuspüren, sowie Fehler im ATLAS MDT System zu finden. Mit Hilfe eines vernetzten PVSS System werden die Temperaturinformationen gesammelt. Nach der Analyse der Daten werden Temperaturgradienten in die COOL Datenbank exportiert und die Temperaturen der MDT Kammern farblich dargestellt.

Für jeden einzelnen Temperatursensor aller MDT Kammern wurde eine Anzahl von Konfigurationsparametern zusammengestellt. Diese enthalten für jeden Sensor Koordinaten, Positionen, Kalibrationskonstanten, Auslesekanäle, Alarmschwellen... Diese Daten wurden in einer Art und Weise gespeichert, welche es anderen ATLAS DCS Projekten und off-line Analyse Programmen ermöglicht auf diese zuzugreifen.

Desweiteren wurde während dieser Diplomarbeit ein Markierungssystem entwickelt, welches es ermöglicht defekte Sensoren zu verwalten. Dieses Datenbank basierte System bietet koheränte und zentral gespeicherte Marker. Das Hauptaugenmerk wurde hierbei auf die Flexibilität des Systems gerichtet um eine einfache Erweiterbarkeit des Systems auf andere Sensoren und Geräte zu ermöglichen. Die positive Resonanz von drei weiteren MDT DCS Projekten, welches dieses System übernommen haben, machen dieses Markierungssystem zu einem gutem Kandidaten für weitergehenden Einsatz.

Nach intensiven Tests und Begutachtungen wurde das MTM Projekt in das ATLAS DCS System integriert und steht nun den Anwendern des ATLAS Kontrollraums zur Verfügung.





# Contents

<b>1. Overview</b>	<b>9</b>
<b>2. Large Hadron Collider</b>	<b>10</b>
2.1. Introduction . . . . .	10
2.2. LHC accelerator . . . . .	10
2.2.1. LHC injector chain . . . . .	12
2.3. Physics program . . . . .	13
2.3.1. Standard Model . . . . .	13
2.3.2. Supersymmetry . . . . .	14
2.3.3. B Physics - CP Violation . . . . .	14
2.4. LHC experiments . . . . .	15
2.4.1. ATLAS . . . . .	15
2.4.2. CMS . . . . .	17
2.4.3. ALICE . . . . .	18
2.4.4. LHCb . . . . .	20
<b>3. The ATLAS Experiment</b>	<b>22</b>
3.1. ATLAS coordinate system . . . . .	23
3.2. Inner detector . . . . .	24
3.3. Calorimeters . . . . .	25
3.3.1. Electromagnetic calorimeter . . . . .	25
3.3.2. Hadronic tile calorimeter . . . . .	26
3.3.3. Hadronic end-cap calorimeter . . . . .	26
3.3.4. Forward calorimeter . . . . .	26
3.4. Muon spectrometer . . . . .	26
3.4.1. Toroid magnets . . . . .	26
3.4.2. Muon system instrumentation . . . . .	28
3.4.3. Alignment system . . . . .	28
3.5. Data Acquisition, High Level Trigger and Detector Control System . . . .	28
<b>4. Monitored Drift Tube system</b>	<b>30</b>
4.1. Layout . . . . .	30
4.1.1. Barrel . . . . .	32
4.1.2. End-cap . . . . .	34
4.2. Local MDT coordinate system . . . . .	35
4.3. Monitored Drift Tube chambers . . . . .	35
4.3.1. Chamber mechanics . . . . .	35

4.3.2.	Chamber electronics . . . . .	37
4.3.3.	Temperature sensors . . . . .	38
4.4.	Temperature distribution . . . . .	44
4.4.1.	MDT chamber temperature distribution . . . . .	48
<b>5.</b>	<b>ATLAS Detector Control System</b>	<b>52</b>
5.1.	Organisation . . . . .	52
5.1.1.	Front-End system . . . . .	52
5.1.2.	Back-End system . . . . .	52
5.2.	Standards . . . . .	53
5.3.	Prozessvisualisierungs- und Steuerungssystem PVSS . . . . .	54
5.3.1.	Evaluation and selection of PVSS . . . . .	54
5.3.2.	Introduction to PVSS II . . . . .	54
5.3.3.	Scripting Language CONTROL . . . . .	55
5.3.4.	System Architecture . . . . .	55
5.3.5.	Concepts . . . . .	57
5.4.	Finite State Machine . . . . .	60
5.4.1.	Finite State Machine concept . . . . .	60
5.4.2.	State Machine Interface (SMI++) . . . . .	62
5.4.3.	Detector Control System integration . . . . .	62
5.4.4.	ATLAS specific FSM . . . . .	64
5.4.5.	ATLAS Detector Control System . . . . .	66
5.5.	Database . . . . .	67
5.5.1.	Database models . . . . .	67
5.5.2.	Database usage in ATLAS . . . . .	68
5.5.3.	Security . . . . .	69
<b>6.</b>	<b>Muon Temperature Monitoring project</b>	<b>70</b>
6.1.	Scope . . . . .	70
6.2.	Data flow . . . . .	70
6.3.	Data collection . . . . .	73
6.3.1.	Collect data script . . . . .	73
6.3.2.	Update script . . . . .	75
6.3.3.	Timeout script . . . . .	76
6.4.	Data mapping . . . . .	76
6.5.	Data evaluation . . . . .	77
6.5.1.	Data Point Functions . . . . .	77
6.5.2.	Alarm handling . . . . .	77
6.5.3.	Flagging system . . . . .	78
6.5.4.	Temperature gradient fit . . . . .	80
6.6.	Data export . . . . .	80
6.7.	MTM project database usage . . . . .	80
6.7.1.	Database tables . . . . .	81
6.7.2.	Views . . . . .	81

6.7.3. Triggers . . . . .	82
6.8. FSM structure . . . . .	82
6.8.1. DAQ partitions for the MTM system . . . . .	82
6.8.2. FSM tree . . . . .	83
6.8.3. Performance considerations . . . . .	85
6.8.4. FSM STATE and STATUS . . . . .	86
6.9. User Interface . . . . .	86
6.9.1. Chamber Panels . . . . .	87
6.9.2. Sector Panels . . . . .	92
6.9.3. Endcap Wheel . . . . .	95
6.9.4. Partition Panels . . . . .	98
6.9.5. Expert Panels . . . . .	102
6.10. Integration . . . . .	107
<b>7. Summary</b>	<b>109</b>
<b>A. FSM STATE and STATUS definitions</b>	<b>110</b>
A.1. Device Unit . . . . .	110
A.2. Logic Unit - Sector . . . . .	111
A.3. Logic Unit - Endcap Wheel . . . . .	111
A.4. Control Unit - Partition . . . . .	112
<b>B. Alarm Levels</b>	<b>113</b>

# 1. Overview

The Muon Temperature Monitoring (MTM) project, a part of the ATLAS detector control system (DCS), is a monitoring system which is designed to run in the ATLAS control room. Its scope is to provide an efficient temperature monitoring of the ATLAS monitored drift tube (MDT) chambers.

The MTM system does not read out hardware by itself, instead it collects the necessary data from specialised readout systems. Then these data is sorted and analysed. After establishing the reliability of the temperature readouts, the state of the MDT chamber temperatures is made available to the shifter using the ATLAS Finite State Machine (FSM) interface. The operator can choose between various panels that provide him with an overview of the temperature of the MDT chambers and the state of the MDT temperature monitoring system itself. An overview panel shows the temperatures of all 1150 MDT chambers in a single view.

Specialised expert panels allow to quickly pinpoint faulty devices and efficiently debug the MDT system.

In this thesis I describe the MTM project, for which I was completely responsible, from the conception until the final implementation. It has been developed within the ATLAS MDT DCS group at the European Organization for Nuclear Research (CERN) in Geneva. Now it is fully operational and is integrated into the ATLAS Control System.

## 2. Large Hadron Collider

### 2.1. Introduction

The Large Hadron Collider (LHC) is a new particle accelerator which is nearing its completion at CERN. Crossing the borders of France and Switzerland it is located in a tunnel with a circumference of 27 km between 50 and 175 m underground. Accelerating protons to create head-on collisions with energies up to 14 TeV, the LHC will enable physicists to test the laws of fundamental interactions.

Approved by the CERN Council in December 1996, the LHC will collide proton bunches with centre of mass energies of 14 TeV every 25 ns at a design luminosity of  $10^{34} \text{ cm}^{-2}\text{s}^{-1}$ . Furthermore the LHC is able to operate in ion mode, in which it will collide heavy ions such as lead nuclei with centre of mass energies of 5.5 TeV at a design luminosity of  $10^{27} \text{ cm}^{-2}\text{s}^{-1}$  [1].

### 2.2. LHC accelerator

The Large Hadron Collider (LHC) is a superconducting particle accelerator, which is being prepared for operation in the 27 km long tunnel of the former Large Electron Positron Collider (LEP). It aims at studying rare events using proton-proton collisions with centre of mass collision energies of up to 14 TeV.

The high luminosity required ( $10^{34} \text{ cm}^{-2}\text{s}^{-1}$ ) makes it virtually impossible to use an antiproton-proton beam as it is used at the Tevatron at Fermilab, near Chicago, due to the very low efficiency of antiproton generation. Instead of using two oppositely charged particles, two proton beams had to be used. Particles with different charge (such as proton and antiproton) could have been diverted in circular orbits using the same orientation of a magnetic field. The consequence of this choice was the necessity of using two beam pipes with two magnetic fields. The high magnetic field strength required to bend the proton beams at these energies to a radius of 2.8 km, made the use of superconducting magnets necessary. For simplicity and reduced costs, both beam pipes and their respective magnet coils are entrenched in the same cryogenic vessel. The LHC accelerator consists of more than 1200 main bending magnets (Fig. 2.1) with a length of 14 m each. In order to keep the beams focused additional quadrupole and sextupole magnets have been inserted. At collision energies of 14 TeV the two circulating beams store about 700 MJ of kinetic energy. Further beam parameters can be found in Tab. 2.1 and [2].

Table 2.1.: LHC beam parameters [2]

Beam Data	Injection	Collision
Proton energy	450 [GeV]	7 000 [GeV]
Particles per bunch	$1.15 \times 10^{11}$	
Number of bunches	2808	
Circulating beam current	0.582 [A]	
Stored energy per beam	23.3 [MJ]	362 [MJ]
Events per bunch crossing	19.02	
Number of collision points	4	
Ring circumference	26658.883 [m]	
Number of main bending magnets	1232	
Length of main bending magnets	14.3 [m]	
Field of main bending magnets	0.535 [T]	8.33 [T]
Bending radius	2803.95 [m]	
Bunch crossing interval	25 [ns]	

## LHC DIPOLE : STANDARD CROSS-SECTION

CERN AC/DI/MM - HE107 - 30 04 1999

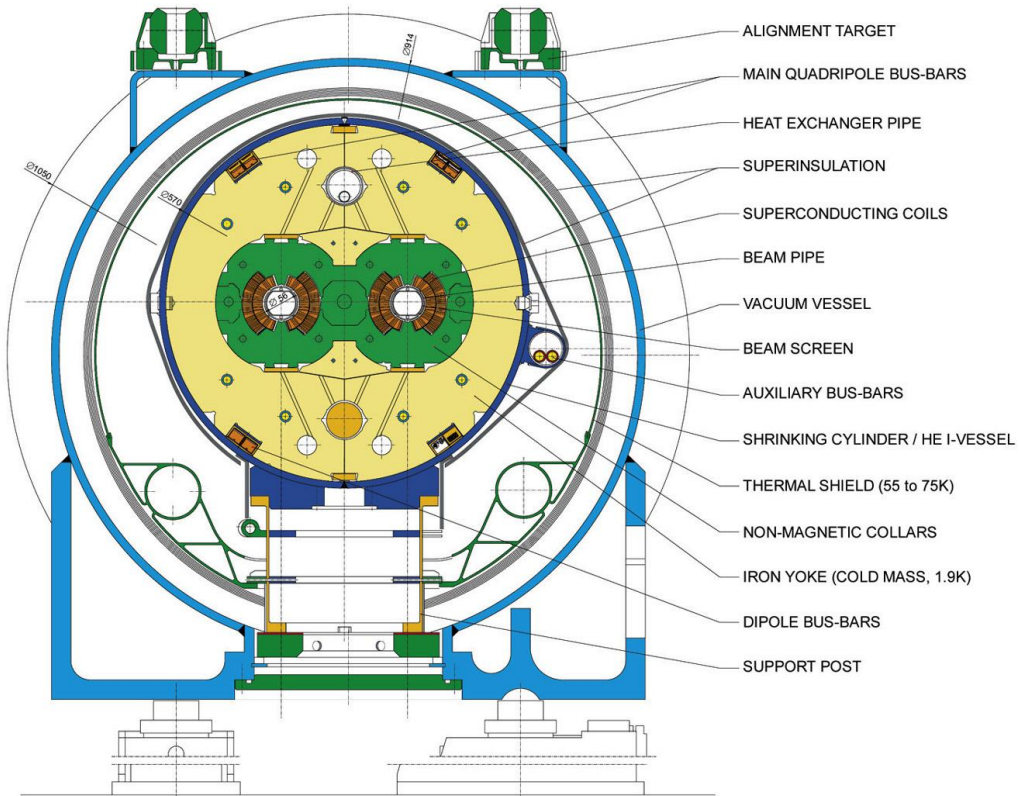


Figure 2.1.: Schematic layout of the LHC cryodipole

### 2.2.1. LHC injector chain

The LHC accelerates protons from 450 GeV to collision energies of 7 TeV. Protons are supplied using already existing accelerator structures at CERN (Fig. 2.2).

Initially protons will be accelerated in Linac 2 to about 30 MeV. After increasing their energy up to 1.4 GeV using the Proton Synchrotron Booster (PSB), they will be injected into the Proton Synchrotron (PS). Boosted to energies of 25 GeV, taking 3.6 s, the Super Proton Synchrotron (SPS) takes over. After reaching the injection energy of 450 GeV, the protons will be injected into the LHC storage rings where they will finally be accelerated to reach the collision energies of 7 TeV per beam. A luminosity lifetime of 14.9 h is anticipated. To fill the LHC, 12 cycles of 21.6 s of the SPS are required. Each fill of the SPS in term requires 3 to 4 cycles of the PS. Along with additional cycles to readjust the machine settings, a total LHC injection time of  $\sim 16$  min can be reached. After injection, the LHC will take about 20 min to increase the beam energy from 450 GeV to 7 TeV per beam. After a beam dump, the magnets need 20 min to ramp down back to injection energies of 450 GeV [2].

The LHC will also be run in ion mode, using a slightly modified injector chain. In this case Linac 1 will accelerate the ions, the ion accumulator will take over and inject them into the PS. The further injection chain is the same as in proton mode [3].

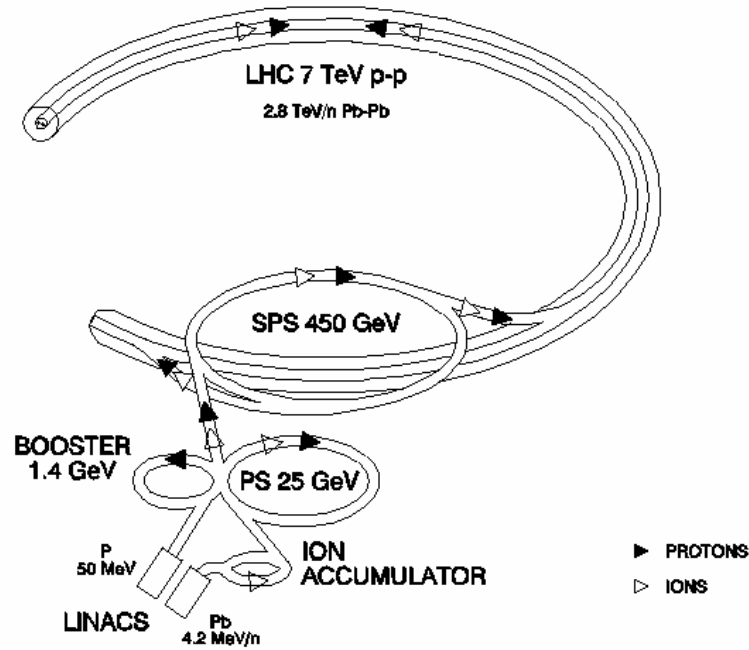


Figure 2.2.: The LHC injector chain [3]



## 2.3. Physics program

### 2.3.1. Standard Model

The Standard Model (SM) of particle physics has been empirically determined through experiments over time. Since its finalisation in the early 1970ies it was subjected to stringent tests. Currently this model seems to accommodate almost all experimental results [4] [5] [6].

With the help of the SM it is possible to classify the fermions (Tab. 2.2), and the gauge bosons (Tab. 2.3). However, experiments have established, that this symmetry is not exact, but in fact broken. This is the reason why quarks and leptons have very different masses (Tab. 2.4).

Table 2.2.: Classification of fermions and quarks [6]

Leptons		Quarks	
electron neutrino	electron	up	down
muon neutrino	muon	charm	strange
tau neutrino	tau	top	bottom

Table 2.3.: Classification of gauge bosons [6]

Interaction	Particle	Mass [GeV/c <sup>2</sup> ]
weak	W <sup>±</sup>	80.4
	Z <sup>0</sup>	91,2
electromagnetic	photon	0
strong	8 gluons	0

Other 'broken' symmetries exist in nature, for example in superconductivity. There a 'technical' solution has been devised to solve the problem. Inspired by this solution a similar concept has been used in the SM. A new scalar field (Higgs field) which permeates the vacuum has been introduced. The interaction of this field with particles generates their respective masses. This mechanism, known as the Higgs mechanism of the SM, would have two observable consequences. Firstly, it relates the masses of the W and Z boson to the electromagnetic mixing angle, a relation which is well confirmed experimentally. Secondly, it would manifest itself in at least one neutral scalar particle with a mass greater than 114.4 GeV [6], the so called Higgs boson. Until now, the Higgs boson escaped detection. One of the goals of the LHC is to search for this particle.

As mentioned before, precision tests of the SM found remarkable concordance between the models predictions and experiments. However, despite the high accuracy, the SM is unable to provide answers to some fundamental questions. The SM needs 26 (free) constants which can only be derived by experiments. This high number of constants suggests that there might be a more fundamental model. Furthermore, the SM cannot explain why there have to be three generations of quarks and leptons, or why there are

three independent symmetry groups. Finally the question remains whether there is any possibility to include gravity into a so called Grand Unified Theory. It is the aim of LHC to address some of these questions [6] [4] [5].

Table 2.4.: Fermion masses [6]

Particle	Mass
electron neutrino	$< 2 \text{ eV}/c^2$
muon neutrino	$< 0.2 \text{ MeV}/c^2$
tau neutrino	$< 18 \text{ MeV}/c^2$
electron	$0.511 \text{ MeV}/c^2$
muon	$105.7 \text{ MeV}/c^2$
tau	$1778 \text{ MeV}/c^2$
up quark	$1.5\text{-}3 \text{ MeV}/c^2$
down quark	$3\text{-}7 \text{ MeV}/c^2$
strange quark	$95 \text{ MeV}/c^2$
charm quark	$1.25 \text{ GeV}/c^2$
bottom quark	$4.2 \text{ GeV}/c^2$
top quark	$174.2 \text{ GeV}/c^2$

### 2.3.2. Supersymmetry

Supersymmetry (SUSY) is a new type of symmetry relating bosons with fermions. SUSY postulates that each known particle has a (supersymmetric) partner with a spin difference of  $\frac{1}{2}$ . The partners of quarks or leptons would then be spin 0 particles called squarks and sleptons. There are various different formulations of SUSY, some of these theories can incorporate gravity, for example the minimal supergravity theory. The supersymmetric particle spectrum is quite rich, while the lightest SUSY particle is often the lightest neutralino  $\chi_1^0$ . This particle is stable and only weakly interacting, which makes its discovery, relying only on the detection of missing energy, difficult.

### 2.3.3. B Physics - CP Violation

CP violation was discovered in 1964 by studying the decay of neutral kaons [7]. The Standard Model generates CP violation in both weak and strong interactions<sup>1</sup>. CP violation in the weak interaction is described by the Cabibbo Kobayashi Maskawa (CKM) matrix [8]. So far the available data is consistent with the theory, but other contributions to the observed phenomena cannot be excluded.

Until now, CP violation has been measured only in the decay amplitudes of  $K_L$  mesons and in neutral B decays. Using the B-meson system and the numerous decay modes available, it is possible to compare the predictions of the SM with the measurements. Therefore it is an attractive place to study CP violation and search for new physics.

<sup>1</sup>Until now CP violation in strong interactions has not been detected

## 2.4. LHC experiments

In total there are four big LHC experiments. ATLAS and CMS are designed for high luminosity proton-proton collisions. LHCb is aiming at B-physics and ALICE is a dedicated ion experiment (Tab. 2.5). A short description of the four bigger experiments is given below.

Table 2.5.: Design luminosity of the LHC experiments [2]

Experiment	Luminosity [ $\text{cm}^{-2}\text{s}^{-1}$ ]	Type
ATLAS	$10^{34}$	proton-proton
CMS	$10^{34}$	proton-proton
LHCb	$10^{32}$	proton-proton
ALICE	$10^{27}$	Pb-Pb or other ions

### 2.4.1. ATLAS

The design concepts, used in the ATLAS experiment, are very different, compared to its competitor CMS. With a diameter of 22 m and a length of 44 m the ATLAS (**A** Toroidal **L**H**C** **A**pparatu**S**) detector is the largest particle physics detector which has ever been built (Fig. 2.3).

The choice of the magnetic field configuration is an important aspect driving the detector design. ATLAS uses large air-core coils to generate a toroidal magnetic field throughout its muon spectrometer. The advantage of a toroidal magnetic field is that the momentum resolution in the forward region increases, compared to the decreasing momentum resolution of a solenoid magnetic field such as the one used by CMS. The open and light structure minimises multiple scattering and allows for excellent muon momentum resolution. Inside the muon spectrometer the position of particles are detected and measured by a series of specialised instruments.

The inner detector is housed inside a thin superconducting solenoid providing a magnetic field of 2 T. Vertex and momentum measurements are achieved using silicon pixel and strip detectors in the inner and straw tube tracking detectors in the outer part of the tracking volume. As electromagnetic calorimeter a high granularity Liquid Argon (LAr) detector was chosen. The energy measurement of hadrons in the barrel region is achieved using a scintillator-tile calorimeter, while in the more forward part of the end-cap region a LAr detector is used. The calorimeter is surrounded by the muon detector [9]. Further information on the ATLAS detector will be given in the following chapter.

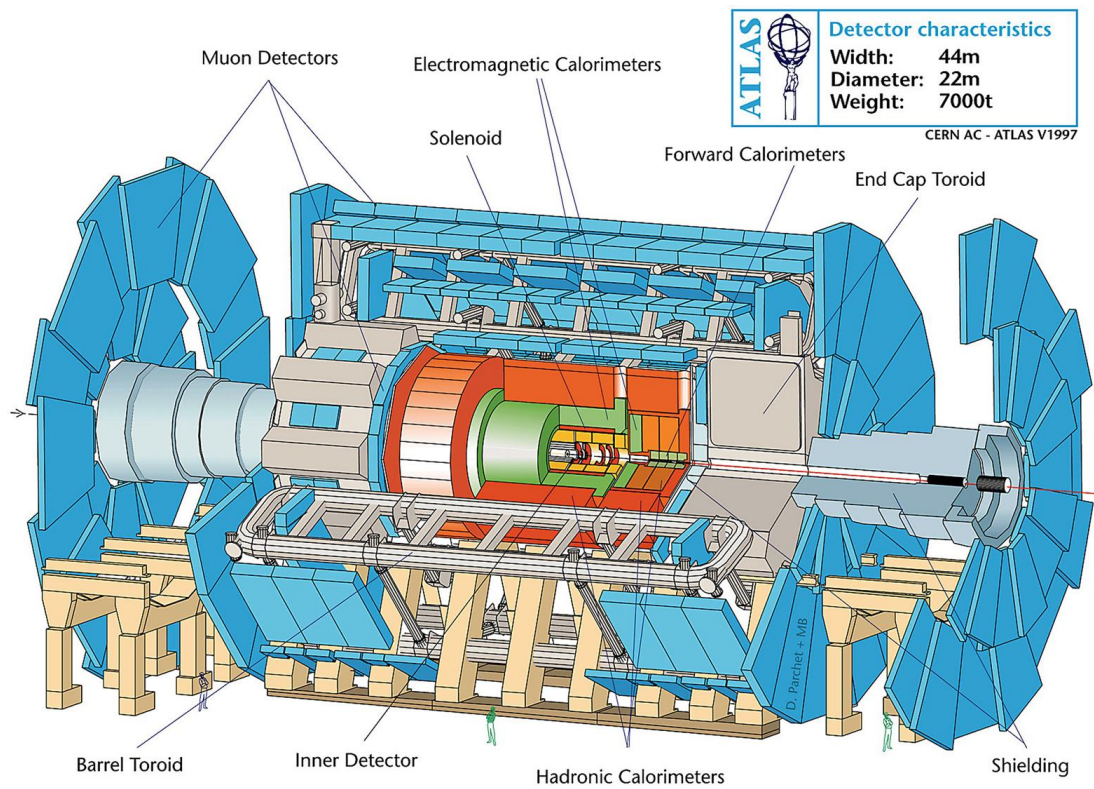


Figure 2.3.: Layout of the ATLAS experiment

### 2.4.2. CMS

The CMS (Compact Muon Solenoid) detector (Fig. 2.4) features a weight of 12,500 tons and is the heaviest detector at the LHC. With a length of 21.6 m and a diameter of 14.6 m, it is considerably more compact than its competitor ATLAS.

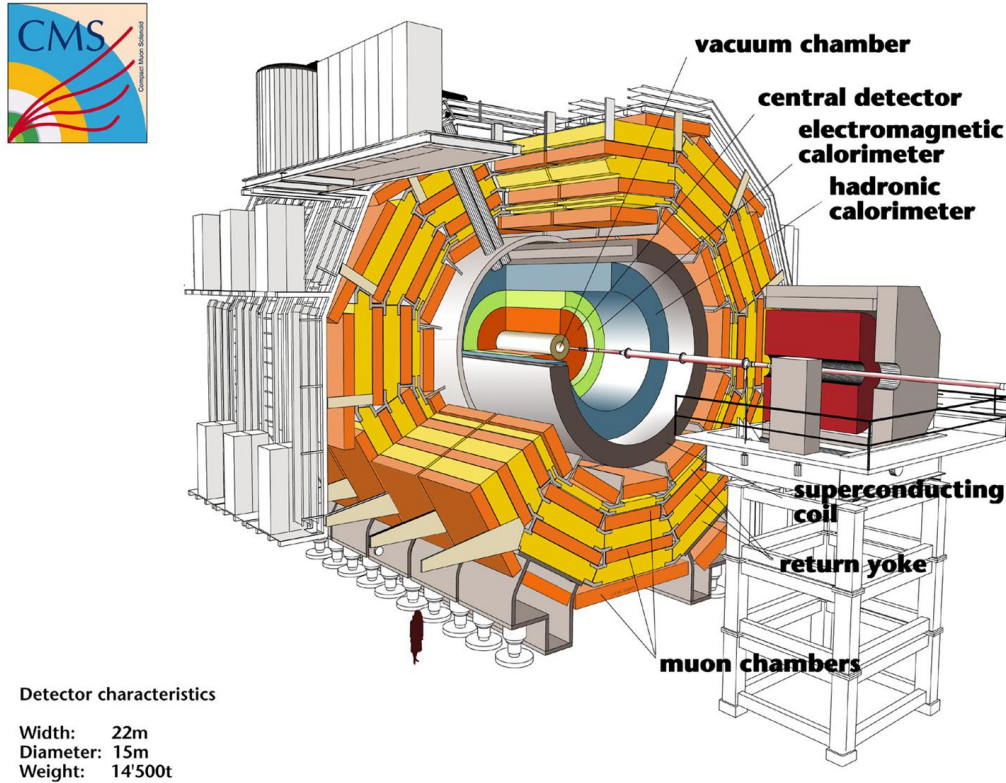


Figure 2.4.: Layout of the CMS experiment

CMS uses a 4 T superconducting solenoid containing 2.7 GJ of energy. The magnetic field returns through an 1.5 m iron yoke. This yoke, which is in saturation, houses four muon stations ensuring nearly full geometric coverage. Their choice of an iron return yoke limits, owing to multiple scattering effects, the resolution of the muon measurement. This limitation is compensated by high resolution particle momentum measurement inside the inner detector. The iron return yoke is the reason for the heaviness of the detector. Each muon station consists of aluminium drift tubes and resistive plate chambers in the barrel region, while in the endcap region the drift tubes have been replaced by cathode strip chambers.

The interior of the solenoid, a cylinder of 5.8 m length and 2.6 m diameter, houses the inner tracker and the calorimeter.

The inner detector contains 13 layers of silicon detectors in order to deal with the high number of tracks. 10 silicon microstrip detectors provide the necessary granularity and precision, while three layers of silicon pixel detectors improve the measurement of impact

parameters and provide the position of secondary decay vertices.

The electromagnetic calorimeter (ECAL) consists of lead tungstate ( $\text{PbWO}_4$ ) crystals producing scintillation light. This light is detected using silicon avalanche photodiodes in the barrel and vacuum phototriodes in the end-cap region. The ECAL is surrounded by a hadron calorimeter using brass as absorber and scintillators as detection element. The wavelength of the scintillation light is transformed using wavelength-shifting fibres in order to be matched to the hybrid photodiodes [10].

### 2.4.3. ALICE

The ALICE (**A** **L**arge **I**on **C**ollision **E**xperiment) experiment is a general-purpose heavy-ion experiment which aims to study strongly interacting matter and quark-gluon plasma in nucleus-nucleus collisions at the LHC [11].

ALICE plans running periods with lead ions and ions lighter than lead, in order to study the energy-density dependence of the measured phenomena. The ALICE physics program also includes data taking during the proton-proton runs (at reduced luminosity) and dedicated proton-ion runs to provide reference data. A specific pp physics program to study low  $p_t$  particles at proton-proton collisions is also planned.

Its design varies significantly from the dedicated pp experiments (ATLAS and CMS). It has to cope with very large particle multiplicities up to 6000 particles per rapidity unit. Starting from the innermost layer the ALICE detector (Fig. 2.5) consists of the Inner Tracking System (ITS), the Time Projection Chamber (TPC), the Transition Radiation Detector (TRD), the Time-Of-Flight detector (TOF), the High-Momentum Particle Identification Detector (HMPID) and the crystal Photon Spectrometer (PHOS). The particle tracking is done mainly by the ITS, TPC and TRD, while particle identification in the central region is performed by the TPC, TRD, TOF, HMPID, PHOS and partly by the ITS.

Further specialised detectors located at large rapidities like the Forward Multiplicity Detector (FMD), V0, T0, the Photon Multiplicity Detector (PMD) and the Zero-Degree Calorimeter (ZMD) are used to characterise the events and to provide interaction triggers.

Forward muons are detected with a dedicated muon spectrometer and a large dipole magnet. Hadrons, electrons and photons are tracked in the central rapidity region ( $-0.9 \leq \eta \leq 0.9$ ) by a complex structure of detectors. The central detectors operate within a moderate magnetic field of about 0.5 T, which is created by a solenoidal magnet with a conventional warm coil. The central detectors and the muon spectrometer, cover both distinct and non overlapping rapidity domains.

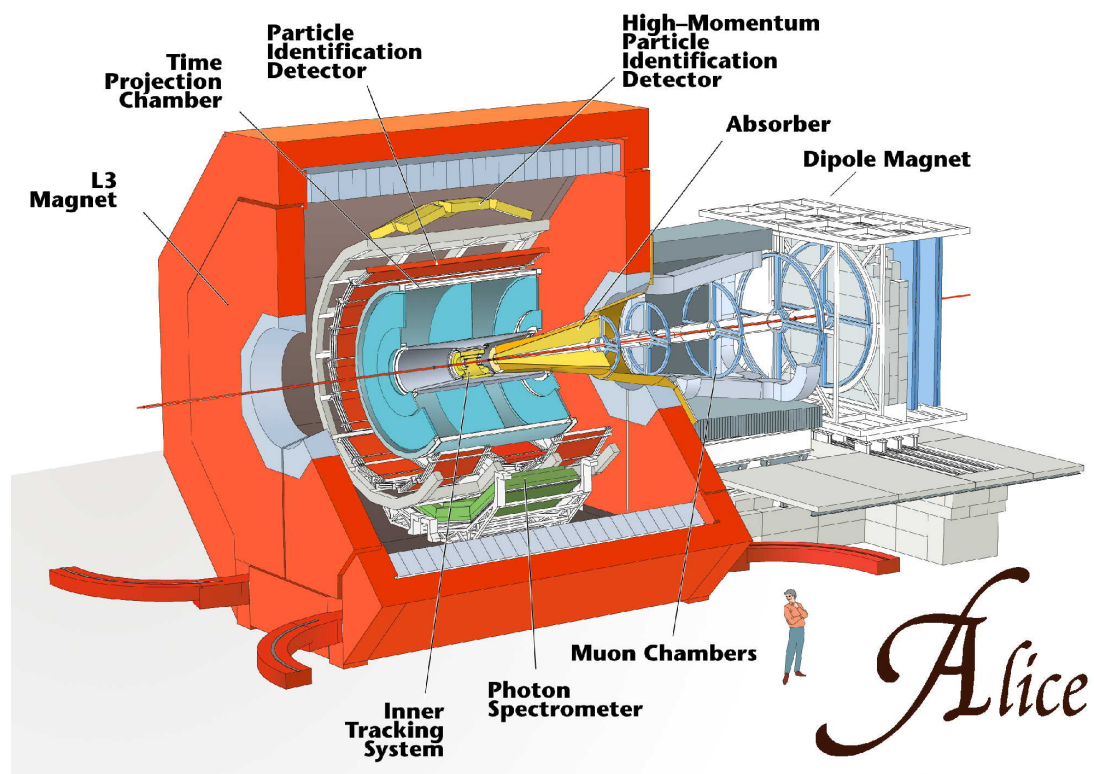


Figure 2.5.: Layout of the ALICE experiment



#### 2.4.4. LHCb

The LHCb experiment is the smallest of the four big LHC experiments. Unlike the other three LHC experiments, the LHCb experiment is a cone shaped single arm spectrometer (Fig. 2.6). This geometry is motivated by the fact that most of the B particles are created in a forward cone.

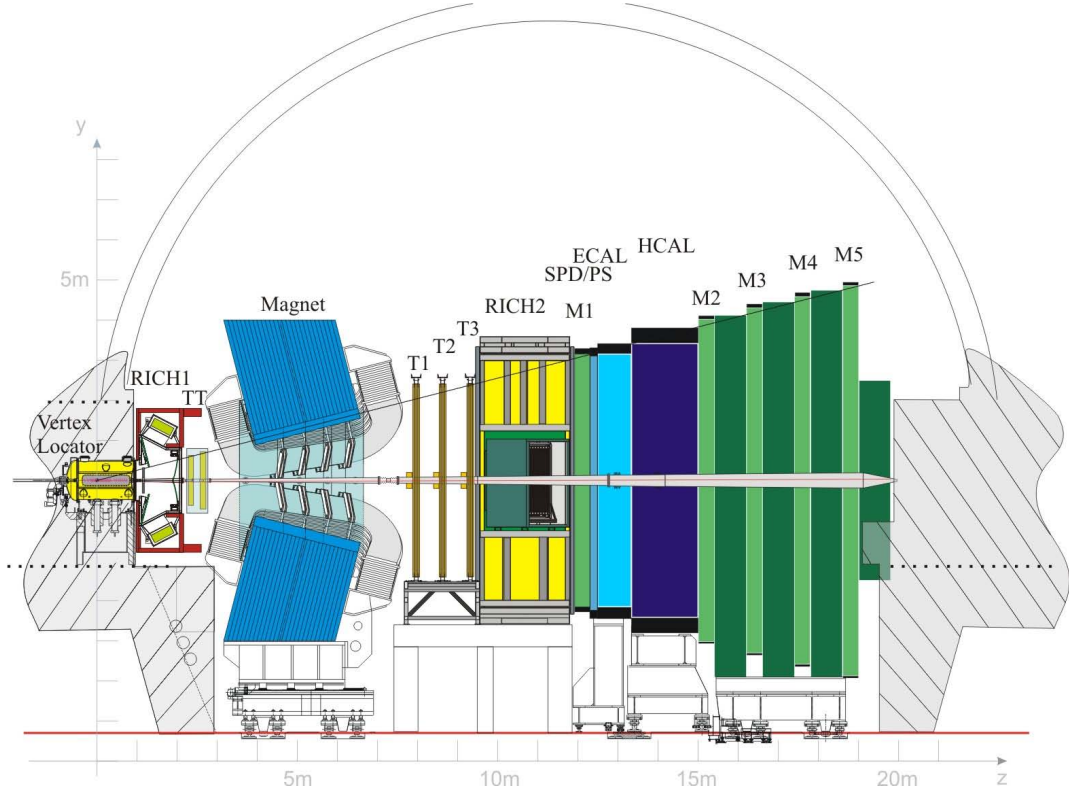


Figure 2.6.: Layout of the LHCb experiment

The Vertex Locator (VELO) consists of 21 stations. Each station consists of two discs of  $220\ \mu\text{m}$  thick silicon detectors with circular and radial strips, giving a resolution of  $40\ \mu\text{m}$  on the impact parameters of high momentum tracks.

A Ring Imaging Cerenkov Detector (RICH) system, consisting of two RICH detectors RICH1 and RICH2 identifies the charged particles with an angular acceptance of  $10 - 330\ \text{mrad}$  over a momentum range of  $1 - 150\ \text{GeV}/c$ . RICH1 consists of a silica aerogel and a  $\text{C}_4\text{F}_{10}$  gas radiator, while RICH2 uses  $\text{CF}_4$  as gas radiator.

A normal conducting magnet provides a vertically oriented field with a maximum value of  $1.1\ \text{T}$  and the possibility to reverse the field to minimise systematic errors.

The tracking system is compromised of four stations (TT, T1, T2 and T3). The Trigger Tracker (TT), located between the magnet and the RICH1 detector, consists of two double layers of silicon strip detectors separated by  $30\ \text{cm}$ . The three remaining sta-



tions, located just behind the magnet and before the RICH2 detector, consist of an inner tracker close to the beam pipe and an outer tracker. While particle fluxes below  $1.4 \times 10^5 \text{ cm}^{-2}\text{s}^{-1}$  permit the use of straw tube detectors in the outer tracking detector, particle fluxes up to  $3.5 \times 10^6 \text{ cm}^{-2}\text{s}^{-1}$  require the use of silicon strip detectors for the inner tracker.

The calorimeter system is formed by the Preshower detector (SPD/PS), the electromagnetic and hadron calorimeter. Using 70 layers of 2 mm thick lead plates and 4 mm thick polystyrene-based scintillator plates the electromagnetic calorimeter reaches a modest, but sufficient energy resolution of  $10 \text{ } \%/ \sqrt{E}$  statistical plus 1.5 % constant. The hadron calorimeter using an iron structure with embedded scintillator tiles reaches an energy resolution of  $80 \text{ } \%/ \sqrt{E}$  statistical plus 5 % constant.

Five muon stations complete the LHCb experiment. The first muon station is located before the calorimetry system. In order to reduce the material budget, this station uses two layers of Multi Wire Proportional Chambers. The remaining four layers consist of Multi-gap Resistive Plate Chambers in the low particle flux regions (below  $5 \times 10^3 \text{ cm}^{-2}\text{s}^{-1}$ ) and Cathode Pad Chambers in the other regions. In total the muon stations have 45,000 readout channels [12] [13].

### 3. The ATLAS Experiment

The **A Toroidal LHC ApparatuS** (ATLAS) detector, is the product of 15 years of dedicated design, research and development. The design goals for the different detector subsystems are listed in Table 3.1. The layout of the ATLAS detector can be seen in Fig. 3.1. In the following an overview of the key components of the ATLAS detector will be given.

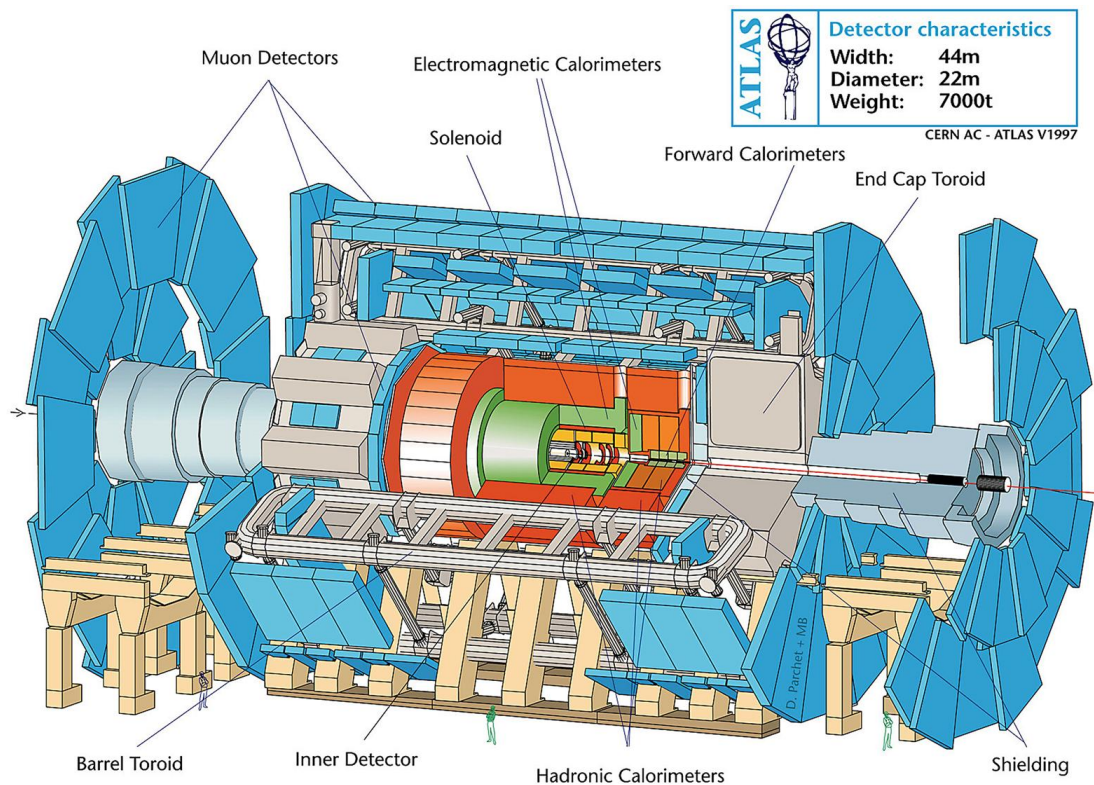


Figure 3.1.: Layout of the ATLAS experiment

Table 3.1.: General performance goals of the ATLAS detector [9]

Detector Component	Required Resolution	$\eta$ coverage	
		Measurement	Trigger
Tracking	$\sigma/p_T = 0.05\%p_T \oplus 1\%$	$\pm 2.5$	
EM calorimetry	$\sigma_E/E = 10\%/\sqrt{E} \oplus 0.7\%$	$\pm 3.2$	$\pm 2.5$
Hadronic calorimetry barrel and end-cap	$\sigma_E/E = 50\%/\sqrt{E} \oplus 3\%$	$\pm 3.2$	$\pm 3.2$
forward	$\sigma_E/E = 100\%/\sqrt{E} \oplus 10\%$	$3.1 <  \eta  < 4.9$	$3.1 <  \eta  < 4.9$
Muon spectrometer	$\sigma/p_T = 10\%$ at $p_T = 1$ TeV	$\pm 2.7$	$\pm 2.4$

### 3.1. ATLAS coordinate system

The ATLAS coordinate system is a right-handed coordinate system whose origin lies in the interaction point (Fig. 3.2). The x-axis points toward the geometric centre of the LHC accelerator circle, the y-axis points toward the surface, while the z-axis points along the beam pipe toward interaction region 8 (ATLAS is installed in interaction region 1).

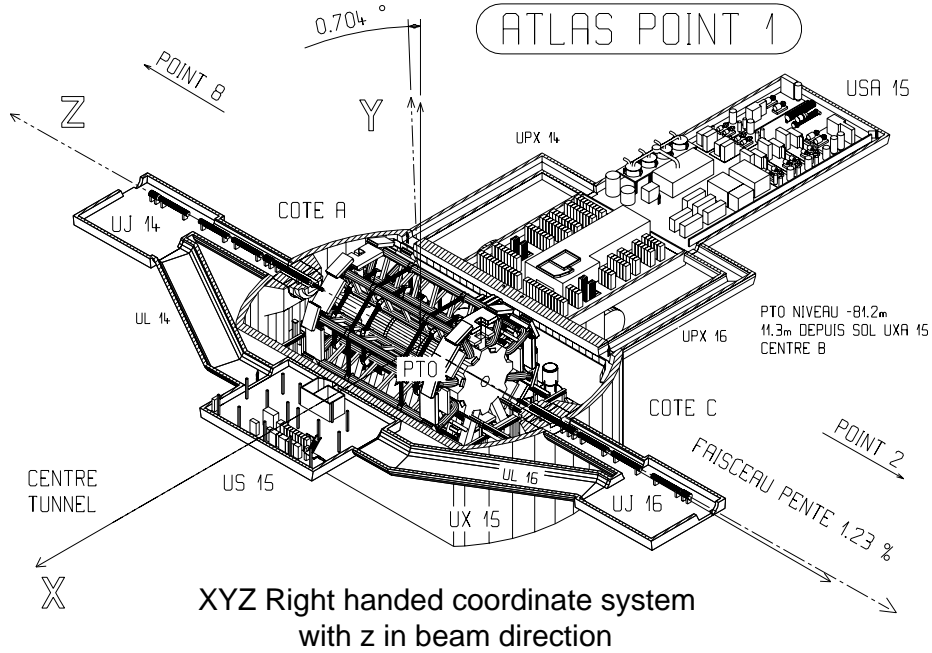


Figure 3.2.: Global ATLAS coordinate system as defined in [14]

The same definition is used for all other LHC experiments and has been used throughout the LEP experiments as well.

The detector is divided into two virtual sides. The side pointing along the positive z-axis

is called side A, while the other side C points in the opposite (negative  $z$ -axis) direction. Side B is located in between side A and C and describes elements at  $z = 0$  (around  $\eta = 0$ ) [15] [14].

### 3.2. Inner detector

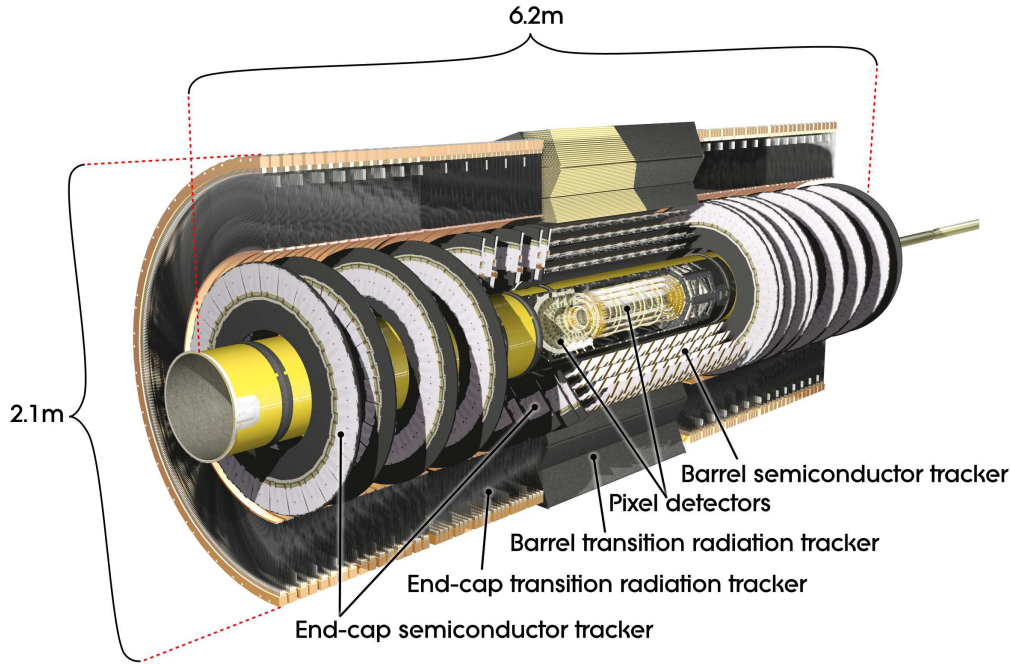


Figure 3.3.: Layout of the ATLAS inner detector

The purpose of the inner detector (ID) (Fig. 3.3) is to track and identify the vertex of the approximately 1000 particles emerging from the collision point every 25 ns. Using silicon pixel and micro-strip (SCT) detectors and the drift tubes of the transition radiation tracker (TRT) it is possible to achieve the momentum and vertex resolution required by the detector performance goals. The ID extends over a length of 6.2 m and a diameter of 2.1 m. It is immersed in a 2 T magnetic field generated by the central solenoid. Three layers of silicon pixel detectors achieve the highest granularity in the vertex region. The active area per pixel is  $50 \times 400 \mu\text{m}^2$  giving a total of 80.4 million readout channels. Another 6.3 million channels are provided by eight layers of SCT which are composed of pairs of daisy-chained sensors with a length of 6.4 cm and a strip pitch of  $80 \mu\text{m}$ . The silicon detectors are surrounded by the TRT. It is composed of 4 mm diameter reinforced carbon fibre drift tubes (also called straw tubes), reaching a measurement accuracy of  $130 \mu\text{m}$  per straw. The straw tubes of the TRT are arranged parallel to the beam axis in the barrel, and radially in the end-cap region. Unlike the silicon detectors, the 351,000 readout channels of the TRT provide only one coordinate

depending on their location ( $\theta$  information in the barrel region, and  $z$  coordinates in the end-cap region). The combination of these detector technologies provides robust pattern recognition and high precision position measurements.

### 3.3. Calorimeters

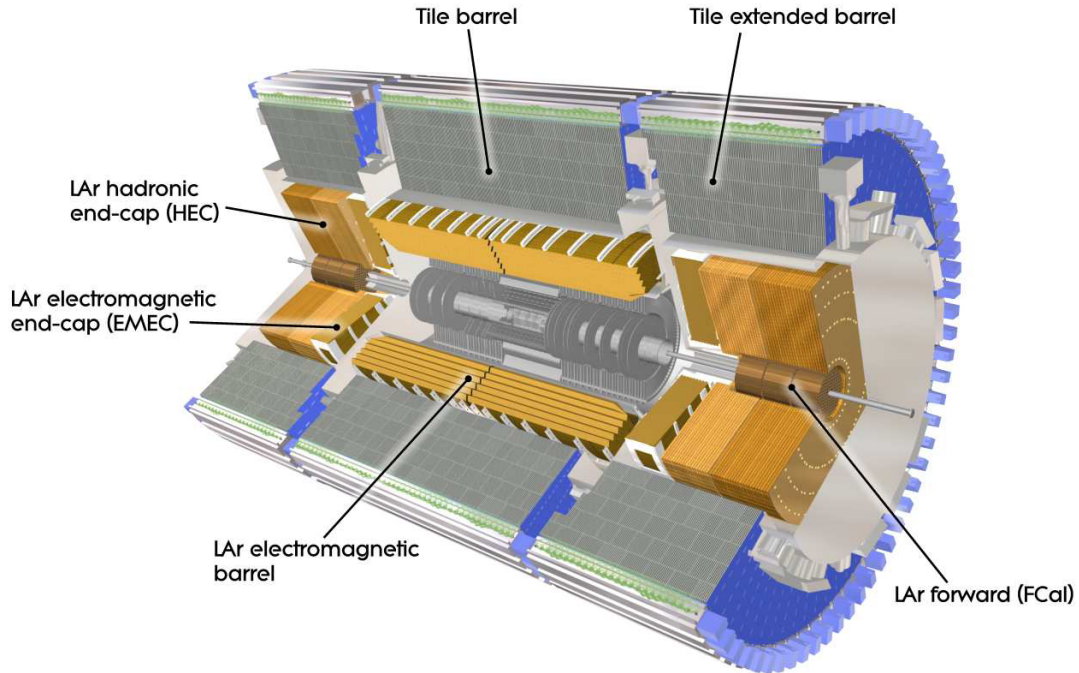


Figure 3.4.: Layout of the ATLAS calorimeter system

The ATLAS calorimeters provide the energy measurements of the particles (Fig. 3.4). They have to be accurate enough to satisfy the physics requirements for jet reconstruction and  $E_T^{miss}$  measurements. Furthermore, they act as absorber for electromagnetic and hadronic particles in order to prevent them from entering the muon detector.

#### 3.3.1. Electromagnetic calorimeter

The electromagnetic calorimeter is a liquid Argon (LAr) detector consisting of accordion-shaped kapton electrodes alternated with lead absorber plates. The specially developed accordion geometry provides complete  $\phi$  symmetry, while the fine-calibrated thickness of the lead plates allows for an optimised detector performance. It consists of a barrel that shares the same cryostat with the LAr preshower detector, the superconducting solenoid and the two end-cap sections. The latter sit in a common cryostat with the hadron end-cap calorimeter and the forward calorimeter.

### 3.3.2. Hadronic tile calorimeter

The tile calorimeter is directly located behind the LAr calorimeter. The 1.97 m thick sampling calorimeter uses 3 mm steel plates as absorber and scintillating tiles as the active element. The scintillating tiles are read out using wavelength shifting fibres and photomultiplier tubes. The tile calorimeter consists of three parts, the barrel and two extended barrel modules in the end-cap region, covering the region  $|\eta| < 1.7$ .

### 3.3.3. Hadronic end-cap calorimeter

The hadronic end-cap calorimeter (HEC) is a liquid argon calorimeter located in the same cryostat as the end-cap EM-LAr calorimeter. It consists in total of four independent wheels, two wheels per side, with a radius of 2.03 m. The HEC uses 25 - 50 mm thick copper plates as absorber interleaved with 8.5 mm liquid argon gaps as active volume. Sharing the cryostat with the EM calorimeter, the HEC covers a range between  $1.5 < |\eta| < 3.2$

### 3.3.4. Forward calorimeter

In order to cover the forward regions, a forward calorimeter (FCal) has been inserted into the end-cap cryostats. It covers a range between  $3.1 < |\eta| < 4.9$ . The FCal is composed of three sections. The innermost sector uses copper as absorber and is designed for electromagnetic measurements. The outer two sections are optimised to measure hadronic interactions using tungsten as absorber.

## 3.4. Muon spectrometer

The ATLAS muon spectrometer was designed to precisely determine the track coordinates and moment of muons independent of the inner detector. It consists of three subsystems: the toroid magnets, the muon system instrumentation and the alignment system. Here only a short overview is given, more details can be found in Chapter 4.

### 3.4.1. Toroid magnets

The magnet system consists of three distinct sets of large air-core toroids (Fig. 3.5) for the barrel and end-cap regions. The magnetic field, produced by this superconducting coils, is between 0.2 and 3.5 T. During operation the ATLAS magnet system will store a total of 1.58 GJ (Tab. 3.2). Precision measurements of the magnetic field will be achieved using a total of 5280 hall probes mounted throughout the muon spectrometer. In the barrel region eight magnet coils, housed in separate cryostats, are situated radially symmetric around the calorimeters. Both end-cap magnets consist of eight smaller magnet coils housed in one large cryostat. The end-cap coils are arranged in a similar way as the barrel coils, but rotated by  $22.5^\circ$  in order to maximise the magnetic field in the overlap region.



Table 3.2.: Parameters of the ATLAS toroid magnets [9]

Parameters	Barrel Toroid	End-cap Toroid (each)
Inner diameter	9.4 m	1.65 m
Outer diameter	20.1 m	10.7 m
Length	25.3 m	5.0 m
Cold mass	370 t	140 t
Nominal current	20.5 kA	20.5 kA
Stored energy	1.08 GJ	0.25 GJ
B-field in the bore	0.2-2.5 T	0.2-3.5 T

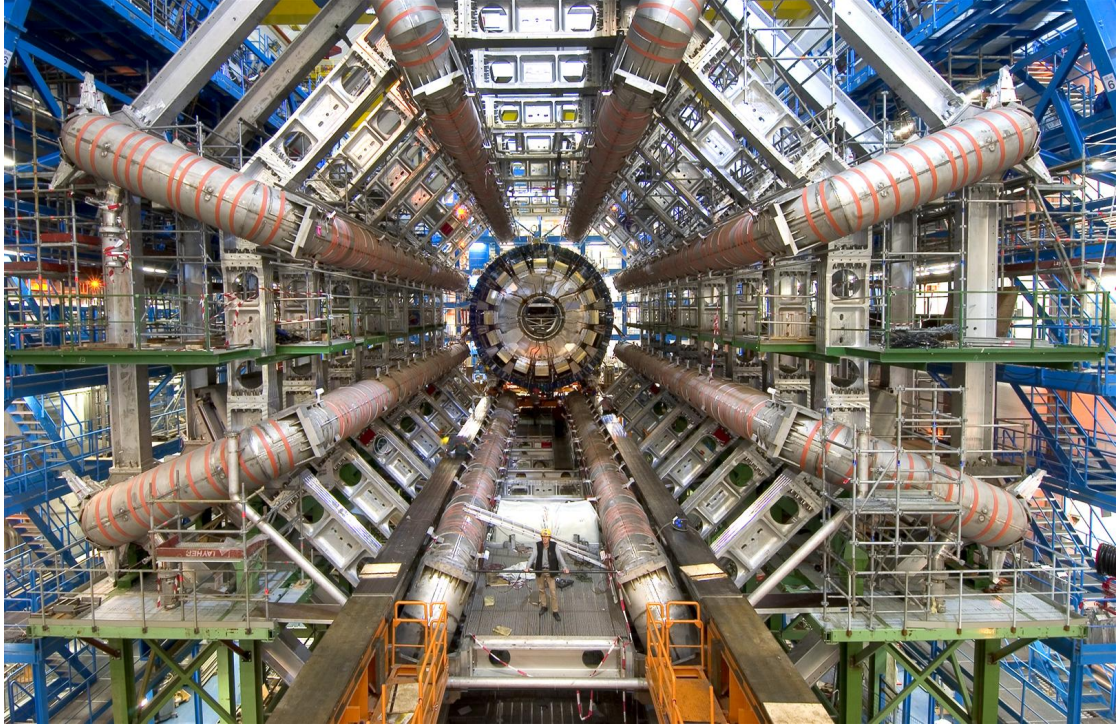


Figure 3.5.: The eight barrel magnet coils of the ATLAS detector. In the background the calorimeter can be seen before it was inserted into the detector.

### 3.4.2. Muon system instrumentation

The muon spectrometer is divided into barrel and end-cap sections, covering a total pseudorapidity range  $|\eta| < 2.7$ . The muon barrel is subdivided into sixteen sectors, each composed of three detector layers. Each end-cap side consists of four independent wheels. Monitored drift tube (MDT) chambers are used as precision chambers to provide the design resolution of  $50 \mu\text{m}$ . Only in the innermost layer of the forward region of the end-cap wheels ( $2 < |\eta| < 2.7$ ) cathode strip (CSC) chambers are used because of their higher rate capability. MDT and CSC chambers are not able to trigger on muons, therefore additional trigger chambers have been added. Using the 355,000 channels of the Resistive Plate Chambers (RPCs) in the Barrel and the 440,000 channels of the multiproportional wire chambers, so called thin gap chambers (TGC), which are mounted on the end-cap wheels, it is possible to generate an independent first-level trigger for the muon system.

### 3.4.3. Alignment system

The relative positions of the muon spectrometer chambers are determined with an accuracy of  $30 \mu\text{m}$  using proximity sensors, axial and projective alignment rays distributed throughout the muon spectrometer. The correction is done during reconstruction, no active correction of the chamber positions is implemented.

## 3.5. Data Acquisition, High Level Trigger and Detector Control System

During normal operations the LHC will collide proton bunches at a frequency of 40 MHz (40,000,000 bunch crossings per second). At design luminosity of  $10^{34} \text{ cm}^{-2}\text{s}^{-1}$  on average 22 inelastic proton-proton collisions will occur at each bunch crossing. The event selection strategy of ATLAS reduces the number of events to store from 40,000,000 to 100 events per second. This is achieved using a staged approach (Fig. 3.6).

The ATLAS detector is read out using Read Out Drivers (ROD). The first-level trigger (LVL1) looks at the data and reduces the initial 40 MHz event rate to a rate of less than 75 kHz. These selected events are transported via the Read Out Links (ROL) into the Read Out Buffers (ROB) where the High Level Trigger system (HLT) takes over. The Level-two trigger (LVL2) looks at selected data from the ROB and reaches its decision in about 1 second (per event). Upon approval by the LVL2 the Event Builder (EB) compiles the events with a size of about  $\sim 1.5 \text{ Mb}$  each. Finally, the data is transported using one of the  $\sim 100$  Sub-Farm Interfaces (SFI) to the Event Filter (EF) which selects events for final archiving [16].



The ATLAS Detector Control System (DCS) supervises the ATLAS experiment. This includes all detector systems, the experimental infrastructure and the communication with external systems such as the LHC accelerator. While safety related aspects are the responsibility of a dedicated Detector Safety System (DSS) and the CERN wide safety and alarm system, DCS interacts with both systems and provides tools for interlocks (in hard- and software). Further details on the ATLAS DCS will be given in Chapter 5 [16].

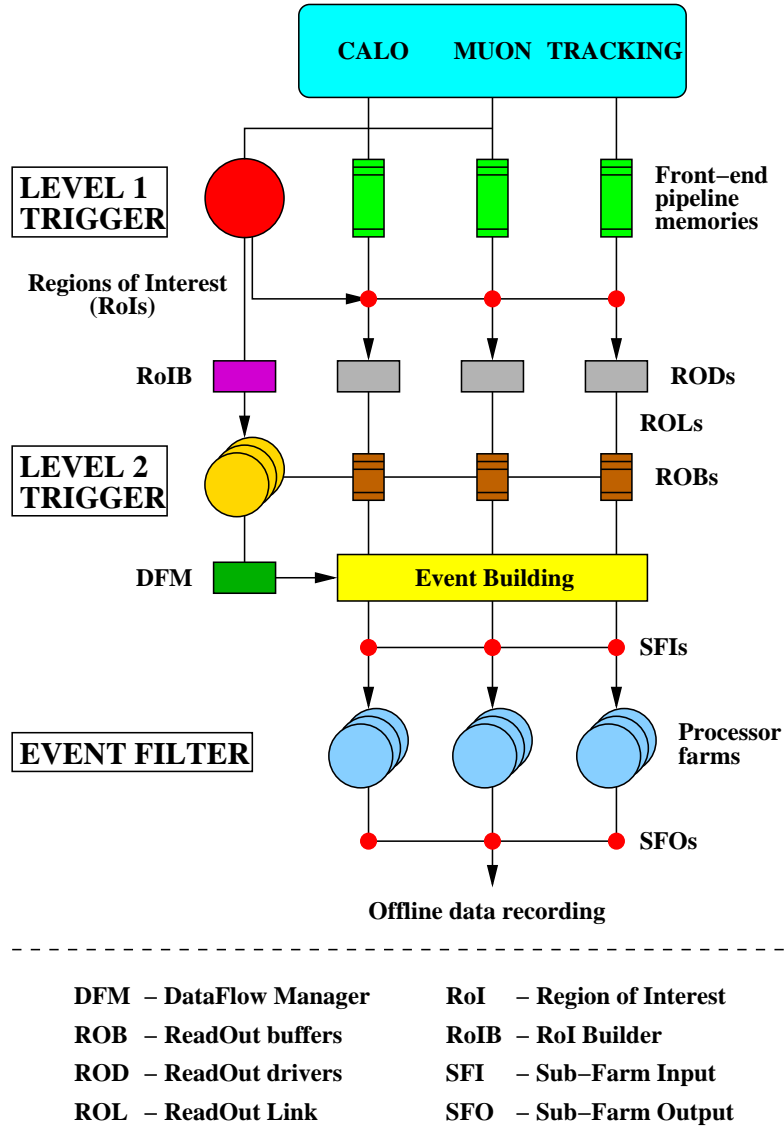


Figure 3.6.: Principal components of the DAQ and HLT systems [16]

## 4. Monitored Drift Tube system

The Monitored Drift Tube system is the part of the ATLAS muon spectrometer. It provides the precision measurements for almost all muon tracks. In the following the layout and design of this system is described and a detailed description of the Muon Drift Tube chambers and their thermal characteristics, being the focus of this thesis, will be given.

### 4.1. Layout

The precision measurement of the muon momentum is done using 1150 Monitored Drift Tube (MDT) chambers<sup>1</sup>, providing a resolution of  $50\text{ }\mu\text{m}$  along the bending direction. The MDT system is divided into three sections: the barrel section, which covers a pseudorapidity range of  $1 > |\eta|$ , and two end-cap sections covering a pseudorapidity range of  $1 < |\eta| < 2.7$ .

The barrel and endcaps are divided into side A or C (see Chapter 3.1), according to their position with respect to the interaction point (Fig. 4.1). Chambers around the interaction point ( $z=0$ ) belong to side B.

Now it is possible to distinguish chambers using the following nomenclature consisting of 7 alphanumeric letters:

- The first two letters determine the section (barrel or end-cap) and the layer
- The third letter usually states whether it is a small or a large chamber
- The first number determines the relative position of the chamber counted from the interaction point
- The letter A or C distinguishes between chambers on side A or C of the detector
- The last two digits code the sector

For example, the chamber BIS4A01, belongs to the innermost layer of the barrel section in sector 1 on side A. It is the fourth small chamber from the interaction point.

---

<sup>1</sup>Only on the innermost ring of the inner sections of the EI wheel Cathode Strip Chambers (CSC) ( $2 < |\eta| < 2.7$ ) are used because of their higher rate capability.

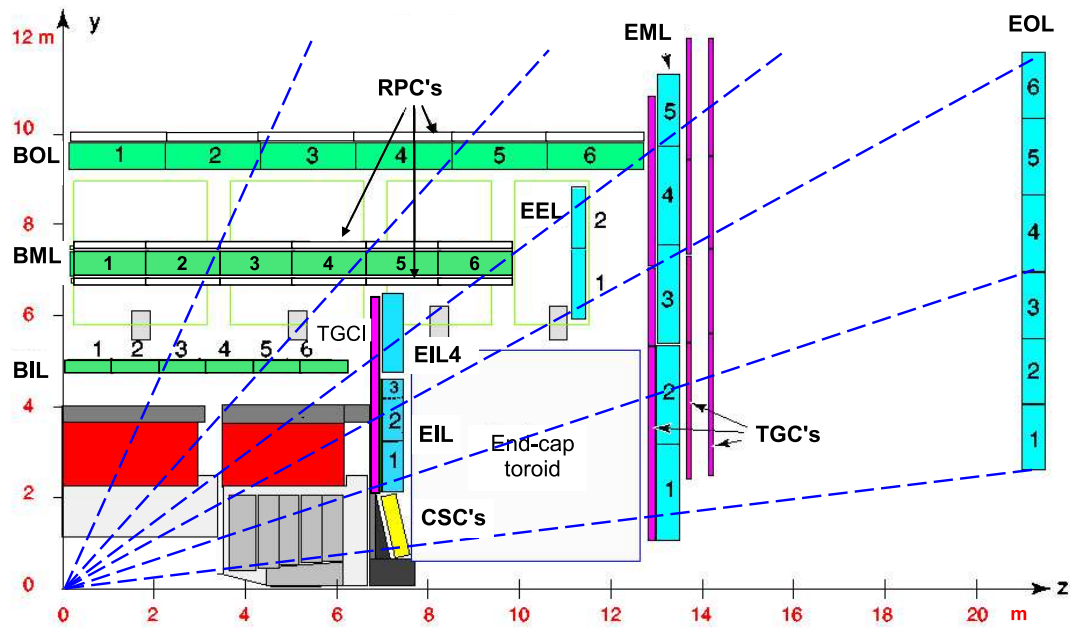


Figure 4.1.: Position and numbering schema of the Monitored Drift Tube (MDT) chambers [15]

#### 4.1.1. Barrel

The Monitored Drift Tube (MDT) chambers are arranged in three cylindrical layers around the calorimeter, so that particles coming from the interaction point have to traverse all three layers (Fig. 4.2 and Tab. 4.1). Starting from the inside, they are called BI, BM and BO. Additional chambers called BEE are mounted on the end-cap magnet cryostats. These are considered barrel chambers, although their functional affiliation belongs to the end-cap.

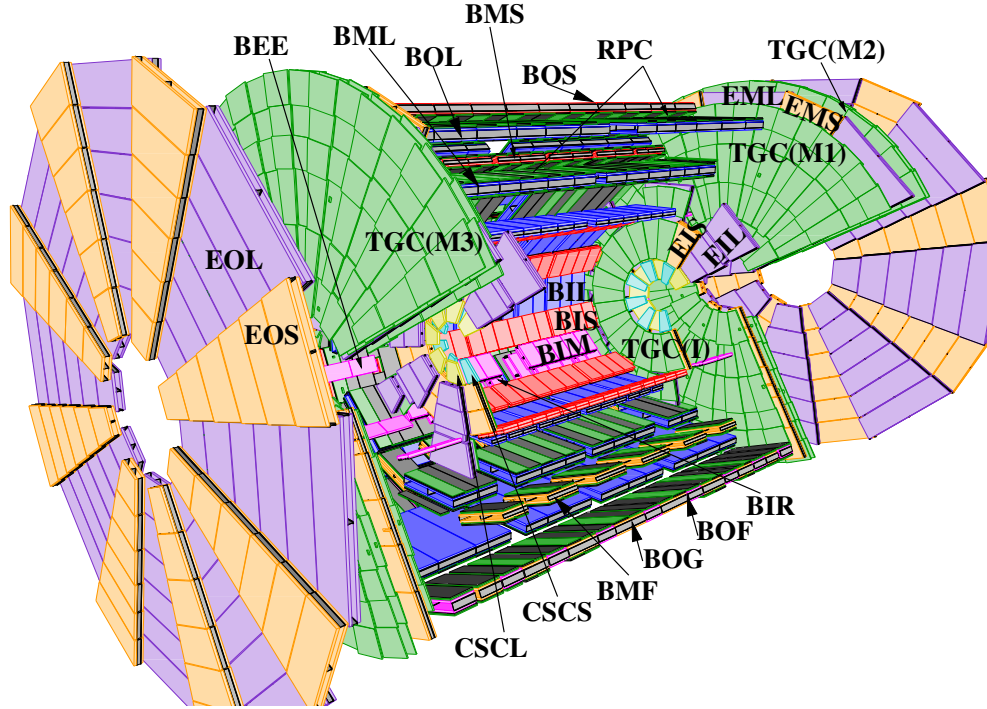


Figure 4.2.: Layout of the ATLAS Muon Spectrometer. All four chamber types, precision (MDT and CSC) and trigger chambers (RPC and TGC) are shown.

The eight magnet coils impose an eightfold azimuthal symmetry on the muon spectrometer. Therefore, both the barrel and the endcaps have been divided into 16 sectors (Fig. 4.3) alternating between small and large sectors numbered from Sector 01 to Sector 16 (Fig. 4.3).

The large sectors cover the regions between the magnet coils, while the small sectors cover the regions around the magnet coils. The azimuthal symmetry is only broken in the lower sectors, where the rails supporting the calorimeter and the supports of the barrel toroid structure require special shaped chambers.

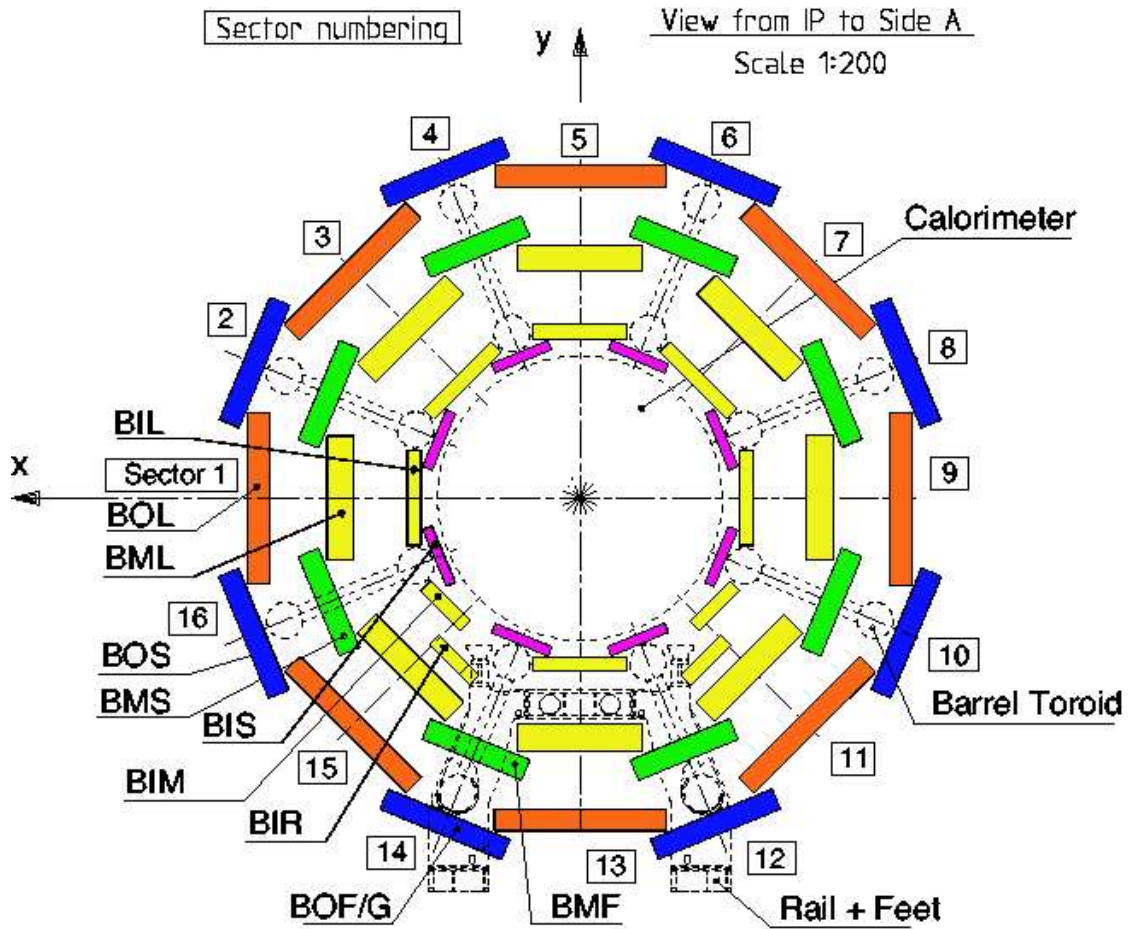


Figure 4.3.: Position and numbering of the 16 ATLAS Muon Spectrometer sectors. The same schema applies to the end-cap section.

The design aimed at minimising the amount of special shaped chambers in order to keep the design and construction costs low. In order to keep the amount of passive material within the muon spectrometer as low as possible, the barrel chambers and a part of the end-cap chambers do not have their own support structure. Instead they are mounted on the barrel toroid support structure.

Table 4.1.: Typical parameters of MDT barrel chambers [17]

Chamber Name	Layer	# of Chambers	Tube layers	Tubes/ layer	Tubes/ chamber	chamber length [mm]
BIS	inner	96	$2 \times 4$	30	240	916
BIL	inner	72	$2 \times 4$	36	288	1096
BMS	middle	72	$2 \times 3$	48	288	1497
BML	middle	94	$2 \times 3$	56	336	1697
BOS	outer	72	$2 \times 3$	72	432	2177
BOL	outer	72	$2 \times 3$	72	432	2177
special chambers						
BIS7	inner	16	$2 \times 4$	30	240	916
BIS8	inner	16	$1 \times 3$	16	48	496
BIM	inner	20	$2 \times 4$	36	288	1096
BIR	inner	24	$2 \times 4$	36	288	916
BEE	middle	32	$1 \times 4$	48	192	1457
BMF	middle	12	$2 \times 3$	64	384	1937
BOF	outer	16	$2 \times 3$	64	384	2177
BOG	outer	18	$2 \times 3$	40	240	1216
Total		656			4080	

#### 4.1.2. End-cap

The end-cap consists of four distinctive wheels on each side of the calorimeter mounted perpendicular to the beam axis, providing the required three point measurement of particles coming from the interaction point (Tab. 4.2).

Starting from the innermost wheel they are called EI, EE, EM and EO. The innermost wheels(EI) are situated next to the calorimeter. The EE wheels, fixed to the barrel section of the MDT system, will be installed at a later stage to increase the coverage at the intersection between barrel and end-cap. The big wheels (EM) are located at the end of the barrel toroid coils. The EI and EM wheels are mounted on rail structures permitting the movement of these wheels along the beam axis to facilitate the accessibility of the calorimeter and inner detector during installation and maintenance. The outer wheels (EO) are fixed to the support structure near the wall of the experimental cavern.

Table 4.2.: Typical parameters of MDT end-cap chambers [17]

Chamber Name	Layer	# of Chambers	Tube layers	Tubes/ layer	Tubes total	chamber length [mm]
EIS	inner	32	$2 \times 4$	36	288	1096
EIL	inner	48	$2 \times 4$	54	432	1637
EES	extra	32	$2 \times 3$	40	240	1216
EEL	extra	30	$2 \times 3$	40	240	1216
EMS	middle	80	$2 \times 3$	64	384	1937
EML	middle	80	$2 \times 3$	64	384	1937
EOS	outer	96	$2 \times 3$	48	288	1457
EOL	outer	96	$2 \times 3$	48	288	1457
Total		494			2544	

## 4.2. Local MDT coordinate system

The local MDT coordinate system defines a coordinate system which is fixed to the chamber [15] [14]. It is a right-handed coordinate system as described in Fig. 4.4.

## 4.3. Monitored Drift Tube chambers

The Monitored Drift Tube chambers are made of individual drift tubes glued on a support structure that incorporates an optical positioning system. Each MDT chamber is composed of two multilayers, sandwiching the support structure. A multilayer consists of 3 or 4 layers of cylindrical aluminium drift tubes. Each aluminium drift tube, having a diameter of 30 mm, is filled with a non-flammable ArCO<sub>2</sub> (93:7) gas mixture at 3 bar absolute pressure. Using a 50  $\mu\text{m}$  W-Re wire at a potential of 3080 V, the optimal drift time and Lorentz angle can be reached, giving a single tube resolution of 80  $\mu\text{m}$ .

### 4.3.1. Chamber mechanics

The physical reference for the track measurement is the wire position within the drift tube. The wire position is determined by the two points where the wire is mounted (in the endplugs) and the gravitational sag of the wire.

In order to limit deviations from the optimal wire position, the tube itself has to follow the wire within 100  $\mu\text{m}$ . The individual drift tubes are glued together, forming layers. Then three or four of such layers are glued together in order to form a multilayer. The thickness of one such multilayer with three layers is about 82 mm. The multilayers are mounted on specially designed very light spacer frames (Fig. 4.5). The spacer frame also houses the in-plane alignment system which monitors chamber deformations.

Temperature sensors have been glued on the multilayers and support frames (Chapter 4.3.3). Up to four B-field sensors (hall probes) per chamber help in reconstructing the magnetic field within the Muon Spectrometer.

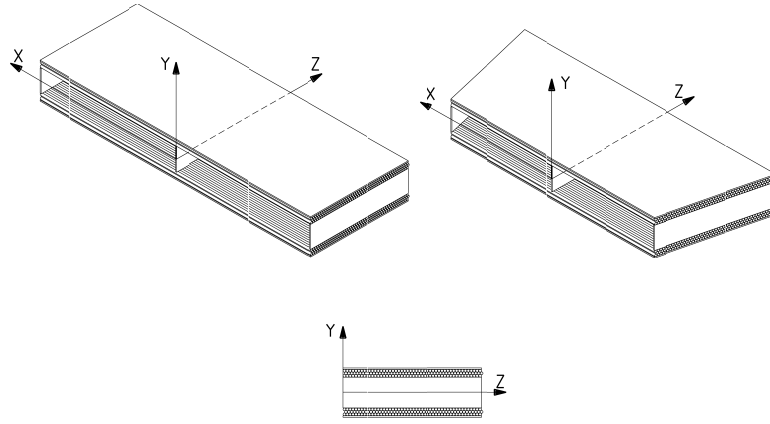


Figure 4.4.: Local MDT chamber coordinate system [15]

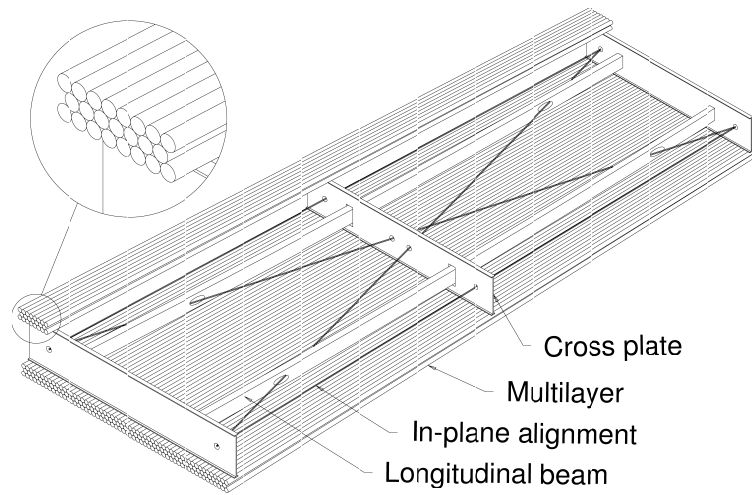


Figure 4.5.: Schematic layout of a MDT chamber [15]



### 4.3.2. Chamber electronics

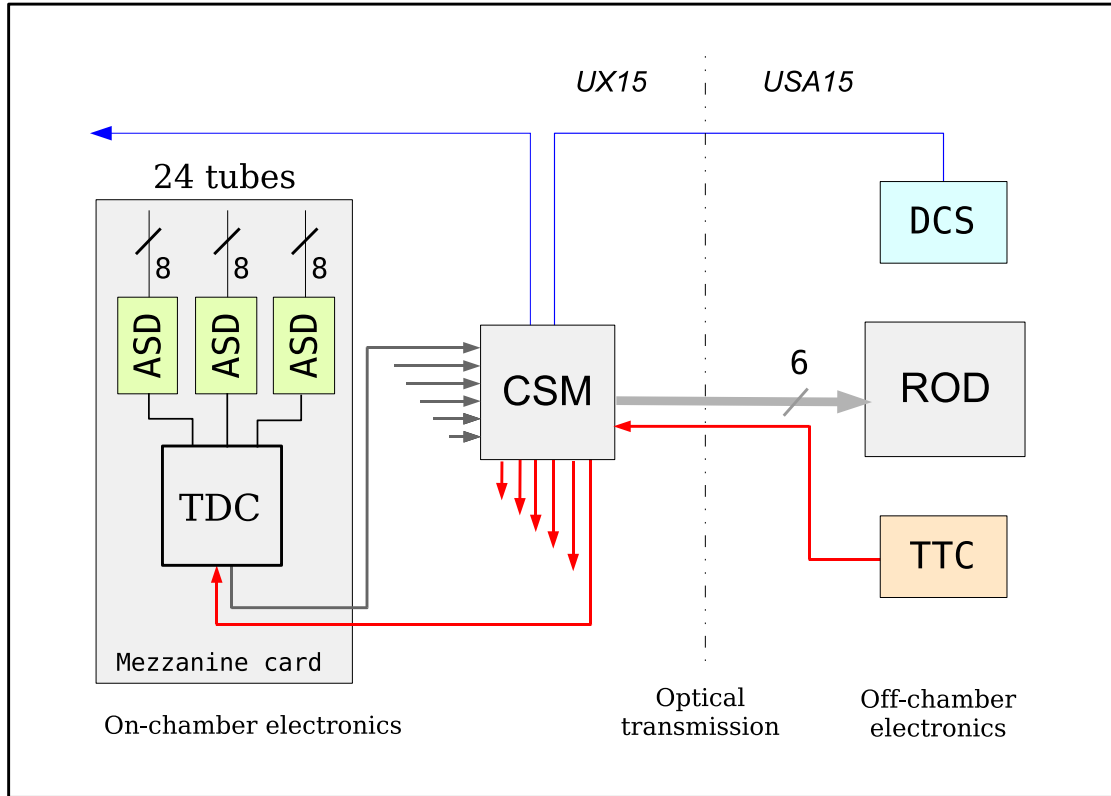


Figure 4.6.: Simplified diagram of the MDT readout electronics [9]

Part of the readout electronics of the MDT chambers are directly mounted at the end of the tubes. At one side the tubes are connected to high voltage, while on the other side the readout electronics (Fig. 4.6) is located. All electronics components are located inside Faraday cages, located on both ends of the MDT chambers. The basic readout element of the MDT chamber is the mezzanine card. Using a printed circuit board as a signal distribution card, it is connected to 24 drift tubes (24 channels). Each mezzanine card contains three monolithic Amplifier/Shaper/Discriminator (ASD) chips connected to a Time-to-Digital-Converter (TDC) chip. Programming of these chips is done using the JTAG protocol.

Each chamber has between 2 and 18 of these mezzanine cards. The mezzanine cards are controlled by a local processor, the Chamber Service Module (CSM) mounted on the chamber itself. The main task of the CSM module is to broadcast the Timing, Trigger, Control (TTC) clock and LVL1 trigger signals to the mezzanine cards, and subsequently collect the signals from them. The hits are then formatted and sent using an optical link to a VME module serving as the Readout Driver (ROD) located in the equipment cavern USA15. A VME module is able to handle up to eight CSMs. Then the data

is transferred to the Readout Buffer (ROB) where the data is stored until the L2 trigger has reached its decision to either store or disregard the data. Figure 4.6 gives an overview of the chamber electronics and the readout chain.

Furthermore, each MDT chamber is equipped with a Muon DCS Module (MDM) box (Fig. 4.7). The MDM box houses an Embedded Local Monitor Board (ELMB), connectors and control chips such as the JTAG control chip. The ELMB has been developed for ATLAS following the specific hardware requirements featuring a 64-channel Analog Digital Converter (ADC), numerous digital in and outputs and a CAN fieldbus interface. Temperature and B-Field sensors are connected to the MDM. Using the CAN fieldbus these sensors are read out by the Detector Control System (DCS).

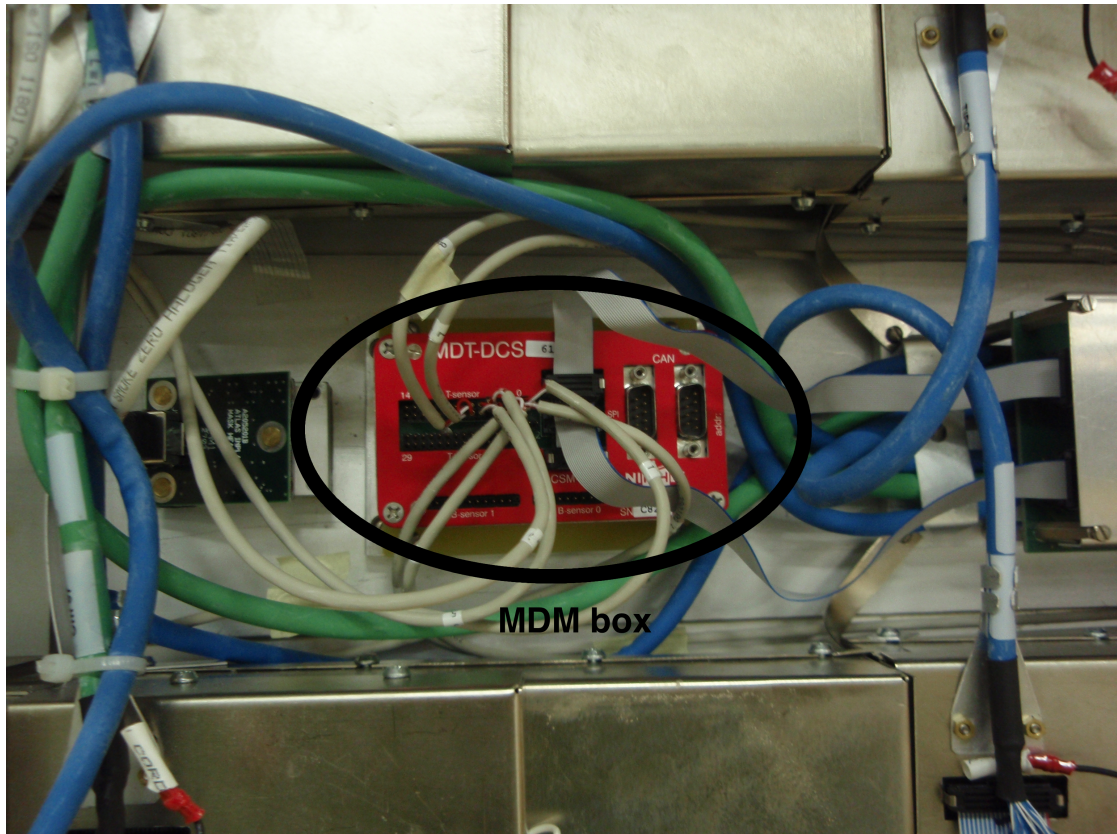


Figure 4.7.: MDM box mounted on a MDT chamber

#### 4.3.3. Temperature sensors

As mentioned before in Chapter 4.3.1, knowledge of the (current) chamber deformations is vital to meet the design resolution requirements. The in-plane optical alignment system is assisted by temperature sensors which are glued to the multilayers and chamber support frames.

However, the temperature of the MDT chamber is not only necessary in order to correct for chamber deformations, furthermore, it is required to reach the required reconstruction precision. The reconstruction of the particle track relies on the drift velocity of the electrons in the gas. Apart from the gas mixture and tube design, the temperature of the gas within the MDT tube has a non negligible influence on this velocity. This requires an effective temperature monitoring system. Depending on the chamber type and size, the number and position of the temperature sensors differs (Tab. 4.3).

## Types

Throughout the whole MDT chambers three different types of temperature sensors, named after their suppliers, have been used:

- NIKHEF sensor: NTC sensor, accuracy:  $0.2^{\circ}\text{C}$
- Washington sensor: Pt100 sensor, accuracy:  $0.1^{\circ}\text{C}$
- Brandeis sensor: 1 kOhm Platinum resistance sensor (RTD), accuracy:  $0.05^{\circ}\text{C}$

It was planned that NIKHEF should supply the temperature sensors for all MDT chambers. However, the University of Washington wanted to install more precise sensors. Initially it was foreseen to install Washington sensors on all EI and EM chambers. During the construction of the chambers, it was unclear whether the calibration of the Washington sensors could be affected by the intense radiation in the forward regions. Therefore it was decided to install less radiation sensitive RTD sensors. In order to study the influence of the radiation on the two sensor types, some chambers have been equipped with Brandeis and Washington sensors [18].

Table 4.3.: MDT chamber types and the corresponding temperature sensor types and numbers

Chamber type	Number and type of T-sensors
BIS	10 NIKHEF
BIS8	3 NIKHEF
BIM	6 NIKHEF
BIR	6 NIKHEF
BIL	6 NIKHEF
BML	10 NIKHEF
BMS	10 NIKHEF
BMF	10 NIKHEF
BOL	18 NIKHEF
BOF	18 NIKHEF
BOG	28 NIKHEF
BOG8	24 NIKHEF
EIS	8 Brandeis
EIS1	20 Washington + 8 Brandeis
EIL	8 Brandeis
EIL1A09	20 Washington + 8 Brandeis
EIL4	20 Washington
EMS	20 Washington
EMS1	8 Brandeis
EML	20 Washington
EML1	20 Washington + 8 Brandeis
EOS	8 NIKHEF
EOL	8 NIKHEF
EES	8 NIKHEF
EEL	8 NIKHEF

## T-Sensor position and naming

Unlike the end-cap temperature sensors, the sensors mounted on the barrel chambers do not follow a clear positioning schema. Each chamber type has optimised sensor positions designed by the chamber manufactures. Furthermore each manufacturer designed their own, incompatible naming schema.

It was intended to find a common way of uniquely naming the temperature sensors, while providing a rough idea of the sensors respective mounting position. It was aimed to stay as close as possible to already existing schemes and numbering. Therefore the running number at the end of the new temperature sensor name, is usually the number given by the chamber manufactures. An already existing schema for naming of the end-cap sensors [18] has been enhanced to make it suitable as a generic naming schema for all sensors. All MDT chambers are virtually subdivided into various sections (Fig. 4.8).

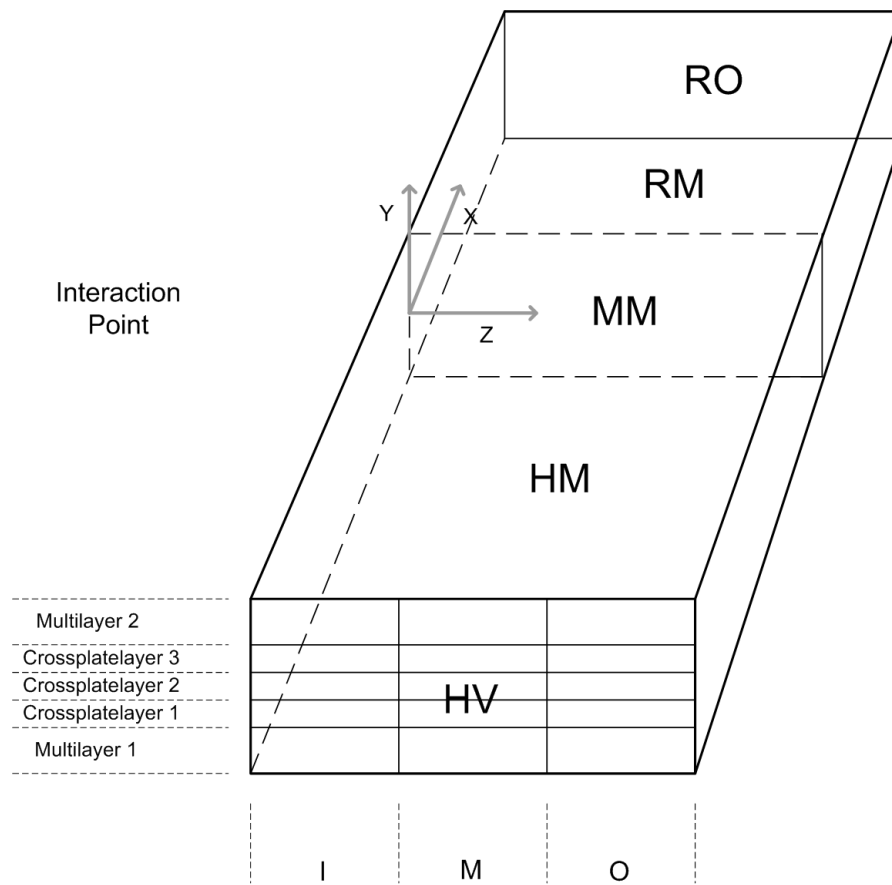


Figure 4.8.: Sections of the barrel chambers [18]

The following generic naming schema is used (Eq. 4.1) [19].

$$T < type > _ < chamber > _ < layer > _ < side > _ < location > _ < number > \quad (4.1)$$

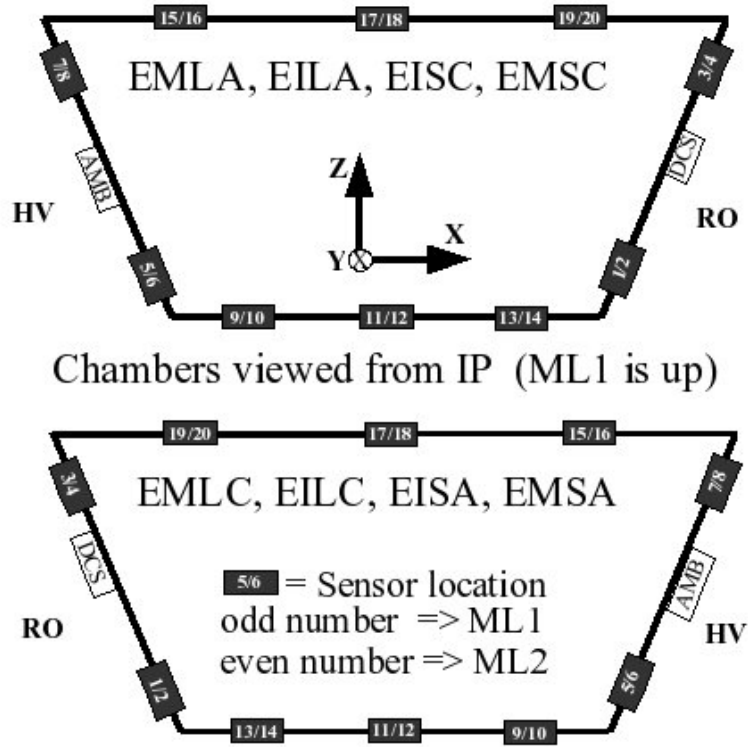


Figure 4.9.: Position of the end-cap temperature sensors [18]

Due to the different shapes and sensor positions on the barrel and end-cap chambers, there are two set of options defined. One used by the barrel sensors (Tab. 4.4), the other one used by the end-cap sensors (Tab. 4.5).

Examples:

**TN\_BOL1A01\_ML1\_HV\_I\_01:** This is a NIKHEF NTC temperature sensor mounted on multilayer 1 at the HV side nearer to the interaction point of the barrel chamber BOL1A01 with the running number 01.

**TW\_EML1C15\_ML1\_RO\_S\_01:** This is a Washington Pt100 temperature sensor mounted on multilayer 1 at the readout end near the short side of the end-cap chamber EML1C15 with the running number 01.

Table 4.4.: Naming options for temperature sensors mounted on MDT barrel chambers

Placeholder	Options	Description and type of T-sensors
< <i>type</i> >	B	Brandeis RTD sensor
	W	Washington Pt100 sensor
	N	NIKHEF NTC sensor
< <i>chamber</i> >	chamber name	name of the MDT chamber, eg.: BOL1A01
< <i>layer</i> >	ML1	Multilayer 1
	ML2	Multilayer 2
	CP1	Crossplatelayer 1
	CP2	Crossplatelayer 2
	CP3	Crossplatelayer 3
< <i>side</i> >	HV	high voltage side
	RO	readout side
	RM	between centre and readout side
	HM	between centre and high voltage side
	MM	on the middle spacer
< <i>location</i> >	I	inner region
	M	middle region
	O	outer region
< <i>number</i> >	00 - 28	Two digits running number

Table 4.5.: Naming options for temperature sensors mounted on MDT end-cap chambers

Placeholder	Options	Description and Type of T-sensors
< <i>type</i> >	B	Brandeis RTD sensor
	W	Washington Pt100 sensor
	N	NIKHEF NTC sensor
< <i>chamber</i> >	chamber name	name of the MDT chamber, eg.: EML1A01
< <i>layer</i> >	ML1	Multilayer 1
	ML2	Multilayer 2
< <i>side</i> >	HV	high voltage side crossbeam
	SB	short side longbeam
	LB	long side longbeam
< <i>location</i> >	S	towards short longbeam side
	L	towards long longbeam side
	H	towards high voltage side
	R	towards readout side
	C	centre of a longbeam
< <i>number</i> >	00 - 28	Two digits running number

### Temperature sensors readout

The NIKHEF and Washington temperature sensors are connected to locally mounted MDM boxes on each chamber. These are read out using a CAN fieldbus by the ATLMDTMDM system. In total 96 CAN fieldbuses are used to read out all chambers. Each readout PC contains 12 CAN fieldbus interface slots, therefore eight readout PCs are required for the whole ATLMDTMDM system. All information on the MDM boxes, this includes the temperature data, is read out at regular intervals<sup>2</sup>.

Brandeis temperature sensors are not connected to the MDM boxes. Owing to the fact that the alignment system uses Brandeis sensors itself, all MDT Brandeis temperature sensors are read out through the alignment system ATLMDTLWDAQ01, which runs on a separate readout PC.

Both readout systems use PVSS and store the temperature data in their respective data point structures.

## 4.4. Temperature distribution

The temperature in the ATLAS cavern is not expected to be homogeneous. The muon system alone, produces approximately 110 kW of thermal energy. Given the fact that fresh air of 17° Celsius is blown into the cavern at the bottom, while the used air exhaust is located at the top of the cavern, a temperature gradient of  $\sim 5$  degrees between the bottom and the ceiling of the cavern is expected.

The CFD group at CERN has performed extensive 3D simulations of the ATLAS ventilation system [20]. During these studies, simulations of the temperature and air velocity distribution of the ATLAS experiment have been made. They provide us with more detailed temperature information (Fig. 4.10) about the ATLAS detector and its cavern [20]. The temperature distribution is caused mainly by heat sources within the detector and by the detector geometry, because of restrictions of free air flow (Fig. 4.11).

First hints of such a temperature distribution can already be measured by the MTM system (Fig. 4.12). However, as these simulations have been performed with a fully functional and running ATLAS detector, the data does not necessarily describe the current temperature distribution of the detector still being in the installation and commissioning phase.

---

<sup>2</sup>At the time this thesis was prepared, the readout interval was set to 30 seconds.



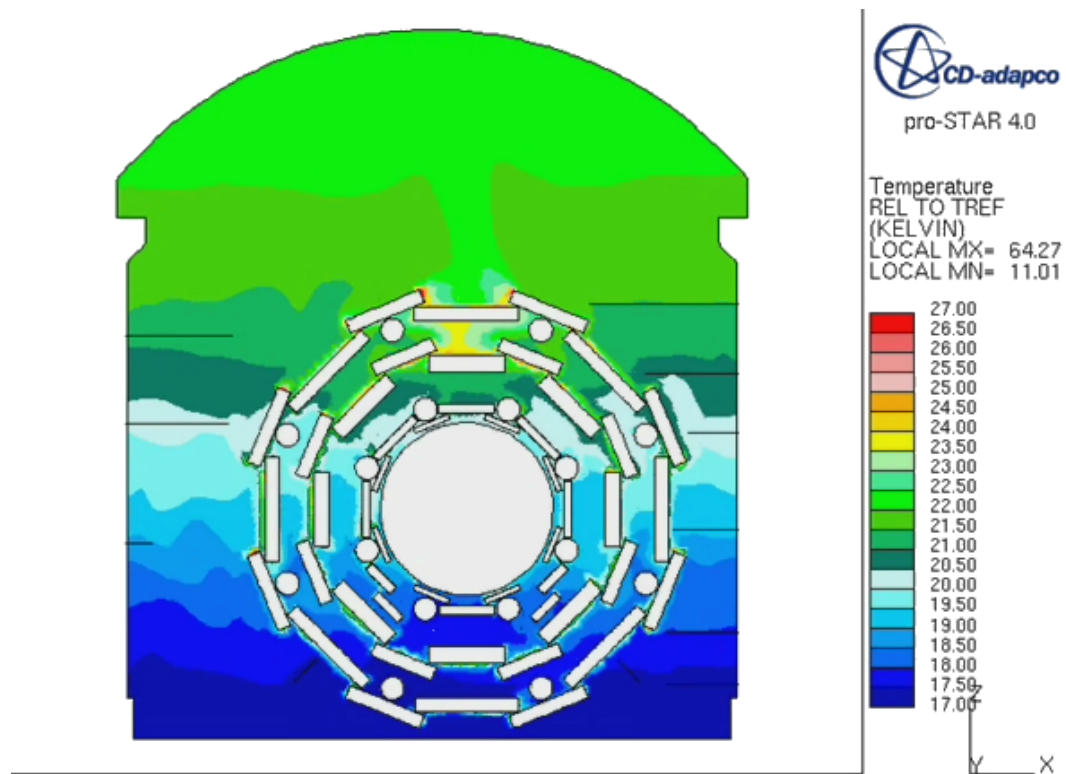


Figure 4.10.: Temperature distribution along a cross section of the ATLAS cavern. The ATLAS experiment is shown within the cavern. [20]

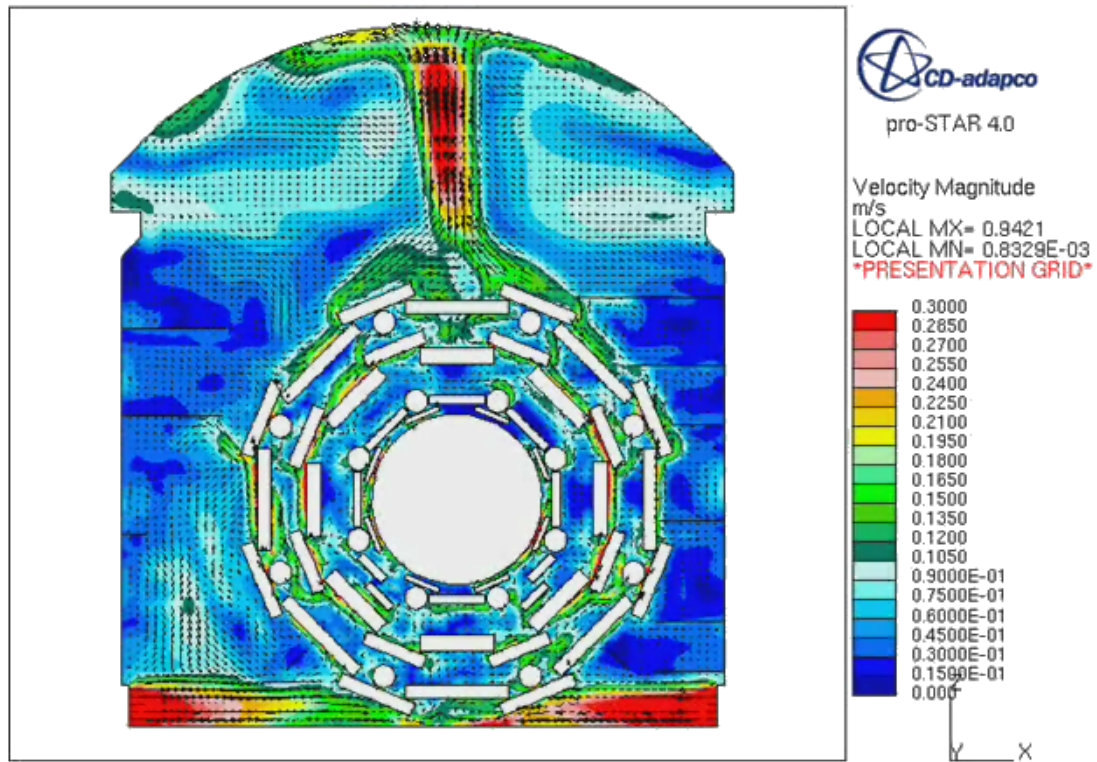


Figure 4.11.: Air velocity distribution along a cross section of the ATLAS cavern. The ATLAS experiment is shown within the cavern. [20]

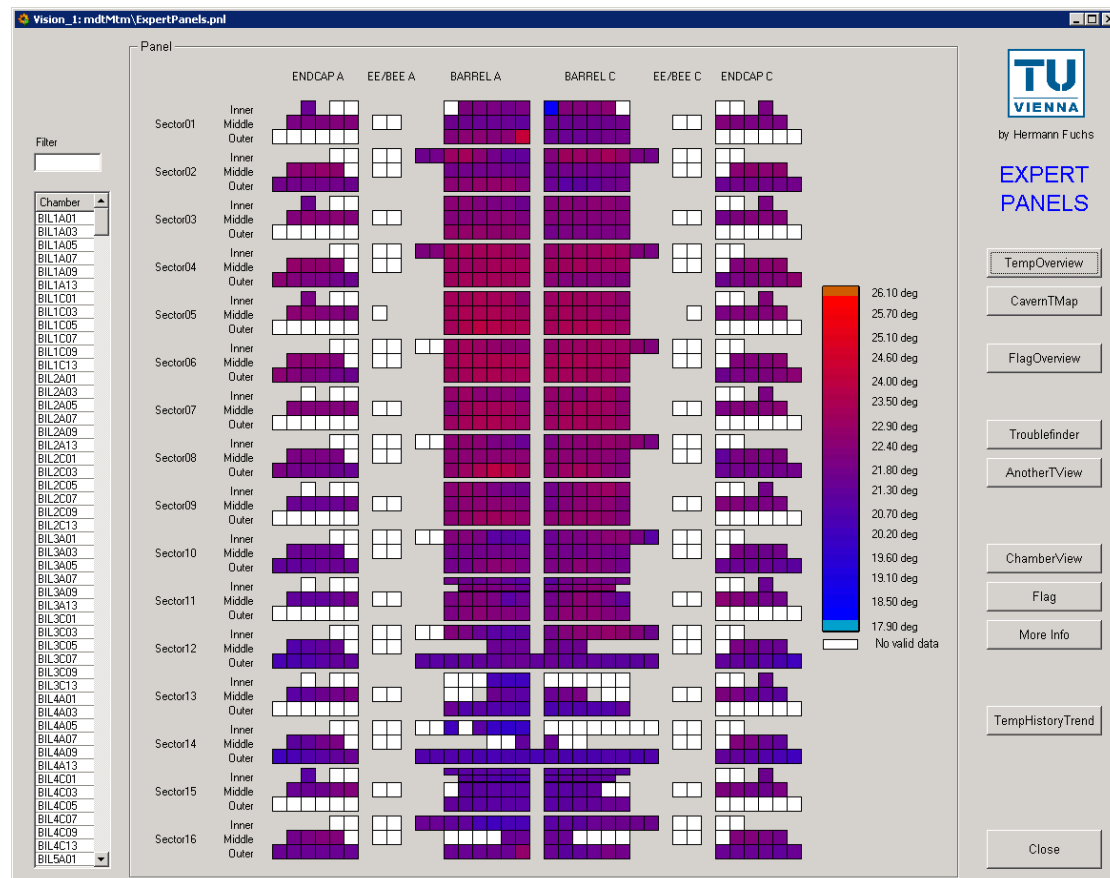


Figure 4.12.: Logical view of the temperature distribution throughout the MDT system during an milestone run of the MDT system (Sectors 3-8 have been powered). Data taken using the MTM project.

#### 4.4.1. MDT chamber temperature distribution

As described in Chapter 4.3.2, the read out electronics is situated at one side of each chamber, opposite to the high voltage connections. While the high voltage supply can be neglected as heat source, the on-chamber read-out electronics consumes around 15 W per board. It is the main heat source on the chamber.

An extended object with a heat source fixed to one side, will, in thermal equilibrium, have a stable temperature distribution. Under ideal circumstances, one should expect an exponential decrease of the temperature along the object. The same applies in first order to the MDT chambers. However, reality is more complicated. The MDT chambers themselves are in a thermal environment that depends on the chamber location, orientation (e.g. the MDT chambers in sector 1 and 9 are mounted vertical while in sector 5 and 13 horizontal), and other heat sources in the vicinity of the chamber.

Furthermore, the number of temperature sensors on each MDT chamber (on average 12) is limited. Most of the temperature sensors are glued to the drift tubes, but rarely more than three along the length of the tubes. Depending on the amount of glue used, a direct thermal contact with the drift tubes can not be guaranteed.

An example of the measured temperature distribution is shown in Fig. 4.13.

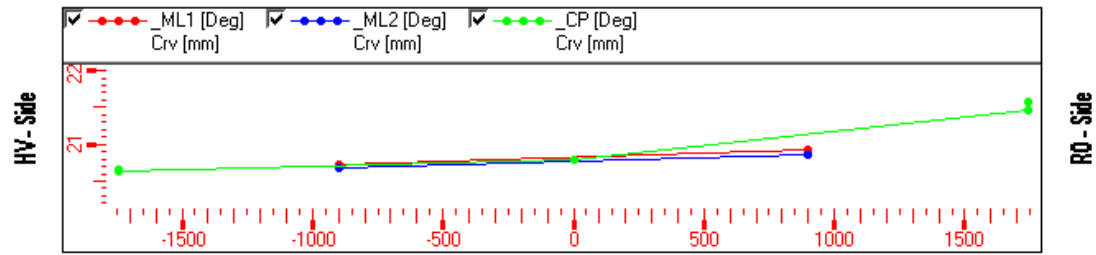


Figure 4.13.: Temperature distribution along the tube axis of a BML chamber in sector 01 (BML5C01) taken with the MTM project using the mounted temperature sensors. The three lines represent sensors mounted on Multilayer 1, Multilayer 2 and the cross-plate respectively.

One of the aims of the MTM project was to provide a parametrisation of the temperature distribution of the MDT chambers. As you can see, the temperature falls almost linear along the tube axis. Depending on the mounting and dimensions of the chambers, different behaviour can be observed (Fig. 4.14, 4.15 and 4.16). Because of the temperature homogeneity of the MDT chambers along the z-axis, a two dimensional temperature parametrisation was chosen. The same approach has been used during the computer simulations of the temperature distribution.

Given the very low number of sensors<sup>3</sup> it was necessary to find a robust fit which can cope with a low number of measurements.

<sup>3</sup>Some chambers only have 4 temperature sensors with only two of them on the same multilayer.

An exponential fit might be the most logical choice concerning temperature distributions. However, the low number of measurements, imposed due to the low number of temperature sensors, makes an exponential fit extremely unreliable and in some cases impossible to calculate.

Therefore, due to its robustness and ease of use, the MTM project uses a two dimensional linear fit to provide a temperature parametrisation. In case a more precise and detailed parametrisation is required, it can be changed easily.

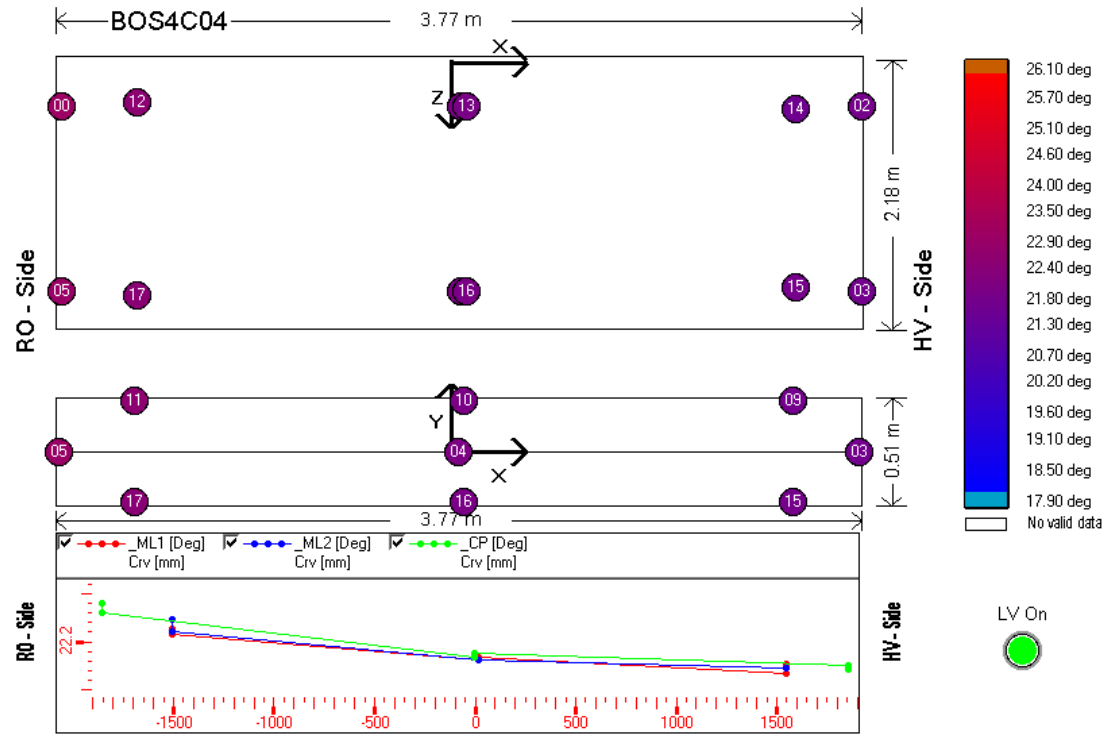


Figure 4.14.: Temperature distribution of a BOS chamber in sector 04 (BOS4C04). The upper part shows the position of the temperature sensors on the chamber. The lower part gives the temperature distribution along the tube axis. The three lines represent sensors mounted on Multilayer 1, Multilayer 2 and the cross-plate respectively.

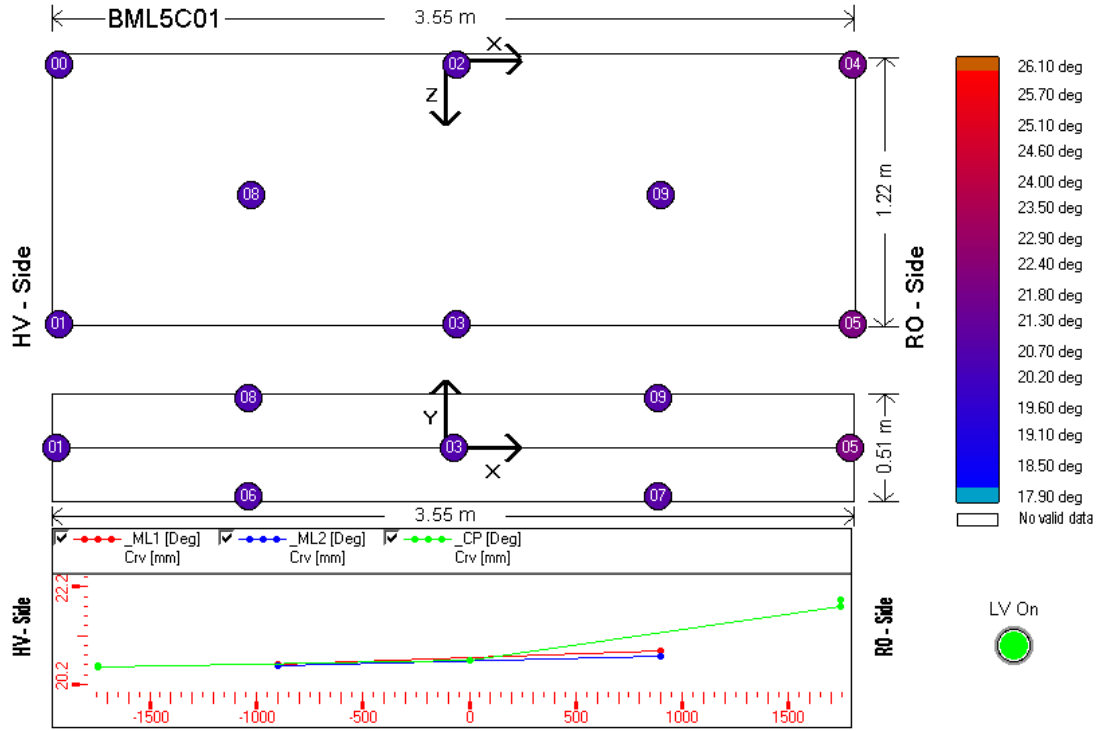


Figure 4.15.: Temperature distribution of a BML chamber in sector 01 (BML5C01). The upper part shows the position of the temperature sensors on the chamber. The lower part gives the temperature distribution along the tube axis. The three lines represent sensors mounted on Multilayer 1, Multilayer 2 and the cross-plate respectively.

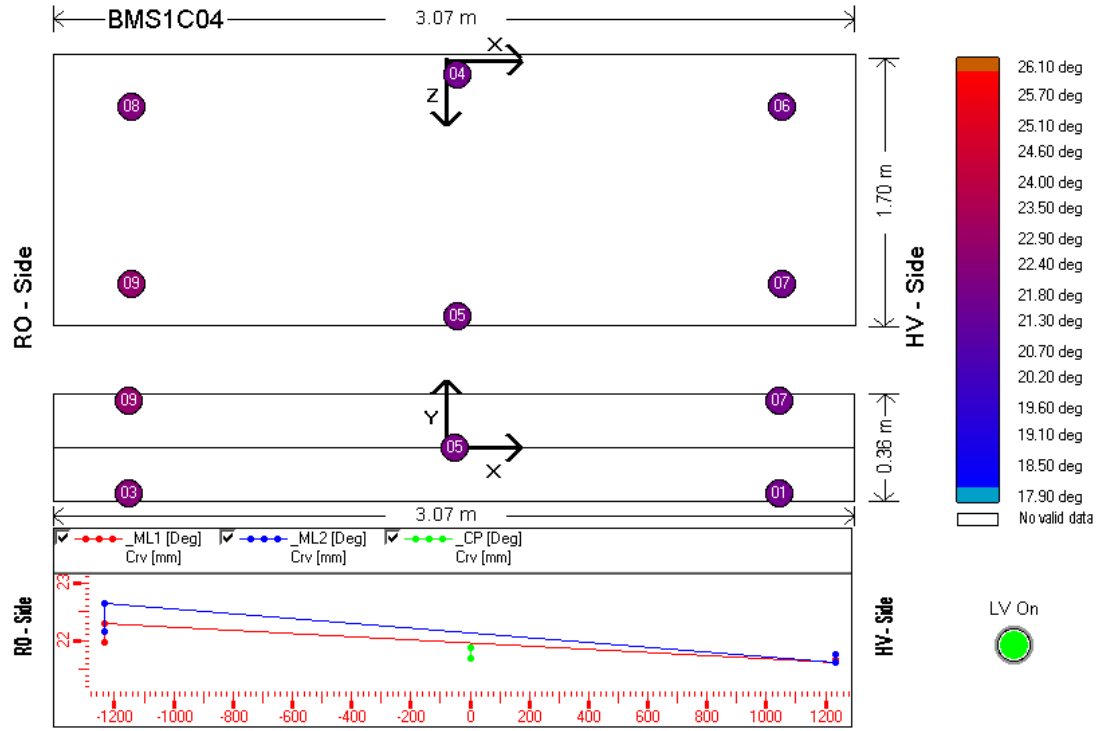


Figure 4.16.: Temperature distribution of a BMS chamber in sector 04 (BMS1C04). The upper part shows the position of the temperature sensors on the chamber. The lower part gives the temperature distribution along the tube axis. The three lines represent sensors mounted on Multilayer 1, Multilayer 2 and the cross-plate respectively.

## 5. ATLAS Detector Control System

The ATLAS Detector Control System (DCS) controls and supervises the coherent and safe operation of the ATLAS experiment. All information and alarms and the (re)actions initiated by the operators concerning the hardware of the detector are handled by the DCS. Some detector components have to operate continuously (i.e. cooling of the magnet system), because interruptions may cause long delays or may affect the performance of the detector altogether. Therefore DCS supervision is needed permanently.

Safety related aspects are not the responsibility of the DCS, but of a dedicated Detector Safety System (DSS) and the CERN wide safety and alarm system, with which DCS interacts. However, DCS provides both systems with tools for interlocks (in hard- and software) [16].

In order to ease development and to reduce maintenance costs of the four big LHC experiments, the Joint Controls Project (JCOP) was formed [21]. Under the auspices of JCOP common software tools have been developed to form a highly modular framework. The idea of this JCOP framework is to provide standardised tools and procedures to facilitate development and maintenance of detector control software.

### 5.1. Organisation

The DCS consists of the Front-End (FE) system and the Back-End (BE) system. The FE system connects directly to the detector hardware while the BE system supplies the supervisory and control layer. Both systems are interconnected using Controller Area Network (CAN) fieldbus and Local Area Network (LAN).

#### 5.1.1. Front-End system

The DCS Front-End (FE) system connects directly to the detector hardware and is distributed over the whole volume of the detector. It executes commands sent by the BE, reads and processes values and transfers data to the BE system. The FE system is the responsibility of the sub-detector groups. Each group developed their own FE components, although it was aimed to use as much as possible standardised components (e.g. the Embedded Local Monitor Boards (ELMB), power supplies).

#### 5.1.2. Back-End system

The Back-End (BE) system of the ATLAS DCS has two main functions. Firstly, it communicates with the FE system and provides supervisory control functions such as data



processing, analysis, display, storage and archiving. Secondly, it relays actions initiated by the operator in the form of commands to the hardware and displays messages and alarms concerning the detector hardware.

The BE system is structured hierarchically in order to map the structure of the experiment (Fig. 5.1). The DCS BE structure follows closely the data acquisition (TDAQ) structure.

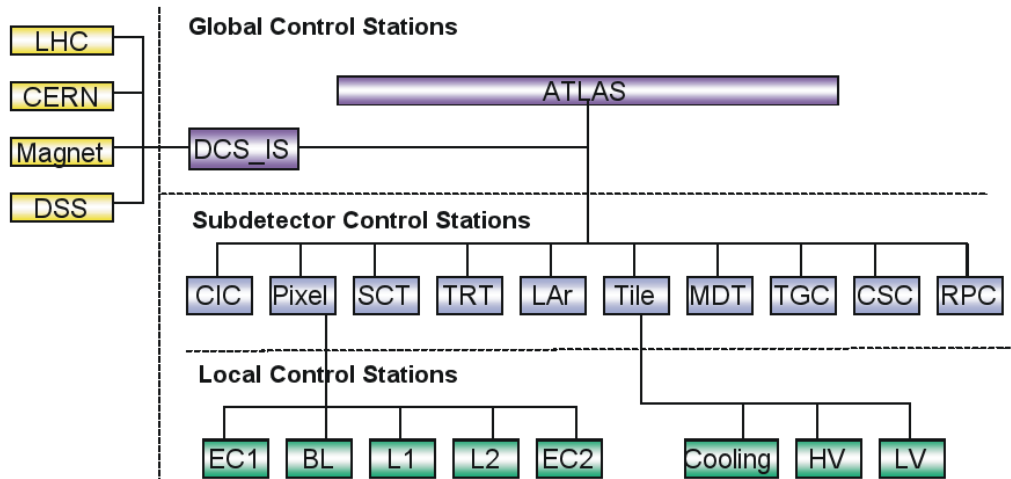


Figure 5.1.: Organization of the ATLAS Back-End DCS system [16]

The hierarchical structure provides the possibility of splitting the ATLAS experiment into partitions which can be operated independently (stand-alone). This is especially important during commissioning where multiple sub-detector elements are be operated and tested in parallel. Additionally it facilitates the debugging of detector elements even during data taking in order to track down faults.

The operation of the sub-detectors will be done using the Finite State Machines (FSM) concept as described in Chapter 5.4.

## 5.2. Standards

In order to standardise the 'look and feel' of the ATLAS DCS, a set of DCS developers guidelines have been prepared [22], [23]. These guidelines specify naming conventions, panel dimensions, backup procedures... Furthermore, the ATLAS DCS requires to use only alert classes defined by the JCOP framework (Tab. 5.1).

Table 5.1.: Alert classes defined by the JCOP framework

Alert Class	Severity	Colour	Comment
FwAlarmFatalUnack	Fatal	Red	Critical alarm demanding immediate investigation.
FwAlarmFatalAck	Fatal	Red	Critical alarm demanding immediate investigation, needs to be acknowledged.
FwAlarmErrorUnack	Error	Orange	Severe alarm demanding investigation.
FwAlarmErrorAck	Error	Orange	Severe alarm demanding investigation, needs to be acknowledged.
FwAlarmWarnUnack	Warning	Yellow	Alarm, no imminent danger.
FwAlarmWarnAck	Warning	Yellow	Alarm, no imminent danger, needs to be acknowledged.

### 5.3. Prozessvisualisierungs- und Steuerungssystem PVSS

#### 5.3.1. Evaluation and selection of PVSS

In order to monitor and control the big LHC experiments, a Supervisory Control And Data Acquisition system (SCADA) was needed. In cooperation the LHC experiments have defined user requirements and a list of selection criteria was established:

- Scalability: Capability of the product to cope with the complexity and size of a LHC experiment, especially in considering the huge number of readout channels.
- Interface/Extensions: The possibility to interface the program with external systems and to add further functionality.
- Performance Evaluation: Ranking of different program architectures and programming approaches (such as polling, event driven...) regarding their performance.
- Support of Large Applications: Capability to support large applications and the provision of suitable tools to develop these.
- Financial Considerations: Stability of the company and costs of the product.

A Technology Survey examined 40 software packages. After rejecting packages that were clearly unsuitable, about 20 products remained. An intensive study was done to compare and rank the remaining products. Finally, in 1999 the four big LHC experiments (ATLAS, CMS, ALICE, LHCb) agreed to use PVSS II as a common SCADA tool. Further information on the selection process can be found in [24].

#### 5.3.2. Introduction to PVSS II

Prozessvisualisierungs- und Steuerungssystem II (PVSS II) is German for process visualisation and control system. It has been developed by the Austrian company ETM.

PVSS is designed as a software package to operate and supervise technical installations by controlling and visualising the current status of an installation. An operator is able to use standard Human Machine Interfaces (HMI), such as a keyboard and mouse, to input commands and can see the response of the system to his actions immediately on his screen. PVSS fulfils all the requirements of a Supervisory Control And Data Acquisition system (SCADA). All the implementations described in the following are written using PVSS II version 3.6 [25] [26] [27].

### 5.3.3. Scripting Language CONTROL

The programming language used throughout PVSS is called CONTROL. The syntax is, apart from some modifications, the same as the one used in C. There are basically two approaches how a programming language can be implemented:

- **Compilation:** The code is translated before the execution of the program to machine code. This machine code can directly be executed by the hardware.
- **Interpretation:** The code is translated step by step during runtime using an interpreter.

Widely used compilation languages are C or C++. While compilation based programming languages provide very efficient and fast program execution, the compiled code is bound to the specific system it was compiled for. An interpreter language is generally slower, but because of the interpretation at runtime, the program can instantly be run on various operating systems and hardware platforms. Commonly used interpreter languages are Perl, Python, or Java. CONTROL is such an interpreter language. PVSS is designed as a SCADA system where the requirements for processing speed are not so stringent. Therefore the disadvantage of slower execution is outweighed by the possibility to run the same program on different platforms. PVSS natively supports Windows and Linux as operation systems and even allows for the cooperation of managers over operation system boundaries.

### 5.3.4. System Architecture

The design of PVSS II is very modular. The main idea is to divide different functionalities into separate functional modules. These functional modules are separate processes, they are called managers. All managers can communicate with each other using the standard TCP/IP protocol. A basic PVSS system is very small and requires only two managers. If additional functionalities are required, it is very easy to add additional managers. On the other hand, if certain functions are not required, the corresponding manager can easily be removed and thus does not consume resources. Managers can be added or removed during runtime, without stopping or restarting the project. This ensures a flexible and scalar system. Figure 5.2 shows a typical PVSS system. In the following the most important manager types are being described.

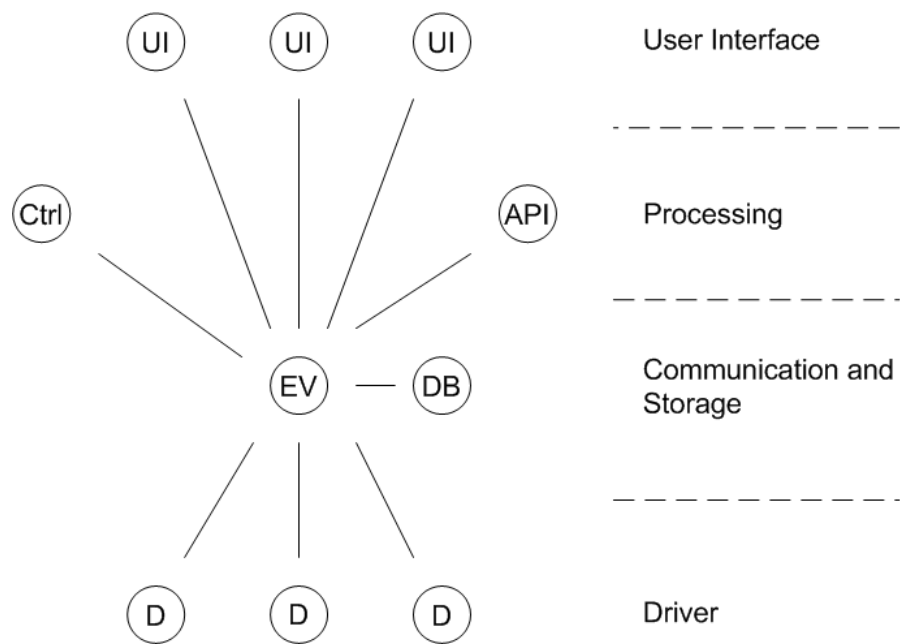


Figure 5.2.: A typical PVSS system

### System Core

The event manager (EV) along with the data manager (DB) constitute the core of any PVSS system. The smallest possible PVSS system consists only of an EV and a DB. Both processes are always required in order to have a functional system.

**Event Manager (EV)** The event manager (EV) manager contains the current state of all variables (process image) and handles the data transfer within the system. All data changes will be processed by the EV. Other managers which need access to data, communicate solely with the EV who will prompt all necessary steps (e.g. query other managers) to provide the data. For example, if a command is sent from a control station, it is first processed by the EV. Then it may be forwarded to the responsible driver who handles the communication with the specific target device (e.g. a power supply). Furthermore, the EV is also responsible for alert handling and some autonomous function calculations (so called data point functions). Both will be explained on the following pages.

**Data Manager (DB)** PVSS uses special databases, called RAIMA databases<sup>1</sup>, to store information. Not only archived (data) values are stored in databases, but also parametrisation data of the project is stored. The data manager (DB) handles the storing and retrieval of the data into and from the database(s). Other processes

<sup>1</sup>The high performance, embedded RAIMA databases have been developed by the homonymus RAIMA cooperation.

only access the DB and not the database(s) itself. For example, if a process needs to access historical or configuration data, the DB provides the requested data directly.

### **Execution of Code**

The two main options for executing code in PVSS are using a Control manager (CTRL) or using an application programming interface (API).

**Control Manager (CTRL)** The Control Manager is able to execute code written in the scripting language CONTROL, designed by ETM. The execution of the code starts as soon as the manager is started.

**Application Programming Interface (API)** The Application Programming Interface is implemented as a C++ library class. Using the API manager it is possible to run custom C++ code as a separated manager.

### **User Interface**

The user interface is a vital component of each SCADA system. It provides the interface between the operator and the control system.

**User Interface Manager (UI)** As the name suggests, the User Interface Manager provides the interface between the operator and the control system by displaying so called panels. These panels provide the user with the necessary control mechanisms and displays to control the system.

**Graphical Editor (GEDI)** The Graphical Editor is a WYSIWYG (What You See Is What You Get) editor with all necessary tools to create UI panels.

**Data Point Editor (PARA)** The Data Point Editor provides an easy way to access and change the PVSS internal data points.

### **Other Managers**

There are various additional managers implemented within PVSS. Only two of them shall be mentioned here briefly. PVSS is able to communicate directly with hardware using Drivers (DR). Furthermore, it is possible to interconnect various PVSS systems so that all systems can share data. This data sharing is coordinated and handled by the Connection Manager (CM).

## **5.3.5. Concepts**

### **Data Processing**

PVSS is not checking (polling) all the time whether there is new data available. Instead it uses an event based approach. Whenever new data arrives, an event is triggered.

The event then leads to the evaluation of the data. This approach is not limited to data processing, but applies as well to communication between separate managers. In the end, this means that processing or communication does only occur when data has changed. This is a very efficient design, as the program is only active when data changes. Therefore PVSS is not producing load if a monitored process is in a stable condition.

## Data Points

PVSS introduces a new concept in grouping variables and data, the so called data point concept. A device type is represented by a data point type. Each device of this type occupies one data point within this data point type. Each variable of a device is represented by a data point element of the corresponding data point.

Let us assume a MDT chamber called 'BIL1A01' which is of type 'MDTChamber'. This chamber contains a number of temperature sensors. The measured temperatures of the temperature sensors would then be data point elements of the data point 'BIL1A01'. This data point would in turn be a member of the data point type 'MDTChamber', which groups together MDT chambers of the same type (tab.:5.2).

Device	Data Structure	Data Point Name
Chamber Type 'MDT chamber'	Data point type	'MDTChamber'
Single MDT chamber	Data point	BIL1A01
Temperature of T-sensor1	Data point element	BIL1A01.temperatureSensor1
Temperature of T-sensor2	Data point element	BIL1A01.temperatureSensor2
Temperature of T-sensor3	Data point element	BIL1A01.temperatureSensor3

Table 5.2.: Example explaining the PVSS data point concept using a simplified MDT chamber

## Scattered System

As we have discussed in Chapter 5.3.4, a PVSS system consists of one EV manager, one DB manager and various optional managers. These managers communicate using the TCP/IP protocol. It is not mandatory that all managers run on the same computer. Certain managers can run on different machines communicating solely over Ethernet. Such a system is called a scattered system. For instance, the event and data manager may run on a server in the experimental area, while the operator is controlling the system from the control room using an UI connected to the EV over Ethernet (Fig. 5.3).

## Distributed System

It is possible to interconnect autonomous PVSS systems using special managers (distributed manager). Such a system is called a distributed system. Distributed systems can share the data of both event and data managers, making it possible to create highly redundant control systems. It is also possible to use distributed systems to control a

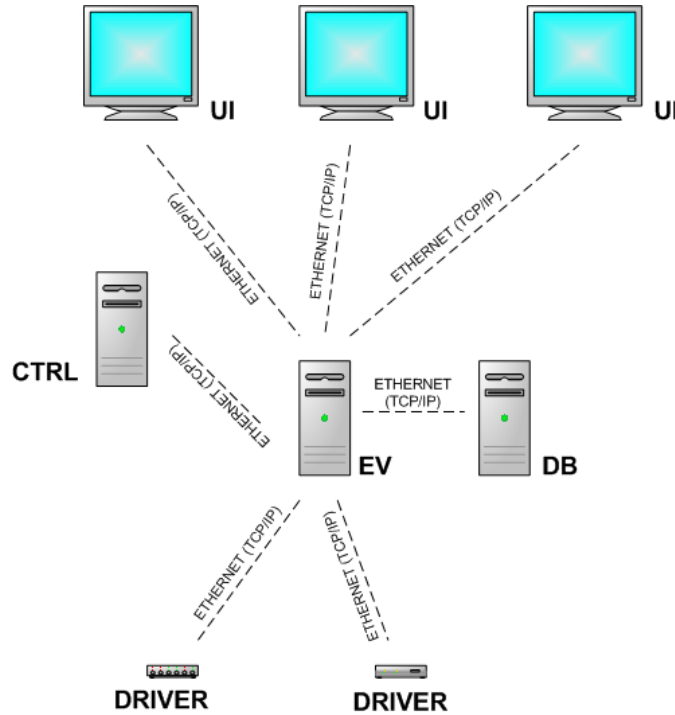


Figure 5.3.: Schematic layout of a PVSS scattered system

bigger experiment, where PVSS projects will control only smaller subsystems. One supervisory project then connects to these subsystems and controls them using a distributed system. This concept is used by all LHC experiments.

### Alerts

PVSS offers the possibility of monitoring certain data point elements and to raise an alarm if this value exceeds predefined alarm limits. The alert definition schema of PVSS is extremely flexible. It is not only possible to define virtually any data point element to be monitored and the according alarm limits, it also allows to define error classes. Raised alerts will be displayed on the alarm screen.

### Summary Alerts

A large number of alerts will quickly fill up the alarm screen, therefore an alarm reduction mechanism, called summary alerts, is included in PVSS. Summary alerts work in a similar way as a floodgate. If few alerts are raised, they are allowed to be shown on the alarm screen. When the number of active alarms becomes too big, the summary alarm kicks in and suppresses alerts from being displayed. Instead of hundreds of single alarm messages, only one message, informing the user that a number of alarms have been filtered out, is displayed. The threshold limit, after which the summary alert becomes active, can be set individually.

## Data Point Functions

Data Point Functions (dpFunctions) are autonomous, standalone functions. DpFunctions are not executed at regular intervals, instead they are evaluated whenever new data arrives or data is updated. Unlike control scripts, dpFunctions are executed directly within the event manager. Whenever the event manager is active, dpFunctions are active as well. As the core of each PVSS project is the event manager, dpFunctions are very robust and reliable. All this features makes them the ideal choice for evaluations, which are only needed to be done when data is updated. If no data is updated, dpFunctions do not consume CPU time. As the name suggests, a dpFunction has to be connected to a data point element, but is not limited to be triggered only from or updating only this element.

PVSS itself comes with a limited number of dpFunctions, mainly for statistical analysis. It is possible to add custom made functions as dpFunctions. In order to do that, these functions have to be written in a library, which has to be loaded by the event manager. Once the functions have been loaded, they are available as dpFunctions. The downside of this approach is, that each change made to the code of a dpFunction, requires a restart of the event manager in order to prompt a reload of the library. Restarting the event manager, being the core of a PVSS project, means restarting the whole PVSS project.

## 5.4. Finite State Machine

High Energy Physics (HEP) experiments are getting more and more complicated [28]. The problem of the increasing complexity of online control systems started to occur at the HEP experiments installed at LHCs predecessor, the LEP. In order to cope with this complexity at the DELPHI experiment, a new concept of control logic has been implemented by P. Aarnio in 1991 [29]. This implementation used an early version of the State Machine Interface (SMI) developed by J. Barlow at CERN [30]. Based on the concept of Finite State Machines (FSM), SMI enabled the development of complex control systems.

### 5.4.1. Finite State Machine concept

A Finite State Machine (FSM) represents the behaviour of a complex system by a limited number of states, transitions and actions. A FSM is event based, that means processing is not continuous, but only occurring in case an event happens (e.g. the arrival of new data). Each sub system is represented by a FSM object. Every FSM object has a main attribute the state, representing the condition of this object. As the name suggests, transitions are change-overs from one state to another. Transitions are described by a set of rules which must be met in order to switch states. Actions are commands send to the FSM object at specified conditions (Fig. 5.4).

The following constraints are necessities in any control system architecture using the FSM concept:



- FSM follows a strict tree hierarchy. Each object can only belong to one other (parent) object. Each parent object can have more than one child object, but parents cannot share children.
- States are always propagated up. The parent is informed when a child changes its state, but not the other way round.
- Furthermore, the parent is able to send actions to the children, but the child isn't.

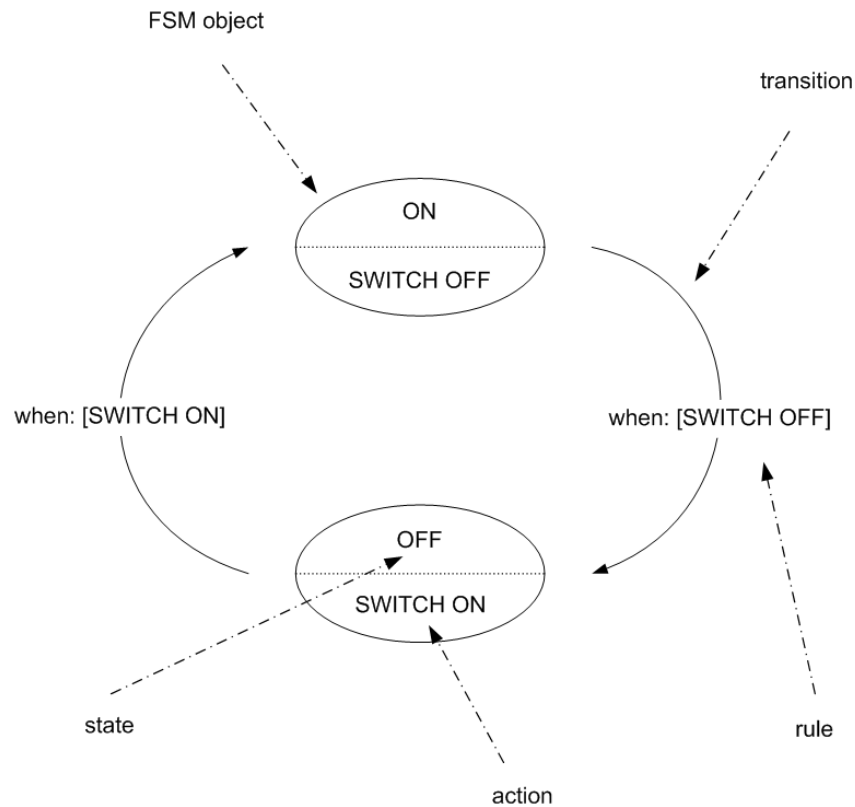


Figure 5.4.: FSM diagram depicting the interaction of states, actions, rules and transitions

### 5.4.2. State Machine Interface (SMI++)

In order to accommodate the needs and flexibility required by the HEP experiments at the LHC, SMI was completely redesigned to form the SMI++ framework [31]. However, the basic operating concepts remained unchanged. Within the SMI++ framework systems can be described as a collection of objects behaving as finite state machines. Objects interact with the device they are attached to. This assures that the corresponding SMI++ object has access to real data in order to calculate the states or to control the devices by sending commands.

However the main attribute of any object remains its corresponding state, only this information is available throughout the SMI++ machinery. SMI++ objects communicate with each other using the DIM protocol<sup>2</sup>.

In order to reduce the complexity of large systems, it is possible to group related objects. This grouping is done using abstract SMI++ objects and domains. Within a domain objects are organised in a hierarchical (FSM) tree structure controlled by abstract objects. Domains can be attached to further abstract objects forming even bigger domains. These basic concepts allow the building of complex control architectures.

For example, there may be several domains, each being a control system of a sub-detector. These sub-detector control systems, can be combined within a superordinate domain, which is then able to control the whole detector (Fig. 5.5).

### 5.4.3. Detector Control System integration

The SMI++ tool kit is written in C++. Using an API manager from PVSS it was possible to integrate SMI++ into the JCOP framework forming the JCOP FSM [32]. Following the habitual language use throughout the ATLAS DCS, the term FSM will refer to JCOP FSM. JCOP FSM combines a FSM display and separate PVSS panels into one detector control system that gives an immediate overview of the detector state, while at the same time detailed information about the monitored system is provided. This is described in more detail in Chapter 5.4.4.

#### Nomenclature and object types

Extending the concept of domains and abstract objects, JCOP FSM uses three distinct object classes:

**Device Unit (DU):** Corresponds to a PVSS object, usually a data point. Normally this is an object which is attached to a hardware device. A DU cannot have children.

**Control Unit (CU):** This an abstract object. Each CU is run as a separate SMI++ process, therefore enabling a CU to be run standalone without superordinate objects. A CU is capable of containing children of every type (CU, LU and DUs).

---

<sup>2</sup>The Distributed Information Management System (DIM) is a lightweight data transfer service based on TCP/IP developed at CERN.

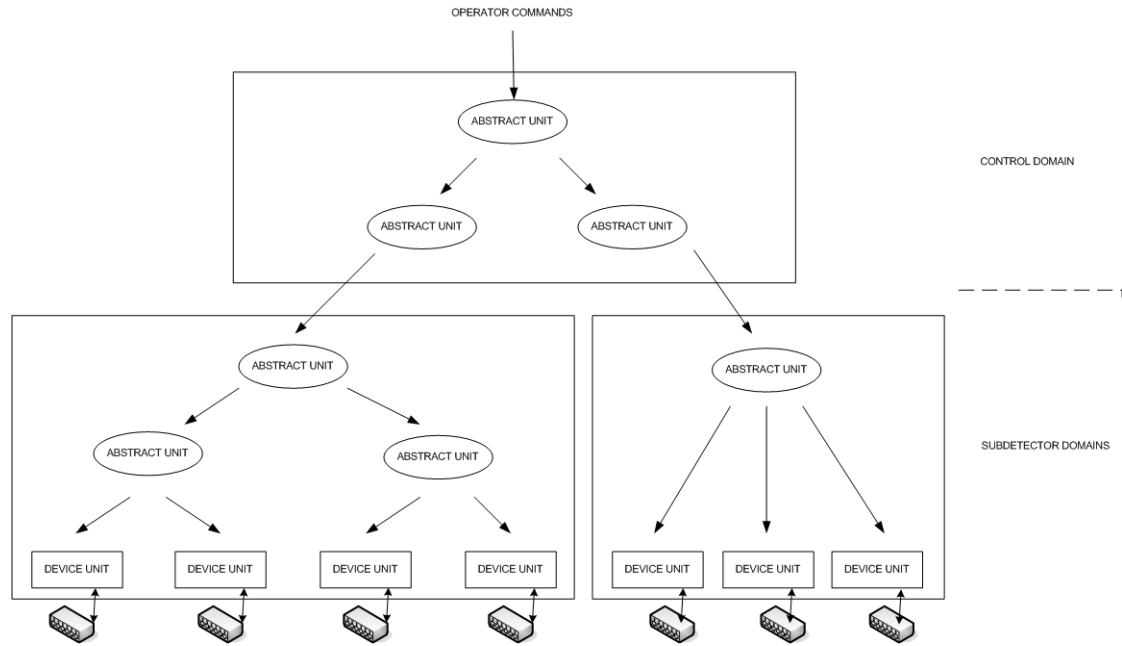


Figure 5.5.: Diagram showing the interaction of two sub-detector domains with a control domain. Each sub detector domain has various abstract objects.

**Logic Unit (LU):** Similar to a CU, however a logic unit (LU) can not run as a separate SMI++ process. Instead (like the DU) it is run within the process of the superordinate CU, therefore improving performance by reducing the number of SMI++ processes. Likewise a LU cannot be run alone without a superordinate CU. A LU is capable of containing children of type LU and DU.

Similar to the PVSS concepts of data point types and corresponding data points, JCOP FSM distinguishes between FSM device types and devices itself. A FSM device type contains the set of rules for a specific device type (e.g. a power supply), while devices (e.g the power supply number 124) are just instances of this device type. Rules and actions can only be defined on a per device type basis.

## Partitioning

HEP detectors are built by a number of groups simultaneously, requiring the possibility to separately operate and control different sub-detectors at the same time. The JCOP FSM provides a partitioning concept, which permits to switch from a central managed detector control to a distributed local control (e.g. for commissioning or debugging). Partitioning introduces the concept of ownership into the FSM concept. States are only received from and commands only sent to objects which are owned by an operator. Each object can only have one owner at the same time. Every CU can partition in or out its children. In order to increase the flexibility of the partitioning concept, the following six

partitioning modes have been defined:

**Included:** An object is included in a FSM hierarchy. It receives commands from and sends states to its parent object.

**Excluded:** An object is excluded from a FSM hierarchy. Neither does it receive commands from, nor does it send state information to its parent.

**StandAlone:** The object does not belong to a FSM hierarchy any more. Instead it has become the root of a new FSM hierarchy.

**CommandsDisabled:** An object is partially excluded from a FSM hierarchy. States are send to its parent object, but received commands are ignored.

**Manual:** An object is partially excluded from a FSM hierarchy. States are send to its parent object, but commands are only accepted from a different owner (e.g. an expert)

**Ignored:** An object is partially excluded from a FSM hierarchy. Commands are still received and obeyed, but states are not sent to the parent object any more.

#### 5.4.4. ATLAS specific FSM

The central DCS team of the ATLAS detector has implemented certain modifications of the JCOP detector control system [23] [28]. The most important change is the introduction of a second FSM state attribute, called STATUS. In ATLAS DCS, STATE and STATUS are defined as follows:

**State:** Defines the operational mode of the system

**Status:** Gives details how well the system is working

The incorporation of the STATUS is done as a special FSM object which is attached to each 'normal' (state) FSM object. Furthermore, ATLAS has modified the JCOP FSM screen (Fig. 5.6). Instead of only one panel showing more detailed information, two panels have been added, allowing for more flexible display and navigation. In addition a table has been implemented, that gives a quick overview of all objects whose states are not okay, therefore demanding investigation.

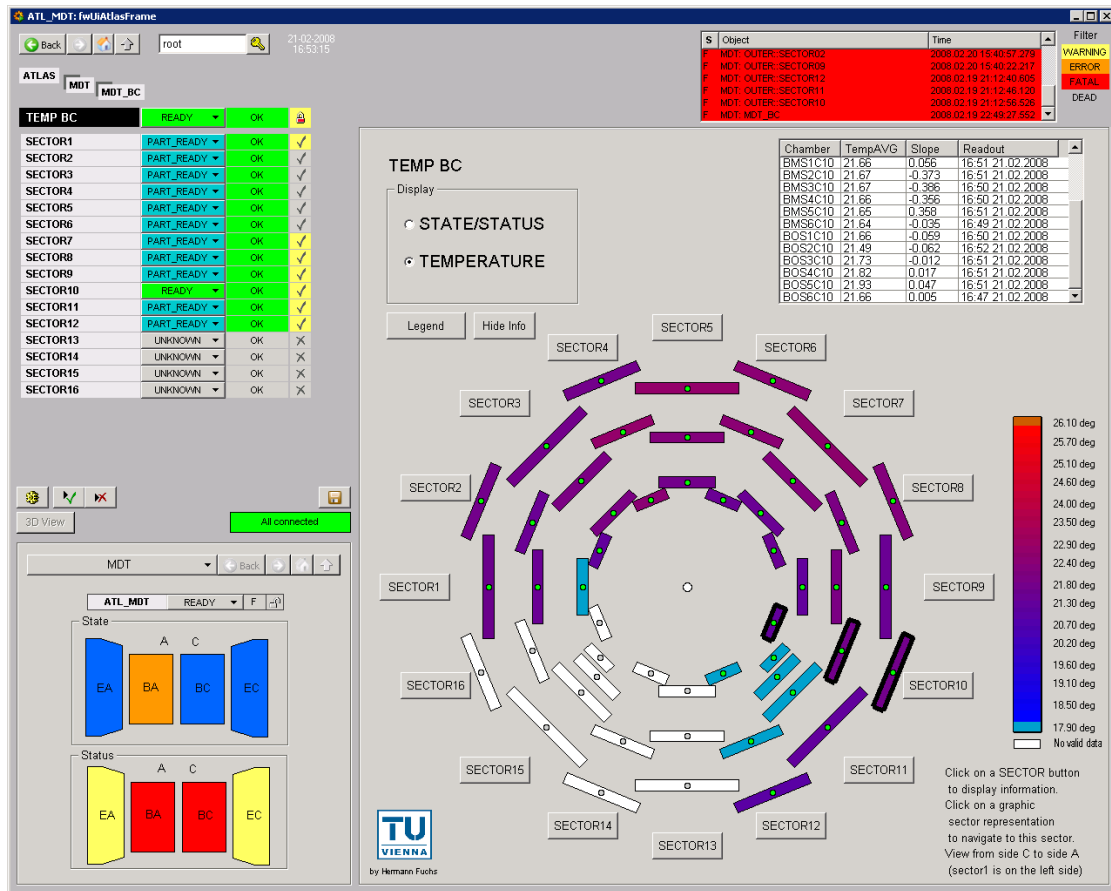


Figure 5.6.: Screen shot of the ATLAS FSM screen, showing a part of the MTM system. On the left side the FSM informations can be found. The panel on the right and the small panel in the lower left corner show more detailed information using PVSS panels. On the upper right part, all FSM objects which demand investigation are shown.

### 5.4.5. ATLAS Detector Control System

The ATLAS Detector Control System (DCS) Back-End is organised in three functional layers (Fig. 5.7). The full control hierarchy is based on the ATLAS FSM implementation. Basically, the detector is broken down into FSMs which in turn are controlled by other FSMs. At the level of Device Units, functional detector elements (e.g. MDT chambers) are foreseen. The detector elements level was chosen, because splitting down these elements further (e.g. to the tube level) would unnecessarily increase the complexity and size of the FSM implementation, while not providing significantly more information. Information below the DU level can only be accessed using the PVSS panels. The DU level is also the lowest level which can receive FSM commands. Therefore it has to be assured, that all commands are correctly sent to the hardware [23].

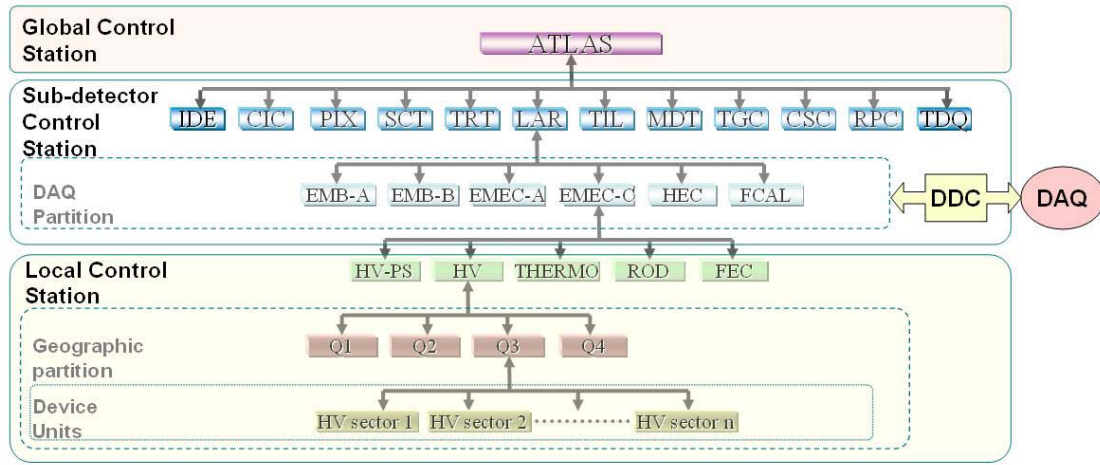


Figure 5.7.: Diagram of the ATLAS FSM Architecture [23]

#### Global Control Station

The Global Control Station is in charge of the overall detector operation. It provides high level monitoring and combines the control of all sub-detectors. All data processing and command execution is handled at lower levels.

#### Sub-detector Control Station

The Sub-detector Control Stations (SCS) form the middle layer. The SCSs allow for full and independent local control of the sub-detector.

At the SCS level the sub-detector is divided in data acquisition (DAQ) partitions which have to follow the hardware readout schema (DAQ TTC partitions). At this level the synchronisation between the detector control system and the physics data taking, using the DAQ-DCS software package, takes place. States of the DAQ partitions are reported

to the DAQ system, which may in turn issue commands which have to be followed by the SCS.

### **Local Control Station**

The lowest level of the ATLAS Detector Control System hierarchy is represented by Local Control Stations (LCS). The LCSs handle the low level control of the hardware and corresponding services of the sub-detector. Each LCS is in charge of a special sub-detector system (e.g. power supplies, gas...). The LCS structure itself is divided into sensible geographical or functional entities. The MTM project forms a LCS.

## **5.5. Database**

Within the ATLAS DCS data has to be easily accessible. It is not only necessary to have hundreds of sets of configuration data for each sub-detector readily available, but also the monitored values have to be stored. Therefore ATLAS DCS relies heavily on databases.

A database is a hard- and software based system, which combines an efficient storing and sharing of data. It contains logically related sets of data. Using queries, it is possible to select, combine and retrieve sets of data. Most commonly these queries use the Structured Query Language (SQL) [33], [34].

### **5.5.1. Database models**

There are various different techniques to efficiently organise data using different data structure models. The most common are the following:

- Hierarchical model: Data is organised in a tree like structure. Each record contains an upward link to the parent folder and a sort field to order records on the same level.
- Network Model: Records are stored with links (pointers) connecting it to other records.
- Relational Model: Data is organised in tables. Multiple tables are related to each other.

Relational database models are used within ATLAS, therefore an overview of this database model will be given.

#### **Relational model**

The basic structure of the relational data model is the table. In a table, data is represented using columns and rows. Columns define the data structure within the table,

while the actual data is contained in the rows. One record belongs to one row. The ordering of rows within the table is of no relevance. Furthermore, there can be no identical rows within the table.

Tables can contain single columns (attributes) or a set of columns which act as a key, which is then used to uniquely identify rows (data) within the table. A set of tables can be related to each other.

A relational database contains multiple tables. In theory whenever a value within one table reoccurs in another table, a relation between this two tables can be made. There are different kinds of relations between tables:

- **1:1** One value in one table corresponds to one value in another table.
- **1:M** One value on one side corresponds to a multiple number of values in another table.
- **M:M** Multiple values on both sides correspond to each other.

Data can be retrieved from a relational database by sending a query. The database answers to such a query by returning a list of rows, containing the data. A SQL query can contain complex calculations and/or filtering of data. Furthermore, it allows the user to access multiple tables and combine the results.

In order to increase the performance of SQL queries and thereby improving the speed of data retrieval, columns, or sets of such, can be indexed.

### **5.5.2. Database usage in ATLAS**

The database system used by ATLAS DCS is the Oracle database system, developed by the homonymous Oracle Corporation. It is based on the relational database model. The Oracle database system combines a software application along with data storage, usually called an Oracle database server. Interactions with the database rely on the Structured Query Language (SQL).

Throughout ATLAS various database variants, based on the Oracle database, exist. The main differences lie in the table structures, the relations between tables and the customised restrictions on the tables.

- **COOL:** The offline analysis tools are based on the Athena project. Athena is a software framework, which uses a special database format, called COOL. COOL is basically an Oracle database with very restrictive table structures and queries.
- **PVSS ORACLE:** Most of the online detector control systems use the PVSS internal mechanism to archive data into a PVSS Oracle archive. This database type is intended for the storage of measurement data. However, while being an Oracle database, this mechanism generates a table structure, which is extremely difficult to access outside from a PVSS project.



- **JCOP ORACLE:** The JCOP alliance introduced a configuration database based on Oracle. The intention of this configuration database is to provide an easy way to set configuration data within a PVSS project. Similar to the PVSS Oracle archives, these Oracle tables are extremely difficult to access from outside of a PVSS project.
- **ORACLE USER TABLES:** Standard Oracle database using user tables are very common as well.

### **5.5.3. Security**

The ATLAS security requirements foresee a complete separation of the DCS network and its storage facilities from the CERN general purpose network. This is a security precaution to ensure a safe and undisturbed detector operation. The planned separation of the networks makes it impossible to access data from the control room which is not located within the ATLAS network.

Therefore all data necessary for the operation of the experiment has to reside in the ATLAS online database, in order to be accessible from the control room.

All data used by the MTM system resides in the ATLAS online database with a duplicate in the offline database server which is updated using Oracle streams.

## 6. Muon Temperature Monitoring project

### 6.1. Scope

In this section the Muon Temperature Monitoring (MTM) Project is described, which was the subject of my diploma thesis. The scope of the MTM project, is to provide an efficient temperature surveillance of the ATLAS monitored drift tube (MDT) chambers. It is part of the ATLAS detector control system (DCS) and designed to run in the ATLAS control room.

The MTM project takes advantage of common ATLAS DCS development tools and development strategies. It is written in PVSS, with the majority of the user interface implemented in the ATLAS Finite State Machine (FSM) interface.

The operator can choose between various panels, providing an overview of the state of the MDT chamber temperature monitoring and of the respective chamber temperatures themselves. In addition, a temperature overview panel is available which provides a quick overview of the temperature distribution within the MDT system.

Specialised expert panels can be used by trained detector experts to quickly pinpoint faulty devices and debug the MDT system.

The MTM project uses a PVSS distributed system to collect the temperature data. After sorting and analysing the data, temperature gradients are exported to COOL and the temperatures of the MDT chambers are displayed.

### 6.2. Data flow

The data flow of the MTM project can be subdivided in the following steps (Fig. 6.1):

**Collect data:** Measurement data is collected from 11 different PVSS-based readout servers. The actual readout of the temperature sensors is done by the ATLMDTMDM system which is distributed over eight servers and the alignment system (ATLMDTLWDAQ01). Only a small fraction of the temperature sensors ( $< 0.25\%$ ) is read out using the latter system. The majority of the temperature sensors is read by the ATLMDTMDM system. Furthermore, the state of the low voltage feed is determined by querying the ATLMDTPS power system which is distributed on two servers.

**Mapping:** Using configuration data from the database, the measurement data received from the source systems is translated from readout channels to the corresponding temperature sensors.

**Flagging:** Automatic checks are carried out to determine the validity of the measured temperature values. A central flag database returns already known faulty sensors. Then these sensors are flagged as faulty. Additionally, the resulting temperatures are checked to detect further faulty sensors.

**Raising alarms:** Using the alarm limits retrieved from a database, the temperature values are checked. If temperature values are above these thresholds, alarms are raised and the shifter is informed visually.

**Calculate temperature gradient:** The temperature gradient along the MDT chambers is calculated.

**Display:** The temperature values are displayed.

**Export:** Using the PVSS archiving, the temperature gradients are exported to COOL.

The steps mentioned above are realised using a combination of control scripts, dp-Functions and alarm configurations described below.

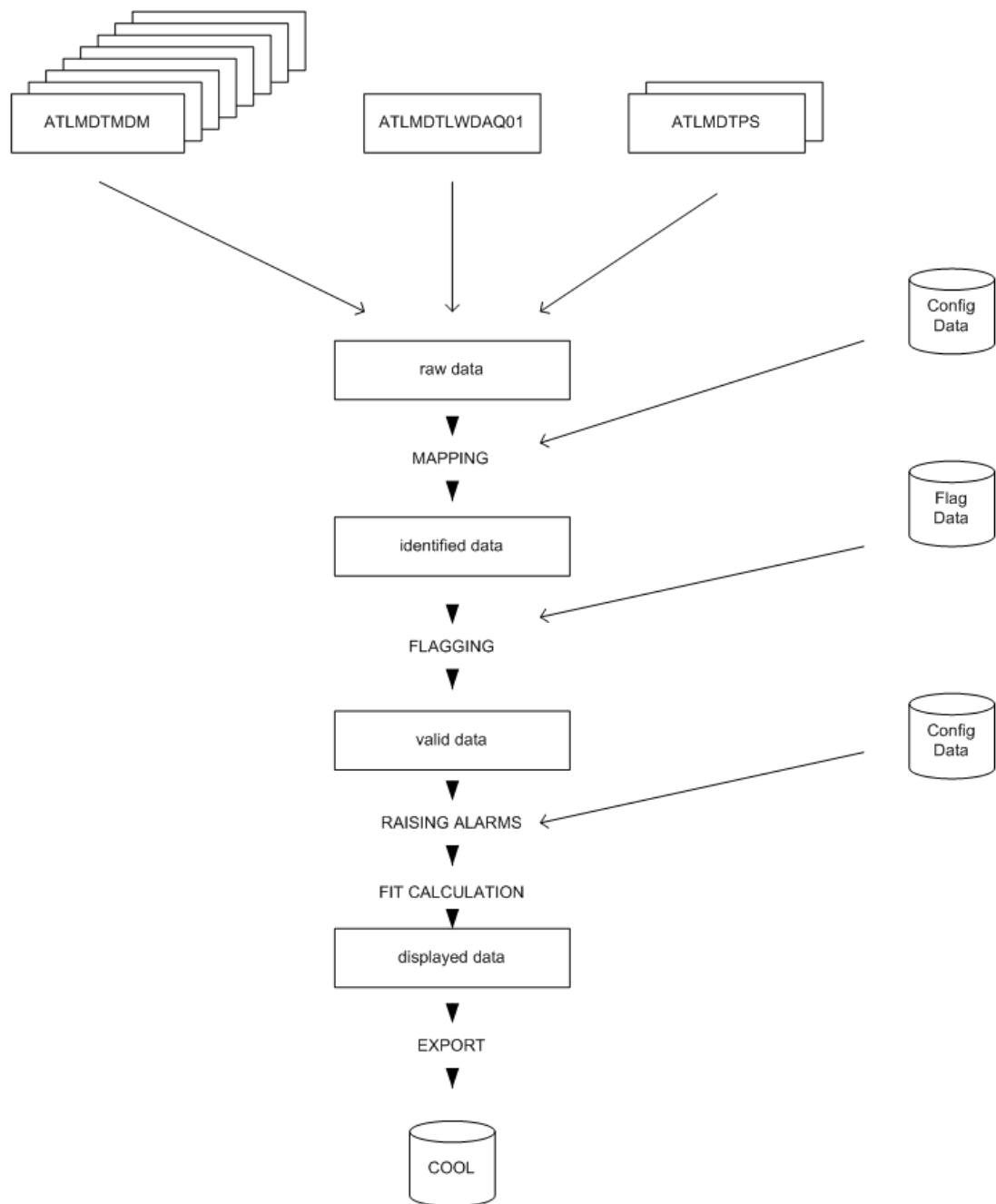


Figure 6.1.: Simplified data flow of the MTM project

## 6.3. Data collection

The MTM system collects configuration and measurement data using PVSS control scripts. In the following all control scripts used by the MTM system will be described. Control scripts contain code written in the scripting language CONTROL. Such scripts are executed in distinct PVSS control managers. All scripts of the MTM project use a special function called `timedFunc` to execute code at defined intervals. To increase the reliability, the MTM project uses three separate control scripts:

- Collect data script
- Update script
- Timeout script

### 6.3.1. Collect data script

The control script `mdtMtmCollectDataScript.ct1` (Fig. 6.2) imports the current temperature data and performs initial processing. The imported values include temperatures, their corresponding readout timestamps and validity flags, the readout state of the MDT chambers, and the state of the low voltage feed.

The data is collected from 11 distributed PVSS systems (Tab. 6.1). Due to the fact, that most of the data is measured by the ATLMDTMDM project, it was decided that the `mdtMtmCollectDataScript.ct1` uses the same collection interval as the ATLMDTMDM project.

The data collection itself is divided in several distinctive and largely independent steps. Each readout system is checked by separate threads, such that all readout systems can be read in parallel, thereby minimising data collection time. Different temperature sensor types and different readout projects use different data point structures, requiring individually adapted functions. It was aimed to keep the tasks and checks of these functions as similar as possible.

- *Check the availability of the source project:* A check is executed to determine whether the source project is available and accessible from the MTM project.
- *Get the chamber list read out by the source project:* Connects to the data points of the readout system and determines the chambers which are read out by this system.
- *Check if chamber exists in the MTM project:* Checks whether this chamber exists and therefore should be read out in the MTM system.
- *Compile the data to be copied:* Determines which data is to be copied and prepares the actual data copy.
- *Copy the data en bloc:* In order to increase copying performance, data is copied en bloc.

- *Check data integrity:* Confirms the integrity of the copied data (data missing, corrupted...).
- *Map data to temperature sensors:* Data copied from the source project is only related to channels. This function connects the correct channel with the corresponding temperature sensor.
- *Check the validity of the data:* Determines whether the data is valid, and should be used (e.g. if the readout of the chamber was deactivated, received data can not be correct)
- *Get list of known faulty sensors:* Queries the database for a list of known faulty temperature sensors.
- *Mark (flag) non working temperature sensors:* With the help of the report of already faulty temperature sensors, an algorithm determines the operation state of the temperature sensors and marks them accordingly. If new faulty sensors are found, they are reported to the database. This algorithm is described in more detail in Chapter 6.5.3.

Table 6.1.: Systems accessed by Collect data script

Project Name	Proj Nr.	Data Read	Source
ATLMDTLWDAQ01	105	Temperature data	Alignment system
ATLMDTMDM1	191	Temperature data	MDM boxes
ATLMDTMDM2	192	Temperature data	MDM boxes
ATLMDTMDM3	193	Temperature data	MDM boxes
ATLMDTMDM4	194	Temperature data	MDM boxes
ATLMDTMDM5	195	Temperature data	MDM boxes
ATLMDTMDM6	196	Temperature data	MDM boxes
ATLMDTMDM7	197	Temperature data	MDM boxes
ATLMDTMDM8	198	Temperature data	MDM boxes
ATLMDTPS2	102	Low voltage feed	Power system
ATLMDTPS3	103	Low voltage feed	Power system

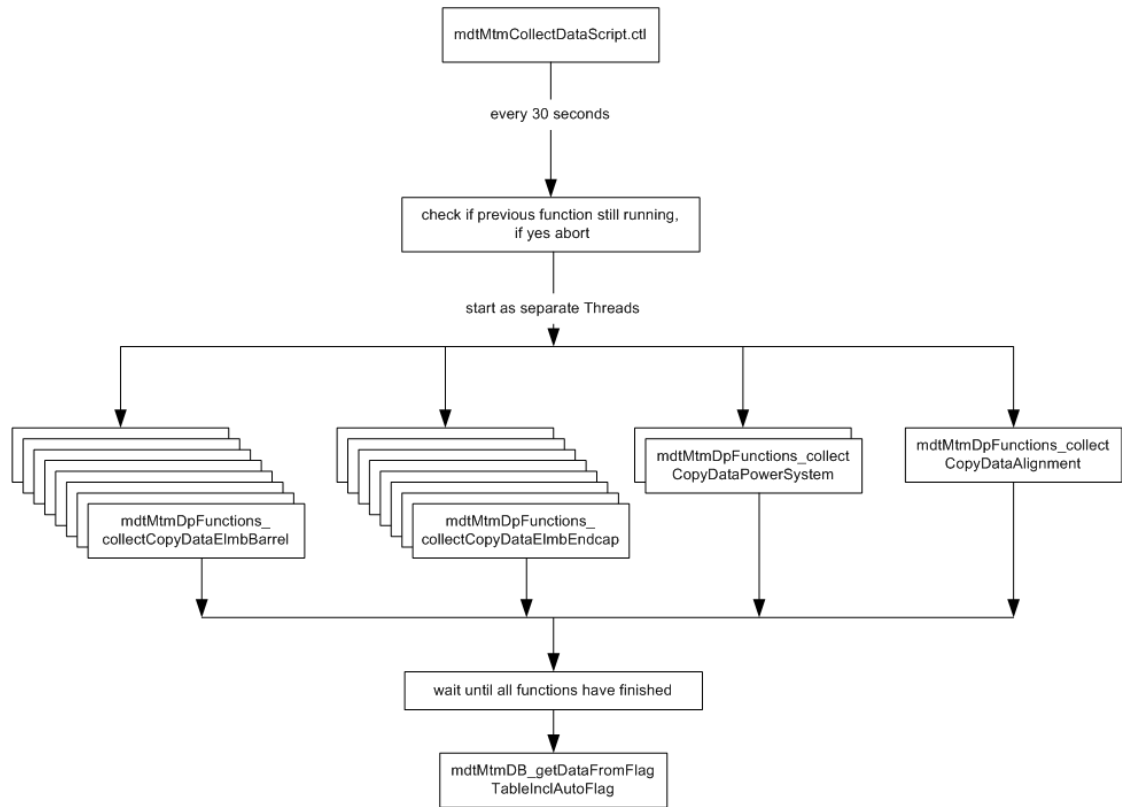


Figure 6.2.: Working schema of the script `mdtMtmCollectDataScript.ctl`, which collects data from 11 different systems

### 6.3.2. Update script

Although the data flow diagram indicates frequent checks in databases, the configuration data is virtually constant. In order to increase performance, it was decided to store this configuration data within the data point structure of the MTM project, and use this stored configuration for most of the calculations. The stored configuration data is updated at regular intervals with the values retrieved from the database, using the control script `mdtMtmDbUpdate.ctl`. An update interval of several hours was chosen in order to minimise the load on the database while still providing optimal data validity. Three different database tables have to be accessed:

- *Temperature sensor configuration:* Specific temperature configuration data (calibration parameters, temperature sensor positions...) is queried from the table `T_SENSOR_INFO` and applied at the data point elements.
- *Chamber configuration:* Configuration data specific to each chamber (chamber APIN, position, rotation...) is applied based on data queried from

T\_SENSOR\_CHAMBER.

- *Alarm threshold:* Chamber specific alarm thresholds for a given operation mode (PHYSICS, STANDBY...) are queried from T\_SENSOR\_ALARM, T\_SENSOR\_ALARM\_GROUP and T\_SENSOR\_ALARM\_GROUP\_LIST and applied to the corresponding data point elements.

### 6.3.3. Timeout script

The task of the `mdtMtmTimeoutCheck.ct1` script is to determine whether temperature sensors have been read or not. The script accesses the readout timestamps and calculates the seconds elapsed since the last readout. In order to have additional redundancy it was decided to make this check a separate control script. That way, crashes of readout systems or a malfunctioning data collection script can be detected easily. This script runs at the same regular intervals as the data collection script.

## 6.4. Data mapping

During the actual readout process each temperature sensor is only identified by its corresponding channel.

Therefore a mechanism had to be developed which automatically translates the temperature sensor address from the readout systems, based on the readout channels, to the MTM project identifier based on the temperature sensor name. This mechanism is called mapping.

A readout channel corresponds to the specific connector on the MDM box the temperature sensor is plugged in (see Chapter 4.3.2). A wiring map, specifying the readout channels of the temperature sensors has been prepared by the chamber builders. Using this wiring map, it is therefore possible to identify the temperature sensors by their corresponding channel.

A major point of consideration was the flexibility of the mapping system. During construction, all temperature sensors were connected to specific readout channels defined by the chamber builders. However, during operation it might be necessary to change the channel allocation (e.g. due to faulty hardware).

Therefore a database based mapping was chosen. Using specially designed Oracle database tables<sup>1</sup>, the temperature sensor names are linked with the corresponding readout channels. Each time new data is queried from the readout system, all temperature values are stored in temporary data point elements. The T-Sensor mapping algorithm accesses the actual channel-temperature-sensor-ID correlation in the database and determines the correct identifier for each temperature value. Invalid data (e.g. in case of data from channels with no attached temperature sensors) is automatically disregarded. After identifying the corresponding temperature sensors, the temperature

---

<sup>1</sup>More details on the used database structure can be found in Chapter 6.7.



values are copied to their final data point elements. All further calculations access only the identified temperature data.

## 6.5. Data evaluation

### 6.5.1. Data Point Functions

The MTM project uses two distinct dpFunctions. An instance of both is attached to each single chamber, giving a total of 2236 dpFunctions.

#### Evaluation of operating conditions of a chamber

The full name of the data point function used is `mdtMtmEventManager_combinedFsmAlarmAndWorking`. It is evaluated every time when temperature or flagging data is updated. The function calculates the number of valid (not flagged) temperature sensors which are in warning, error or fatal range.

Furthermore, it evaluates how many percent of the total number of temperature sensors per chamber are working, the so called percentage of working sensors. This percentage does not take into account sensors which are known to be dead. On average there are 12 temperature sensors per chamber. It is obvious that the values of the temperature sensors on the same chamber should agree within a few degrees. For example, an obvious case of a malfunctioning sensor is when 11 sensors report 22° Celsius while one sensor reports 350° Celsius. Another case might be a miss-calibrated sensor which has an offset of a few degrees.

Obviously a single sensor is not enough in order to determine if the temperature of a chamber is out of the normal operating range. Therefore a percentage of sensor agreement is calculated. This percentage indicates how many sensors of the chamber agree that the temperature is out of the normal operating range.

#### Calculation of fit parameters

The internal name of this data point function is `mdtMtmEventManager_calcAndWriteLinFitParameters`. It was determined that a reasonably good, but not necessarily the best description of the temperature distribution within a MDT chamber with the given number of sensors, is a linear distribution along the tubes (x-axis). Therefore it was decided to calculate and store the temperature gradient and average temperature per chamber using an established linear fit algorithm. Additional to this, linear fits are done separately for each multilayer and the cross-plate layer. More information on the difficulty of finding a reasonable description of the temperature distribution can be found in Chapter 6.5.4.

### 6.5.2. Alarm handling

All alarms raised in the MTM project correspond to the FSM STATE and STATUS. Therefore alert definitions are usually configured on the same data point elements which

are used by the FSM evaluation. Monitored are data point elements indicating whether the chamber is read, the temperatures have been updated, the temperatures are in warning, error or fatal ranges, a sufficient number of sensors is working, the sensors agree whether the chamber temperature is out of normal operating conditions and whether the values are archived.

All alerts raised by a PVSS project, connected to the central DCS, will be displayed on the ATLAS alarm screen. A huge number of alerts would quickly fill up this alarm screen. Therefore it is necessary to have an efficient alarm reduction mechanism. This is realized using internal PVSS Summary Alerts (see Chapter 5.3.5). In case of the MTM project, all summary alerts are defined with a threshold limit of five, that means if more than five alerts of the same type appear, they will be suppressed. Summary Alerts have been defined on a partition basis.

All configured alerts of the MTM project can be found in Appendix B.

### 6.5.3. Flagging system

The ATLAS experiment is scheduled to run more than 10 years [9]. The construction of the detector has been done with utmost precision and care. Despite the frequent quality controls and durability tests, it is inevitable that some components (e.g. power supplies) fail over time. While some of the detector parts can and will be replaced over the lifetime of the experiment, others won't.

Most of the temperature sensors on the MDT chambers are glued to their respective position, making them very difficult to replace.

It is not currently foreseen to replace temperature sensors. As a consequence the Muon Temperature Monitoring project will have to cope with faulty temperature sensors. In order to do that, a standardised flagging system has been developed to mark defective sensors [35]. Currently three other MDT projects are using the same flag definitions (MDTMTM, MDTELTX, MDTBMON) defined in the following.

#### Faulty sensors

Faulty sensors will normally have one or a combination of the following faults:

- *Noisy*: A sensor reports only noise and no useful data.
- *Dead*: A sensor does not report any value.
- *Miss calibrated*: Values reported by a sensor contain an offset, or need to be calibrated in order to be correct.

#### Flag definitions

A flag contains information on the working condition of a device (e.g. a temperature sensor), some information why it has been flagged and information who issued that flag and when. Such a flag is attached to each component or device.

A flag contains all information stated in Tab. 6.2. The operating conditions (Tab. 6.3) of a flag differ in some points from the ones mentioned before (Chapter 6.5.3). This is due to the fact that the flag definition has been created for maximum flexibility in order to be able to use this definition in other projects and with other devices as well [35].

Table 6.2.: Contents of a flag [35]

Flag Component	Data Type	Description
Flag state	Integer	Working condition of the device. A detailed list of allowed integers can be found in Tab. 6.3.
Flag info	String	Details why this flag has been set
Since time	Timestamp	Start of validity for this flag
Until time	Timestamp	End of validity for this flag
Flag system	String	Through which system the flag has been set
Flag source	String	Person or system which authorised the flag
Flag parent element	String	Parent structure the device belongs to

Table 6.3.: Flag states [35]

Flag State	Displayed	Description
0	OK	Device is working normal
1	DECLARED DEAD	Device has been declared dead by an expert
2	DUBIOUS	Data from this device can not be trusted
3	NO RESPONSE	Device has not been responding for some time
4	RECALIBRATION NEEDED	Device needs to be recalibrated or renormalised

All flags are stored in a central database, the ATLAS CONDITION DB (ATONR) and are only exchanged through this repository, ensuring that all systems using standardised flags have coherent and correct flag information. While the user or system accessing the database will see complete and readable flags, the database tables themselves are divided in order to optimise performance. This is possible by using database procedures which are customised to the need of the individual projects, however, accessing the same database tables. More details on the database structure can be found in [36].

## **MTM flagging system implementation**

The MTM project uses a simple dead band algorithm to detect faulty sensors. Whenever the value of a temperature sensor is out of a given valid range, the sensor will be flagged automatically as defective. Furthermore, previously known issues and flags from other systems (such as the readout system itself) will be read from the database and taken into account. An expert can then take a closer look and decide what to do with this sensor.

### **6.5.4. Temperature gradient fit**

One of the aims of the MTM project was to provide data which can be used for further analysis and for the calibration centres. Calibration centres do not need the granularity given by the single temperature sensors, therefore it was decided to export only a parametrisation of the temperature distribution within the MDT chambers. This helps to reduce the necessary data volume needed to transfer.

Four separate temperature gradients are calculated, one for each multilayer and the cross-plate, and a global chamber temperature gradient using all temperature sensors of the chamber. As mentioned in Chapter 4.4.1 a two dimensional linear fit algorithm was chosen to calculate the temperature gradients. In case a more detailed parametrised temperature distribution is required it can easily be changed.

## **6.6. Data export**

To reduce the strain on the databases it was decided, that the MTM project should export as little data as possible. Therefore the MTM project exports only the temperature gradient fit to be used for off-line analysis and the calibration centres (Chapter 4.4.1)

Offline analysis groups use the Athena framework. Part of this framework is a specialised kind of database called COOL (Chapter 5.5.2), making it necessary to export the data into the COOL database. PVSS provides us with an easy way to store values from a data point into an Oracle database. Due to the fact that COOL is some kind of an Oracle database, it was decided to use a two step approach. Using PVSS internal functions, the temperature gradients are taken from their respective data points and exported into an Oracle database. An external task is executed at regular intervals to convert data from the Oracle database into the COOL database. This task is a new component under development by the JCOP framework. The MTM project was one of the first projects to integrate the first stable development version into the MTM project, providing valuable data for the MDT community and valuable feedback for further development.

## **6.7. MTM project database usage**

In the early stages of this project, it was already clear that a lot of configuration data had to be stored. For each temperature sensor a number of configuration parameters

have been collected. This included coordinates, location, calibration constants, readout channels, alarm levels...

It was decided, that this data should be stored in a way which would enable other ATLAS DCS projects and even offline analysis tools to access this data.

While the COOL database might have been a good storage place for the offline analysis, it would have been nearly impossible to read the data using any PVSS based DCS project. For the opposite reasons, it was not possible to use the PVSS Oracle archive either. Being an ATLAS DCS project, the logical choice of storage would have been the JCOP configuration database. While this is an excellent way to quickly access data using a PVSS project, the special table structures and identifiers make it very hard to access it using offline analysis tools. A special translation step would have been required.

After long evaluation a compromise was reached. In order to enable everyone to easily access the data, it was decided to store the configuration data in standard Oracle user tables. Although the data is not exported into the COOL database, the chosen storage format does make it easy to do so if necessary.

Another issue was the availability of the configuration data. The MTM project is an online detector monitoring system, designed to be used in the ATLAS control room. The ATLAS security requirements foresee a complete separation of the detector control system and its storage facilities from the CERN general purpose network.

Therefore all necessary data has to reside in the online database in order to be accessible from the control room. However, while this works fine for all DCS projects, the access for offline analysis tools would have been impossible. The following solution was adopted: While the data remains on the online database, inaccessible for the offline analysis, the data will be replicated to another database server, available on the CERN general purpose network. This is realised using a replication technique called an Oracle stream.

Further information on the database use of the MTM project, can be found in [37].

### **6.7.1. Database tables**

Using the input of other DCS projects and the offline requirements, a data model has been developed specifically for the MTM project [37]. Following this data model, a set of Oracle user tables have been created (Tab. 6.4). This set of tables can be broken down into four subsets, dealing with temperature sensors configuration, MDT chamber information, alarm configurations and history values.

### **6.7.2. Views**

Oracle databases offer the possibility to compile data using views. A view is a virtual table. It behaves like a real table, but contains data which is calculated and compiled every time the view is accessed.

Table 6.4.: Database tables used for configuration data by the MTM project

Database table	Content
T_SENSOR_INFO	Informations related to single temperature sensors
T_SENSOR_MAPPING_SCHEME	Lists the different naming schemes for temperature sensors
T_SENSOR_MAPPING_NAMES	T-Sensor designations in different naming schemes
T_SENSOR_INFO_HISTORY	As soon as new configuration data is entered, the previous configuration data is archived here
T_SENSOR_CHAMBER	Information related to MDT chambers
T_SENSOR_ALARM	Alarm level definitions
T_SENSOR_ALARM_GROUP	Alarm modes (PHYSICS, CALIBRATION...)
T_SENSOR_ALARM_GROUP_LIST	Alarm thresholds

The data model of the MTM project contains only one view `T_SENSOR_INFO_GLOBAL`. It was created to suit the specific requirements of the offline analysis group. This view contains all information of the table `T_SENSOR_INFO` and additionally the calculated global positions of each temperature sensor using the ATLAS coordinate system.

### 6.7.3. Triggers

In order to perform user defined actions whenever data is removed or inserted, Oracle databases offer a trigger mechanism. The actions executed when such a trigger occurs are defined using SQL commands.

Within the MTM project database tables, triggers are used for three tasks. First of all, whenever a new row is inserted, a trigger generates a unique key. Whenever information is changed within the tables, a trigger automatically updates the field indicating the latest change to the current date. Finally, as mentioned before, a table exists which contains history data. Whenever calibration data is edited, the previous calibration data is marked with a time stamp and stored within the `T_SENSOR_INFO_HISTORY` table, providing a history of changes for the most sensitive parameters.

## 6.8. FSM structure

### 6.8.1. DAQ partitions for the MTM system

Following the ATLAS FSM integration guidelines [23], which requires all sub detector control systems to follow the DAQ partitions, the MTM project FSM structure has been split into four partitions.

The Barrel has been divided into two distinct partitions BA and BC. BA stands for Barrel side A and consists of half of the barrel from the interaction point upstream (side A), while BC is the abbreviation of Barrel side C and covers the downstream half of the barrel. Following the same convention, the end-cap is divided into two partitions (ECC and ECA) as well. Like in the barrel partitions ECC represents the C side of the end-cap (all four wheels situated on side C) while ECA stands for side A.

While in general the DAQ partitions follow the geographical sections of the detector, there are a few exceptions (Tab. 6.5). The most prominent exceptions concern chambers situated around the interaction point ( $z = 0$ ). According to naming conventions (Chapter 4.1) these chambers belong to detector region B. As this region contains only two chambers located in sector 12 and 14, no separate DAQ partition has been made. By convention all chambers of region B belong to the DAQ partition BA.

Furthermore, in the overlap region between the barrel and the end-cap, a few barrel chambers, namely chambers of type BIS7 and BIS8, are read out through the end-cap system. Therefore these chambers are part of the end-cap partitions.

Table 6.5.: Chambers in the DAQ partitions, not following the standard classification

Chamber	Partition	Comment
BOG0B12	BA	Chambers of side B belong to the DAQ BA partition.
BOG0B14	BA	Chambers of side B belong to the DAQ BA partition.
BIS7A	ECA	These chambers are read out using the ECA partition.
BIS8A	ECA	These chambers are read out using the ECA partition.
BIS7C	ECC	These chambers are read out using the ECC partition.
BIS7C	ECC	These chambers are read out using the ECC partition.

### 6.8.2. FSM tree

The FSM tree of the MTM project is shown in Fig. 6.3. The four DAQ partitions form the only four control units of the MTM FSM tree because it was not considered necessary to independently operate smaller parts of the temperature monitoring system (e.g. only one sector of an end-cap wheel).

Below the end-cap partitions, the four end-cap wheels are represented using Logic units. Under the individual end-cap wheels, further Logic units, representing the 16 sectors, are located. Finally, below the sectors the appropriate device units (chambers) are situated. As the barrel does not have an additional superstructure like the end-cap wheels, the sector level is attached directly below the barrel partitions.

Each chamber is represented by a device unit. The individual sensors mounted on the chamber (on average 12) are not represented in the FSM structure. Operators requiring this level of granularity have to use the PVSS panels included in the ATLAS FSM implementation [22] [23].

In the following the FSM units of the MTM system will be discussed.

In total, the FSM tree of the MTM project consists of:

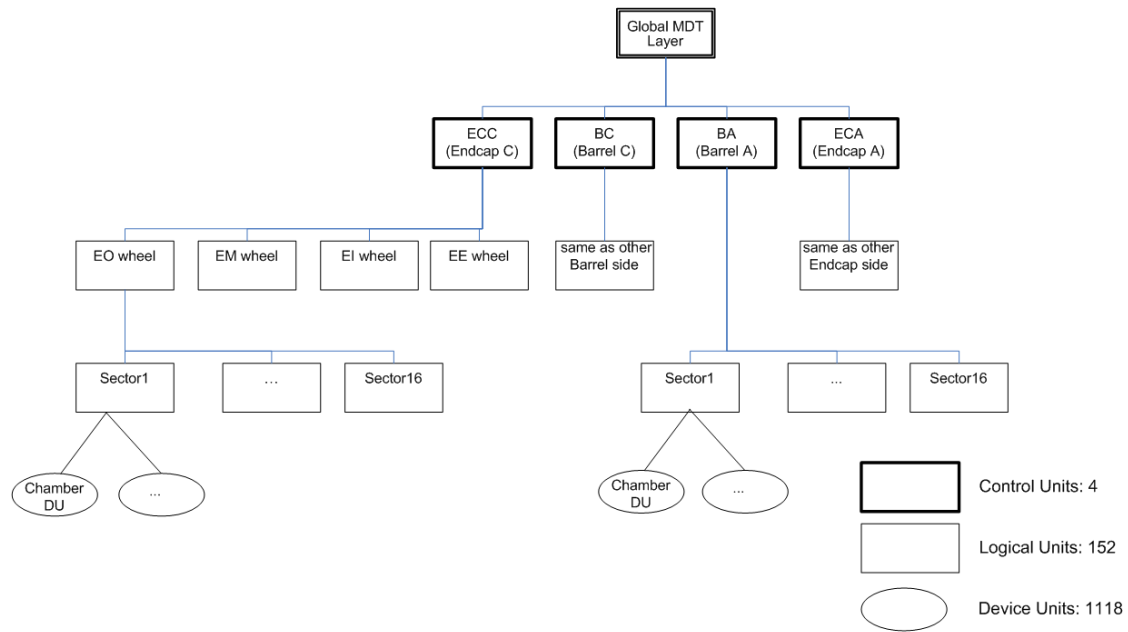


Figure 6.3.: FSM tree structure of the MTM project

- 4 Control Units: DAQ partitions
- 152 Logic Units: wheels and sectors
- 1118 Device Units: MDT chambers

### Chamber Level - Device Unit

A device unit, representing a single MDT chamber, is the fundamental unit of the MTM FSM tree. The STATE and STATUS evaluations are based on values of the corresponding data points and therefore recalculated whenever new data is received. However, while it is expected that STATE and STATUS of a temperature monitoring project are quite stable, data is updated at regular intervals. This would lead to frequent recalculations of the FSM states. Whenever a FSM state is re-evaluated, no matter if the state changes or not, the resulting state will be transmitted to the parent, causing it to re-evaluate its state as well. In order to avoid unnecessary evaluations, a suitable course of action was sought to limit state evaluations to situations when it is likely that a state change is the probable outcome of the evaluation.

Using the PVSS integrated alert handling, a solution to this problem was found. The main idea is that alerts serve a similar function as FSM states, which, provided a suitable alarm configuration, should change at the same time as the FSM states. For example,



when the chamber temperature becomes critically high an alarm is issued, while at the same time the FSM state reflects this condition as well. It should be sufficient to link the FSM states to the alarm handling, but sometimes additional factors have to be included in one of these two (either alarm handling or FSM evaluation).

Therefore within the MTM project the re-evaluation of the FSM states is triggered by alerts, but not governed by it. The actual evaluation of the FSM state is independent of the alarm handling, giving the possibility to take additional parameters into account. All alarm handlings of a device unit are combined to be used as a trigger. The actual triggering is done using a dpFunction which connects to all alarm handlings. Whenever an alarm is issued, the dpFunction causes the FSM state to be re-evaluated, while the state evaluations themselves are completely independent. A list of all defined STATES (Tab. A.1) and STATUS (Tab. A.2) conditions can be found in Appendix A.

### **Sector Level - Logic Unit**

The logic unit (LU) of type Sector is the lowest LU level of the MTM FSM tree, directly above the device unit (DU) level. It groups the DUs belonging to the same sector together and has the same STATE and STATUS states as the DUs below. Due to the fact that LUs are abstract objects, their STATE/STATUS evaluations are based on a logic decision using only the STATE and STATUS objects of the DUs as input. A list of all defined STATES (Tab. A.3) and STATUS (Tab. A.4) states can be found in Appendix A.

### **Endcap Wheel - Logic Unit**

The logic unit of type end-cap wheel exists only for the end-cap partitions and is located above the sector level, grouping the sector LUs and DUs belonging to the corresponding wheel. The STATE (Tab. A.5) and STATUS (Tab. A.6) evaluations are very similar to the sector LU. More information can be found in Appendix A.

### **Partition Level - Control Unit**

The topmost level of the MTM FSM tree consists of control units. As the FSM layers above do only accept ATLAS standard STATE and STATUS states, the partition CU does the 'translation' between these states.

The only non standard state the MTM FSM uses is PART\_READY to provide a more finely structured monitoring. The partition CU translates all PART\_READY states to READY. The full list of STATE (Tab. A.7) and STATUS (Tab. A.2) states can be found in the appendix.

### **6.8.3. Performance considerations**

Tests have been done to evaluate the ATLAS FSM implementation [23]. Owing to the DIM protocol used for communication between FSM objects, FSM trees are not bound or limited to one machine. Therefore, if the FSM tree is spread over multiple systems,

the size of the FSM tree does not seem to be limited.

However, this does not eliminate performance bottlenecks on single machines. In order to facilitate the design a robust hierarchy with adequate performance, recommendations on the maximum number of FSM elements are given (Tab. 6.6) in the ATLAS FSM integration guidelines [23].

Object Type	Recommended Limit
Control Unit	50
Logic Unit	500
Device Unit	1000

Table 6.6.: Recommandatations on the number of FSM elements per PVSS PC [23]

Comparing the recommendations with the actual number of FSM elements used by the MTM project some potential problems can be seen. The number of device units within the MTM FSM tree exceeds the recommended number of device units by 11 %. This excess is balanced by going below the other recommended limits. Furthermore, these recommended limits depend on the actual PC hardware. Using a eight-core server with 8 gigabyte of RAM as in the MTM project, these limitations should be less severe. This is supported by intense performance tests done with the final MTM FSM tree that have not unveiled any performance problems under any operating conditions.

#### 6.8.4. FSM STATE and STATUS

The project is a pure monitoring project, therefore no FSM actions need to be issued or accepted. This simplifies the FSM design considerably, as states do not need to be checked for possible incompatibilities with commands. Following ATLAS standards, all STATE and STATUS states are written in capital letters. In the MTM project FSM STATE and STATUS have two different functions. FSM STATES display the operation conditions of the temperature sensors, while the FSM STATUS represent the temperature of the MDT chambers. Further details can be found in Appendix A.

### 6.9. User Interface

An essential element of a monitoring system is its user interface. It has to provide an efficient and easy-to-use overview of the whole system. In the following the user interface of the Muon Temperature Monitoring (MTM) project and its underlying structure will be described. As a part of the necessary features, such as alarm handling is already provided by the PVSS software suite itself, the focus lies on the FSM panels and objects the shifter interacts with. The FSM monitoring is designed to be used as a standard control and surveillance system. It is optimised to provide all functionality needed on a regular basis for the shifter in the ATLAS control room.

### 6.9.1. Chamber Panels

The User Interface (UI) on the chamber level consists of a set of three panels (main, more info and flag panel), which display information for selected chambers. It allows the user to get information about the chamber, to interact with the MTM system.

In order to increase readability of the MTM panels, the default FSM panel is removed, displaying only the embedded MTM specific panels in all the following figures. Switching between the three panels is possible by pressing the selection buttons in the lower right corner.

#### Main Panel

The main panel (Fig. 6.4) is displayed whenever a specific MDT chamber is selected in the FSM. It is designed to give a quick overview of the chamber temperature and the working conditions of its temperature sensors.

In the upper part of the panel a graphic depicting the shape of the chamber is drawn. It consists of a top view and a side view, similar to engineering drawings. The graphic is reshaped to follow the actual shape of the chamber (rectangular for the rectangular barrel chambers and trapezoid for the trapezoid end-cap chambers). Within this graphic the temperature sensors (represented as circles) attached to this chamber are shown in their correct locations. These circles are coloured according to the temperatures of the corresponding sensors. Malfunctioning sensors are indicated by white coloured circles. A tooltip is available to show the sensor names and temperatures. For reference a temperature bar is provided on the right hand side.

Below the chamber graphic a two dimensional temperature trend is displayed. This temperature trend shows the measured temperature along the tubes (chamber x-axis). Three colours are used to differentiate between sensors mounted on Multilayer 1, Multilayer 2 and the crossplates. Malfunctioning sensors (flagged sensors) are not shown in this trend.

On the right hand side of this temperature trend a LED depicts whether the read out electronic is powered (i.e. producing heat) or not.

The lower part of the Main Panel is divided into three columns:

The column on the left side displays the name of each temperature sensor along with the measured temperature and the corresponding readout time stamp. Malfunctioning sensors (flagged sensors) are coloured grey. Values which raise an alert are coloured accordingly.

The middle column displays calculated temperature gradients of the MTM chamber, while the column on the right hand side gives a summary of the status of the temperature sensors.

#### More Info Panel

The More Info Panel (Fig. 6.5) is designed to supplement the Main Panel by providing additional informations which might be necessary in case of problems.

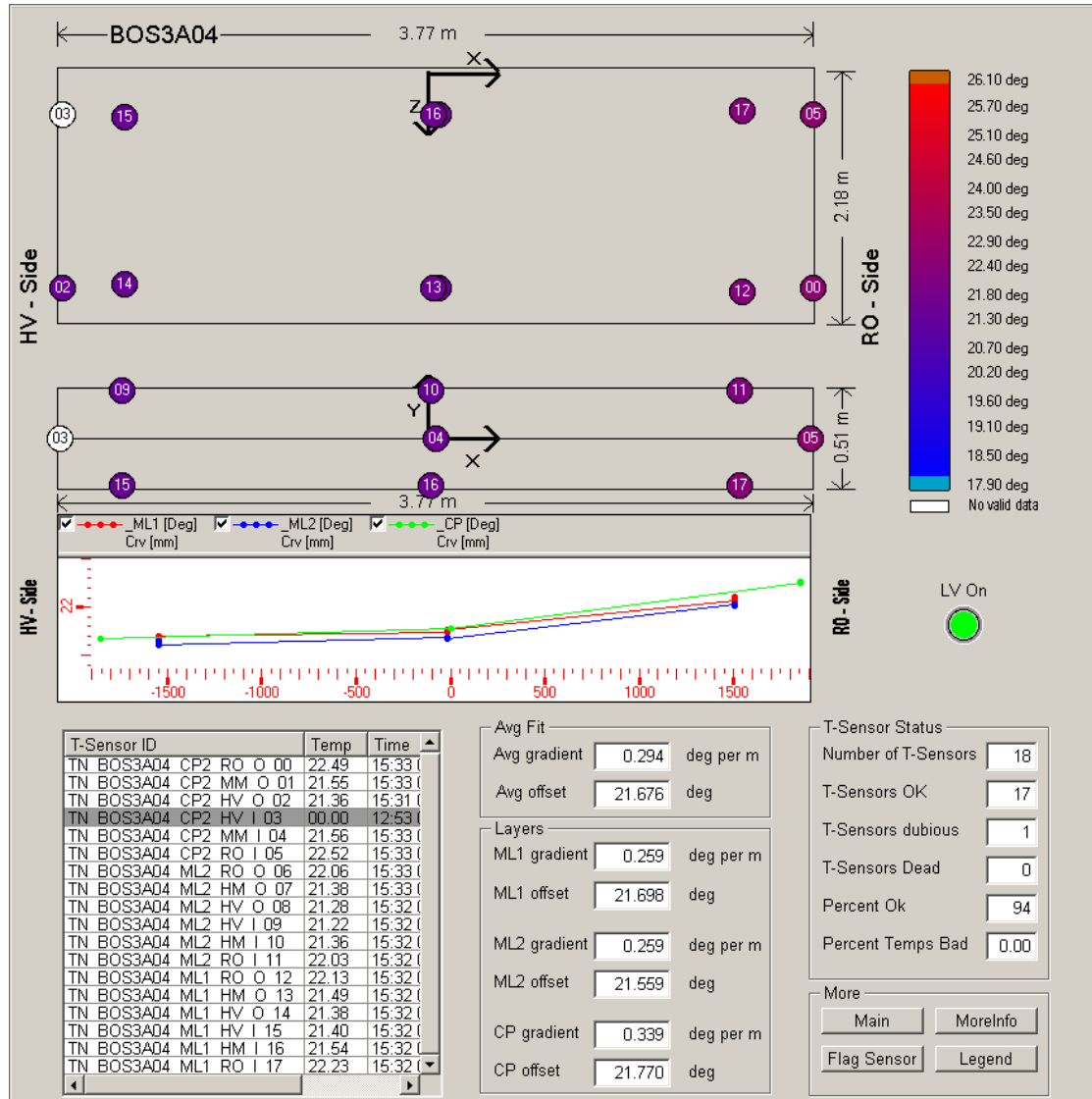


Figure 6.4.: Main MTM panel for a device unit (chamber), showing as an example the chamber BOS3A04.

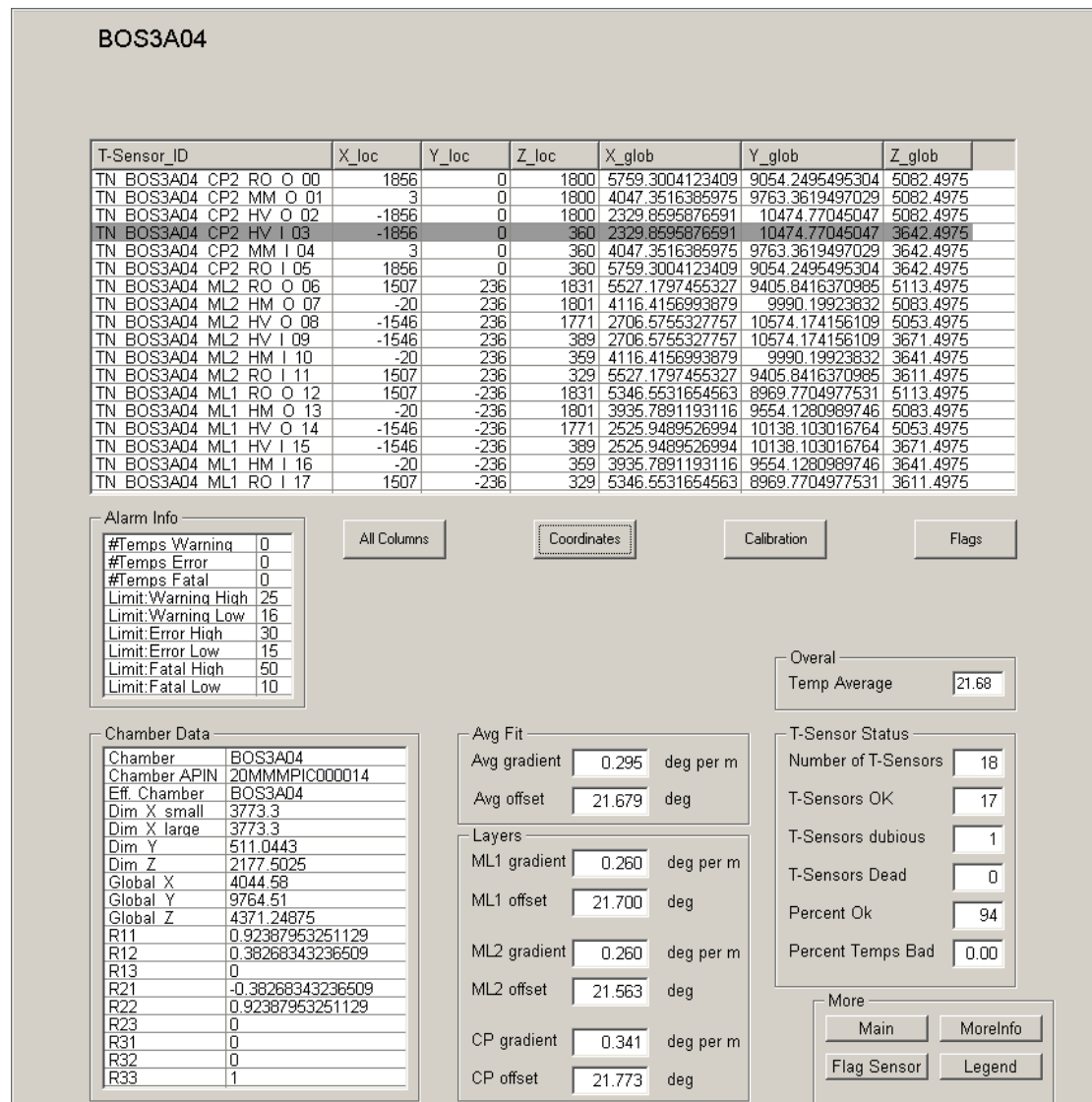


Figure 6.5.: More Info panel for a device unit (chamber), showing as an example the chamber BOS3A04.

The topmost table displays all information available concerning the temperature sensors mounted on this chamber such as names, positions, calibration constants, flags, temperature values and readout timestamps. In order to provide a better readability the displayed columns can be changed using the buttons below.

The small Alarm Info field on the left hand provides information about the number of alarms raised and the limits applied for this chamber.

The table in the lower left corner depicts geometric information about the chamber itself,

such as dimensions, position and within the ATLAS experiment and the unique ATLAS part identifier (APIN).

The temperature gradients and sensor status displays complete this panel.

### **Flag Panel**

The Flag Panel (Fig. 6.6) allows the user to view and change the flags for single or multiple temperature sensors. This panel is access-controlled limiting certain actions to experts.

In the upper part of the panel a two dimensional temperature trend, the same as on the Main Panel, is displayed. Below that a sensor table gives the sensor names, temperatures, average chamber temperature and current flags is located. One or multiple sensors can be selected by clicking on them. Together with the two dimensional temperature trend these two displays are sufficient to locate a malfunctioning sensor.

The lower part of the panel is divided into two sections. The left side features a drop-down menu to select a new flag for the selected sensor. Certain actions, such as declaring sensors dead or reviving dead sensors, can only be selected by experts. This is accomplished by identifying the user logged in into the ATLAS FSM system and checking its authorisation using the JCOP access control module. The user field below the drop-down field is filled in automatically by the access control, though it can be changed manually. The 'Comment' field has to be filled in manually with a reason why a certain flag was issued. The right hand side displays the new flag values which will be set, thereby offering a cross check possibility. Invalid entries are detected and signalled to the user.

The 'Flag It' button at the bottom of the panel changes the flags of the selected temperature sensors to the values specified above and reports the new flag to the database. Due to the complexity of the MTM program and the flagging procedure it may take up to 30 seconds until the new flag is taken into account.

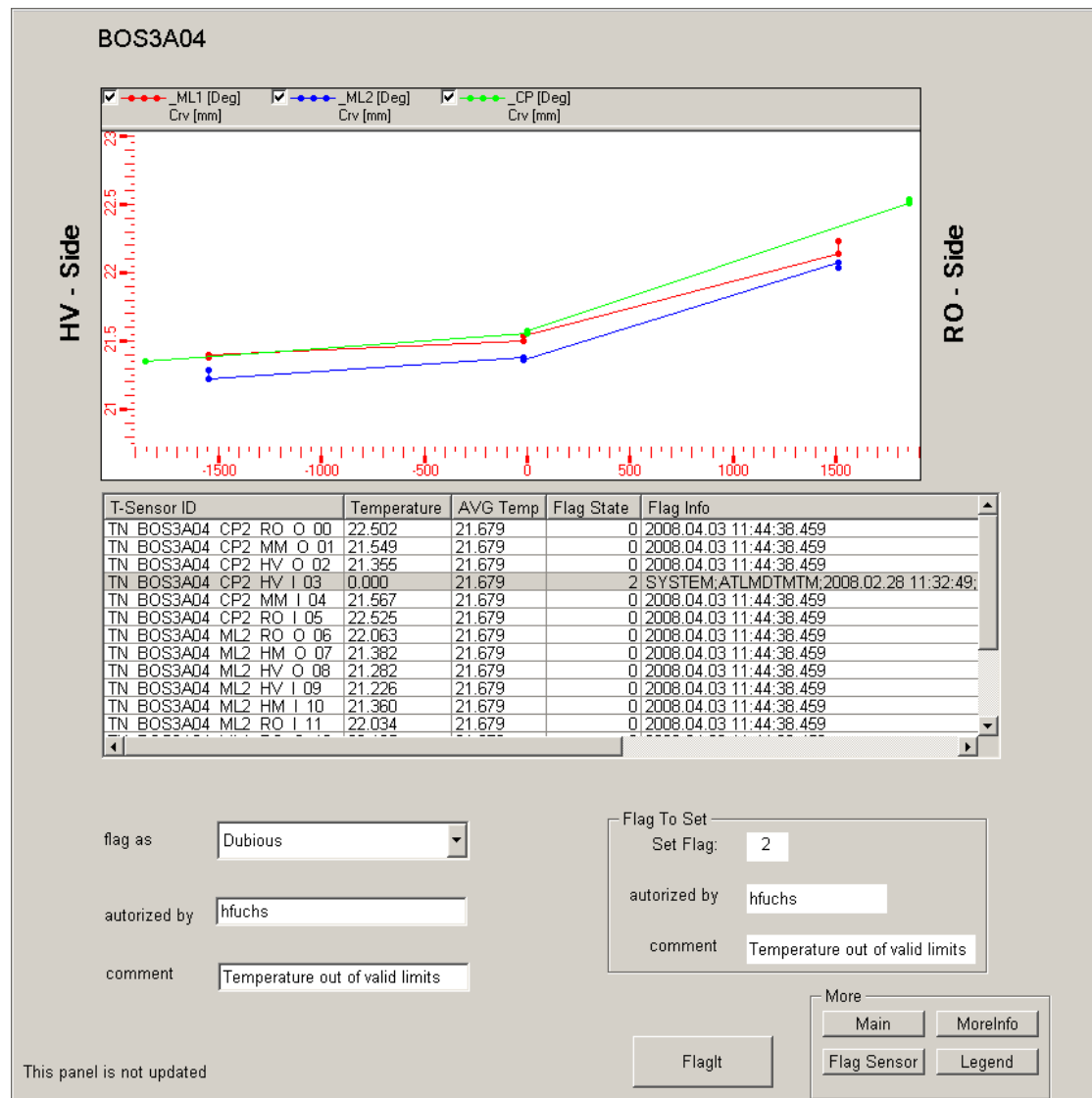


Figure 6.6.: Flag panel of the device unit level, showing as an example the chamber BOS3A04. It enables the user to change and set flags for individual temperature sensors.

## 6.9.2. Sector Panels

The ATLAS muon system features two different geometries, a cylindrical barrel and disc-like endcaps, making it necessary to introduce different display panels.

### Endcap Sector Panel

The Endcap Sector Panel (Fig. 6.7 and Fig. 6.8) has the same functionality as the Endcap Wheel Panel described below. It is automatically skipped by the MTM system during navigation due to its limited use. There it is only to fulfill the FSM requirements. Further information can be found in Chapter 6.9.3.

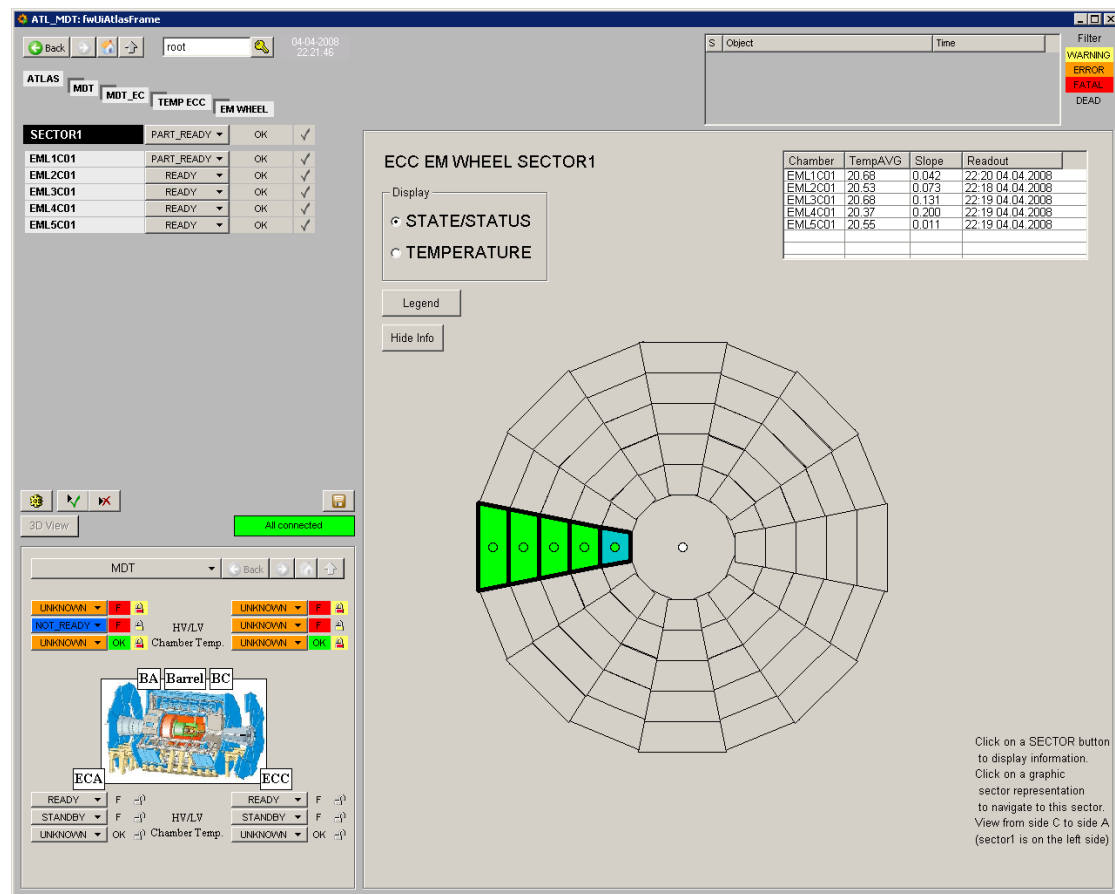


Figure 6.7.: Endcap Sector Panel showing an overview of the FSM STATE/STATUS of the MDT chambers.



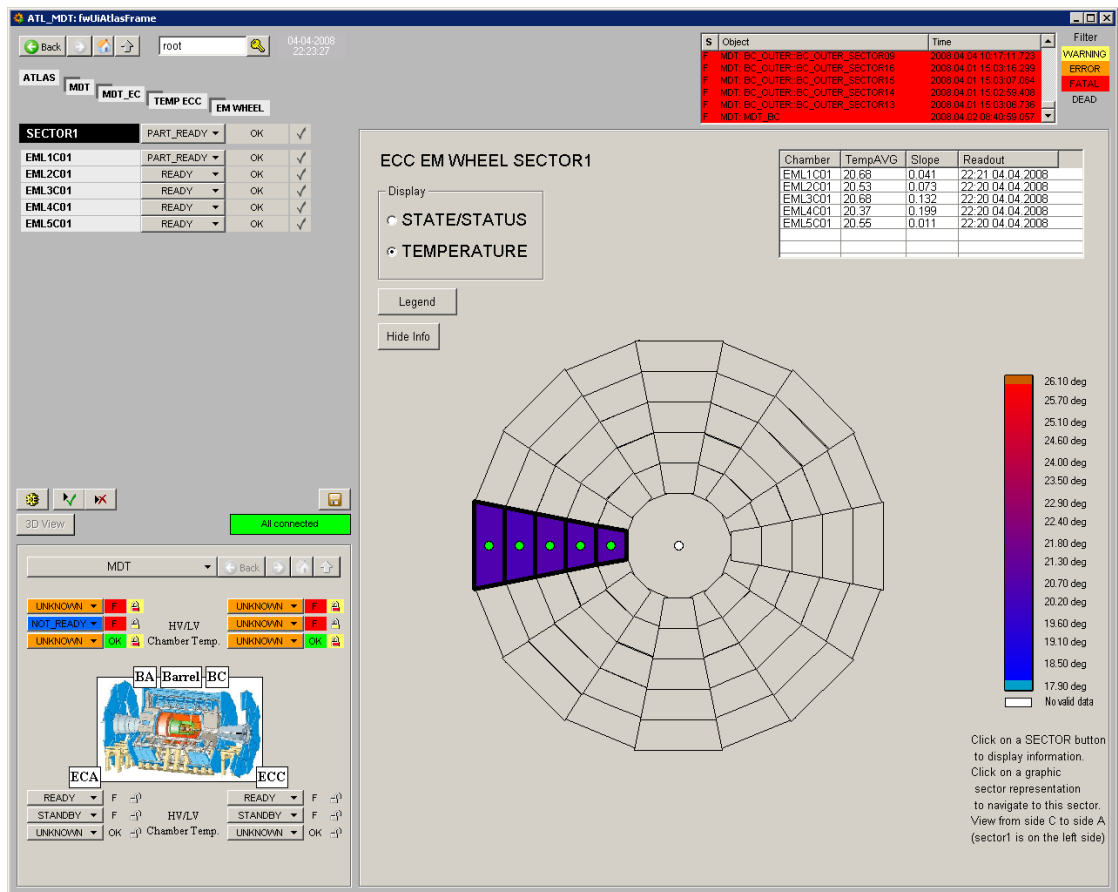


Figure 6.8.: Endcap Sector Panel showing an overview of the temperatures of the MDT chambers.

## Barrel Sector Panel

The Barrel Sector Panel (Fig. 6.9 and Fig. 6.10) depicts all chambers belonging to a sector. Like all other FSM panels<sup>2</sup> of the MTM system it has two display modes, which can be switched using the radio buttons in the 'Display' field on the left side. In the standard display mode the panel displays the FSM STATE/STATUS information as required in the ATLAS FSM integration guidelines [23]. The other display mode shows temperature information instead of the FSM STATE information.

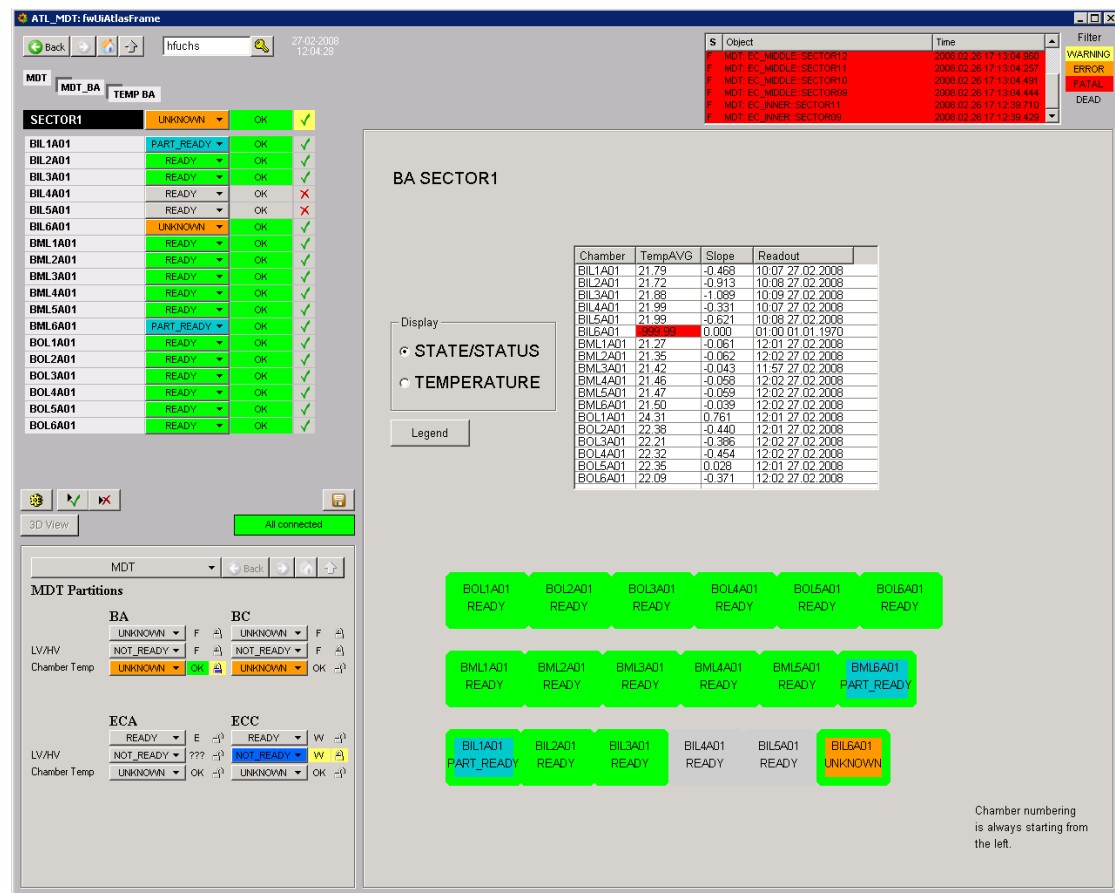


Figure 6.9.: Barrel Sector Panel showing an overview of the FSM STATE/STATUS of the MDT chambers.

In the upper part of the panel an overview table is located, showing key values of the MDT chambers below, allowing a quick overview without having to navigate up and down. Potential alarms are indicated by colouring the corresponding cells in the appropriate alarm colour.

<sup>2</sup>The panels on the device unit (chamber) level do not have two display modes.

Below the overview table a graphic representation of all chambers belonging to this sector is shown. The chamber facsimiles represent the order and location of the chambers within the ATLAS experiment, although sizes and proportions may not be correct. Each chamber facsimile is filled with the standardised FSM colour depicting the STATE or the temperature, depending on the display mode. The border of the chambers are always coloured according to the FSM STATUS. Within the chamber rectangles the chamber designation and FSM STATE or temperature are written. The same information is available via tool tips. Clicking on a specific chamber navigates to this chamber.

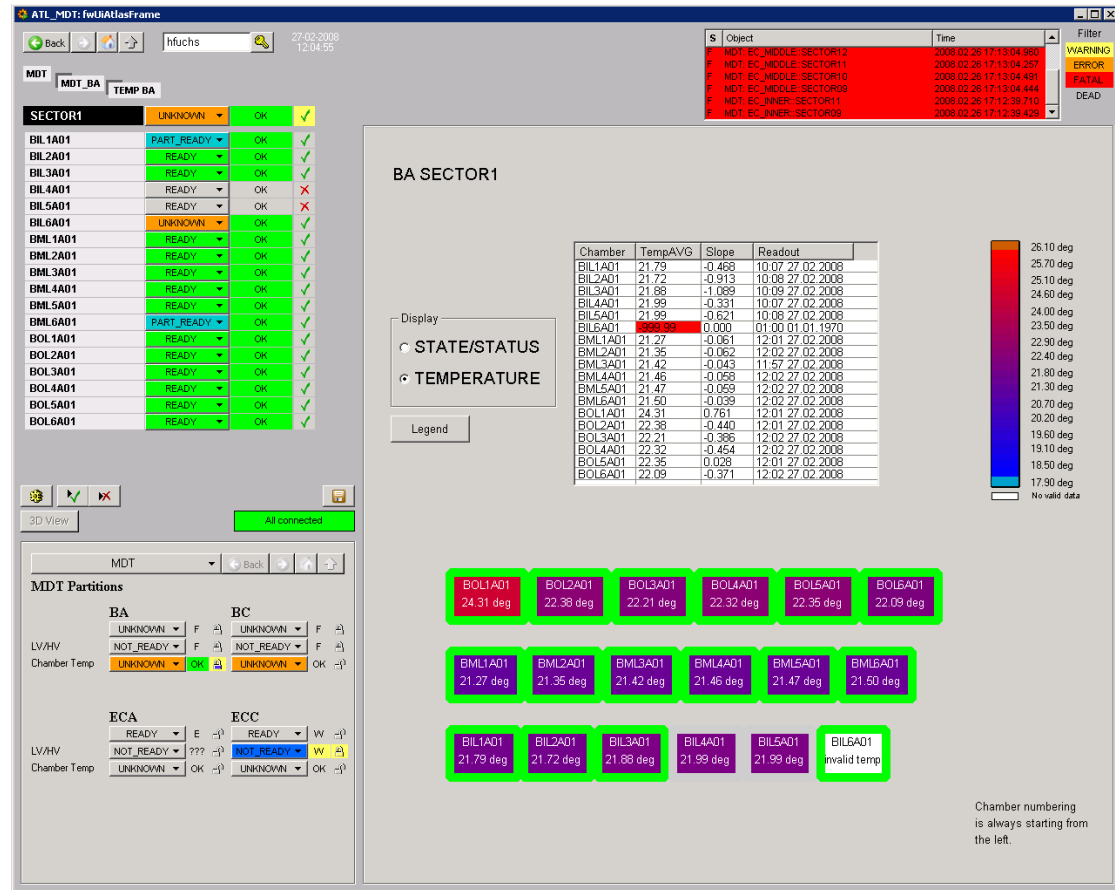


Figure 6.10.: Barrel Sector Panel showing an overview of the temperatures of the MDT chambers.

### 6.9.3. Endcap Wheel

Although four different wheel types (requiring three different display sizes) exist, it is possible to use the same layout and functionality in all of them. The only difference between them is the shape of the depicted wheel.

Like all other FSM panels (except the chamber level panels) of the MTM system it has

two display modes, which can be switched using the radio buttons in the display field on the left side.

The biggest part of the Endcap Wheel panel (Fig. 6.11 and Fig. 6.12) is filled with a graphical representation of the corresponding end-cap wheel.

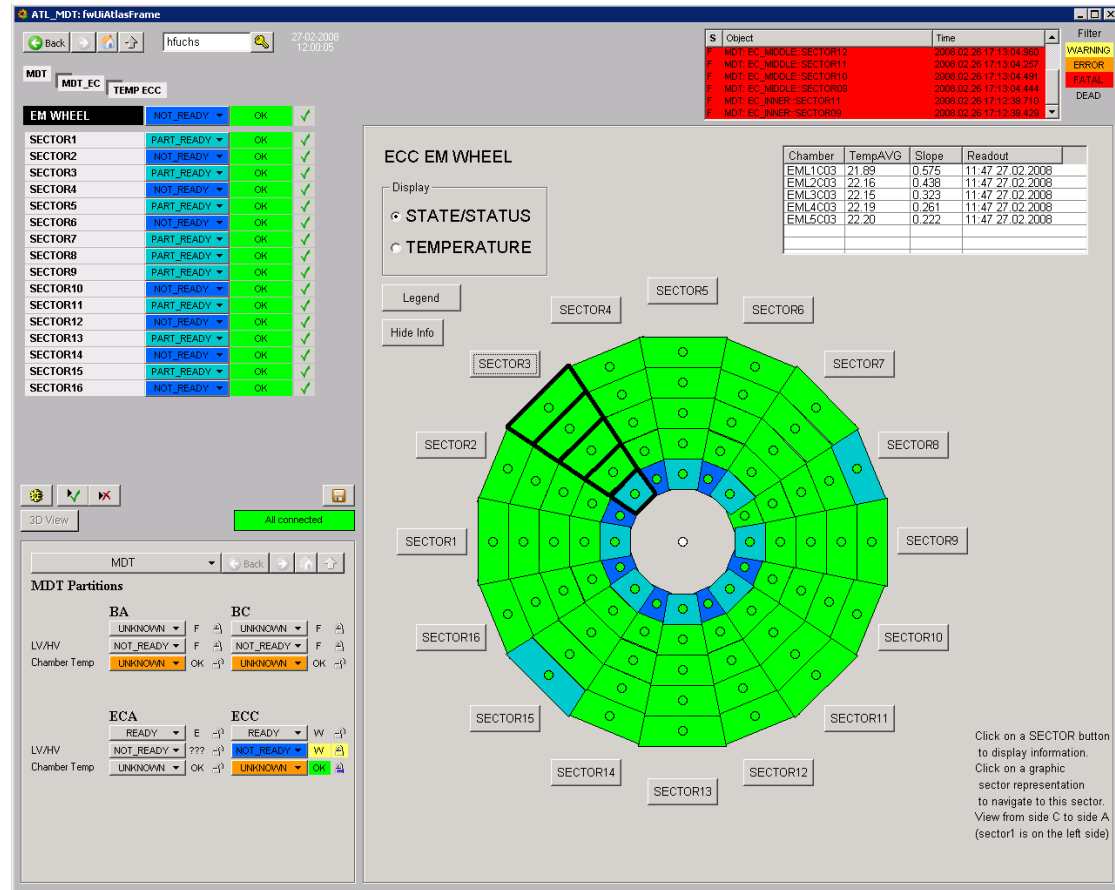


Figure 6.11.: Endcap Wheel Panel showing an overview of the FSM STATE/STATUS of the MDT chambers.

The chamber facsimiles are filled with the FSM STATE or the temperature colour, depending on the display mode. Each facsimile is equipped with a small circle which is filled according to the FSM STATUS colour.

Surrounding the wheel are buttons with the corresponding sector label. When pressed, the selected sector is highlighted and more detailed information on the chambers belonging to this sector is shown in the overview panel located in the upper right corner. In case values are in an alarm range, the background colour of the corresponding cell changes (see the temp view below for example).

Clicking on a chamber facsimile navigates to the corresponding chamber.

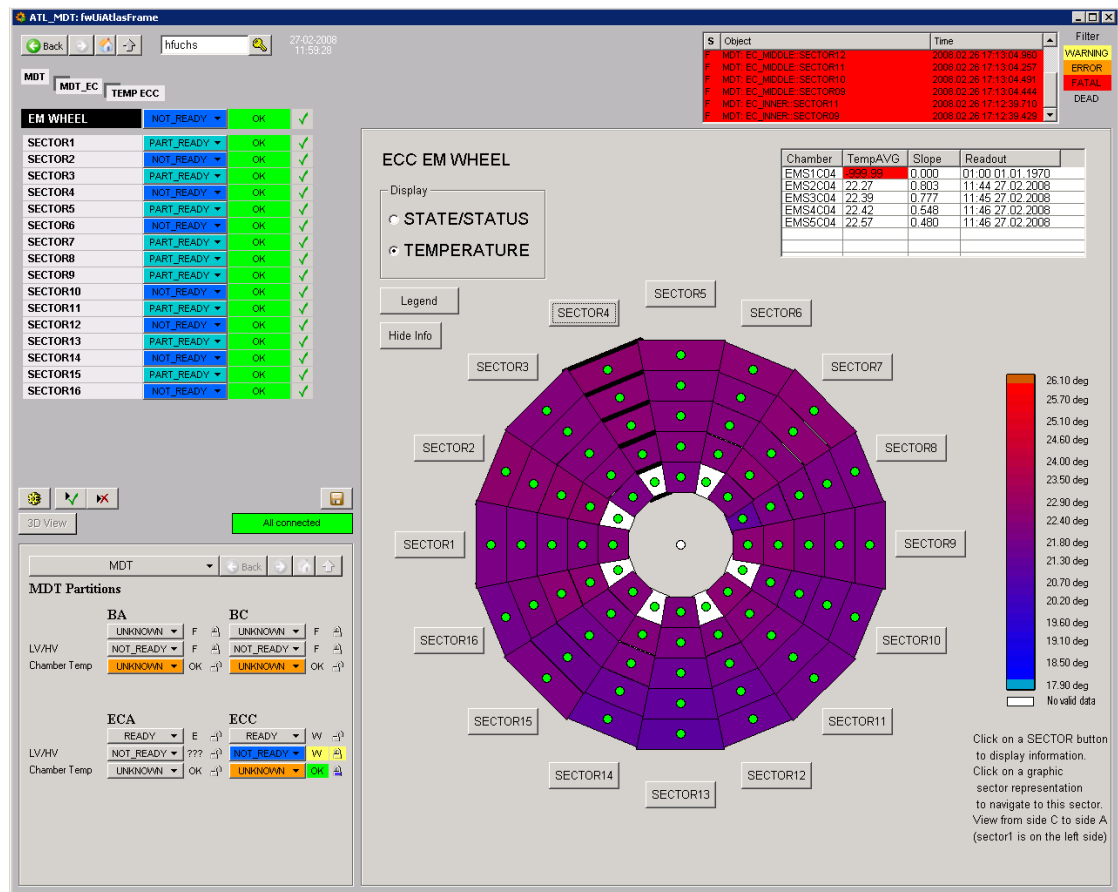


Figure 6.12.: Endcap Wheel Panel showing an overview of the temperatures of the MDT chambers.

#### 6.9.4. Partition Panels

The main purpose of the partition level is not to provide a detailed view, but a quick and easy overview of the operating conditions of all chambers of the selected partition. Because of the two different geometries, the User Interface of the partition level consists of two different panels, depending on the geometry of the partition (barrel or end-cap).

##### Endcap Partition Panel

The Endcap Partition Panel (Fig. 6.13 and Fig. 6.14) gives a complete overview of the selected partition, depicting all four corresponding end-cap wheels and the exceptional BIS7 and BIS8 chambers at one glance. Like all other FSM panels (except the chamber level panels) of the MTM system it has two display modes, which can be switched using the radio buttons in the 'Display' field on the left side.

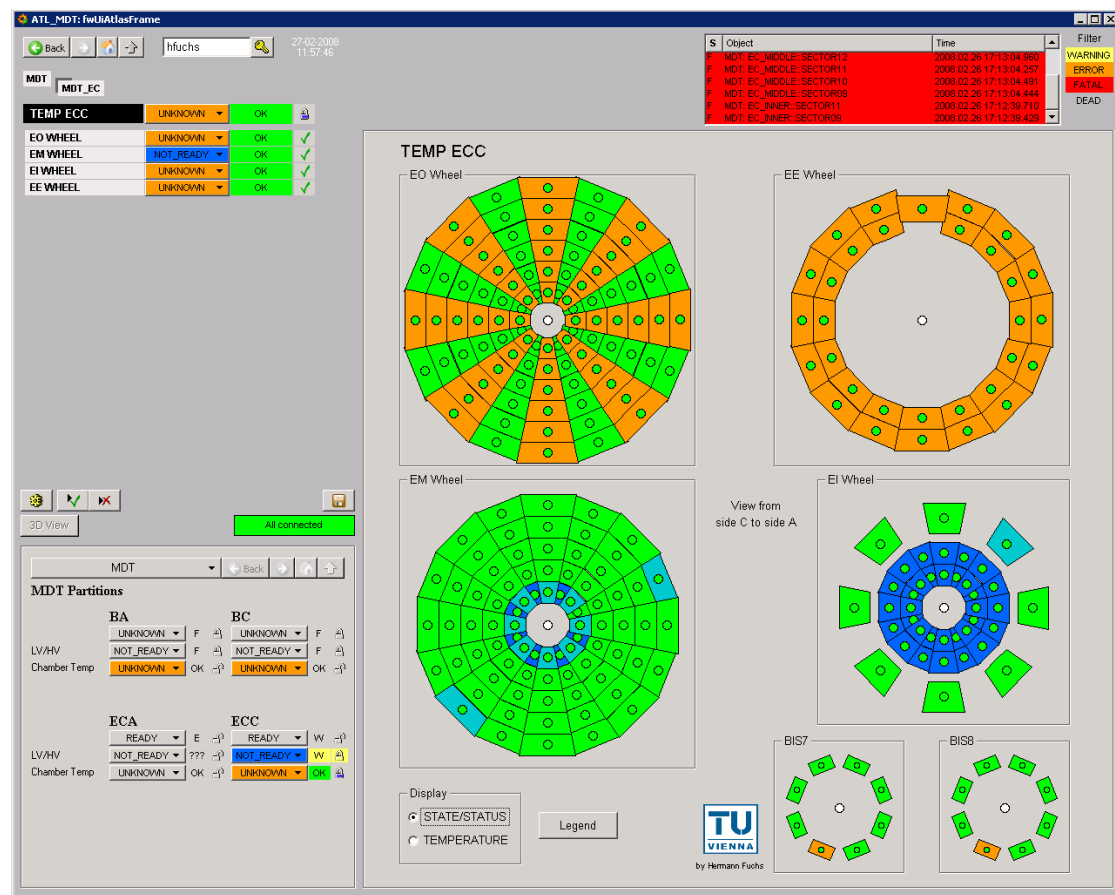


Figure 6.13.: Endcap Partition Panel showing an overview of the FSM STATE/STATUS of the MDT chambers.

Due to the large number of FSM objects queried for this panel (all chambers of this partition have to be evaluated), a special staged loading and display function had to be developed in order to keep loading times within limits. Without this staged loading the opening of this panel took up to 20 seconds.

The chamber facsimiles depict FSM STATE/STATUS and temperatures in the same way as the Endcap Wheel Panel in Chapter 6.9.3. Clicking on a wheel navigates to the corresponding Endcap Wheel Panel.

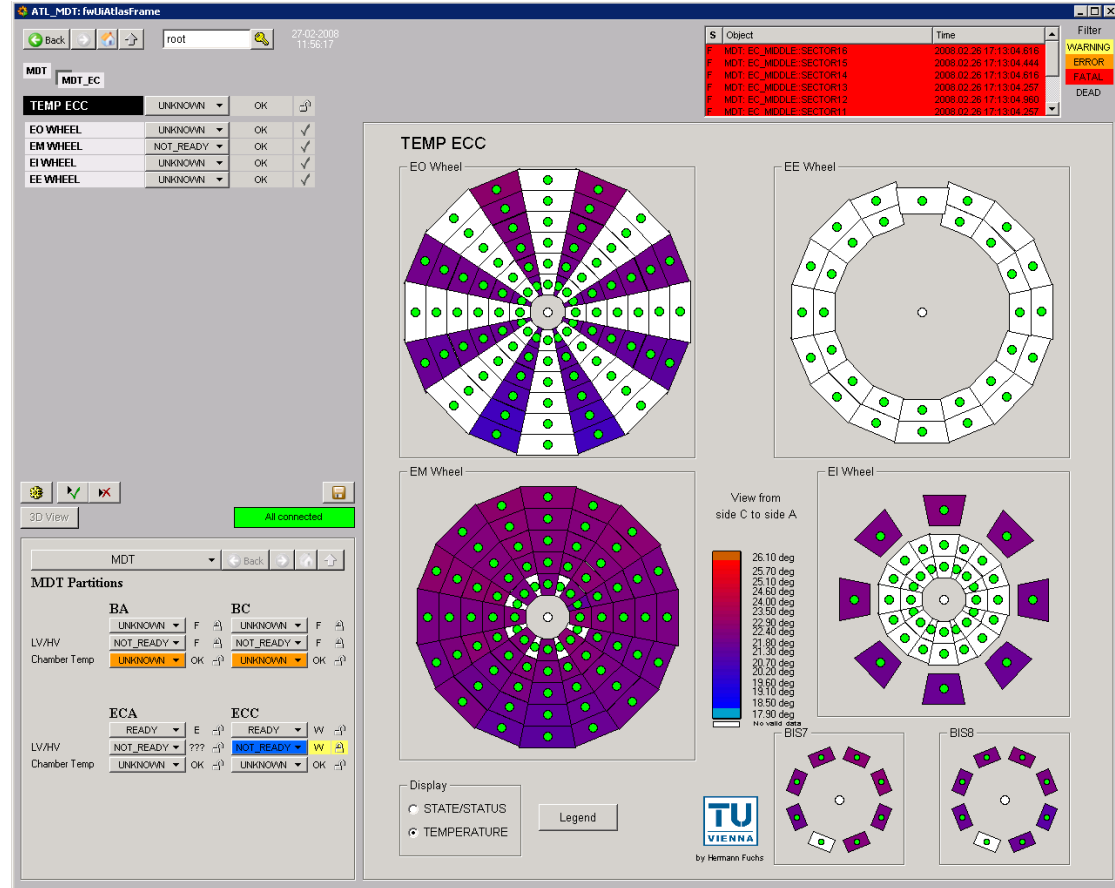


Figure 6.14.: Endcap Partition Panel showing an overview of the temperatures of the MDT chambers.

## Barrel Partition Panel

The partition level of the barrel side is different from the end-cap panel. The geometry of the Barrel makes it very hard to display all chamber at a glance and keep the processing times within range. Therefore instead of displaying all chambers, only a cross section of the Barrel is displayed.

The layout and functioning (e.g. two mode display, overview panel) of the Barrel

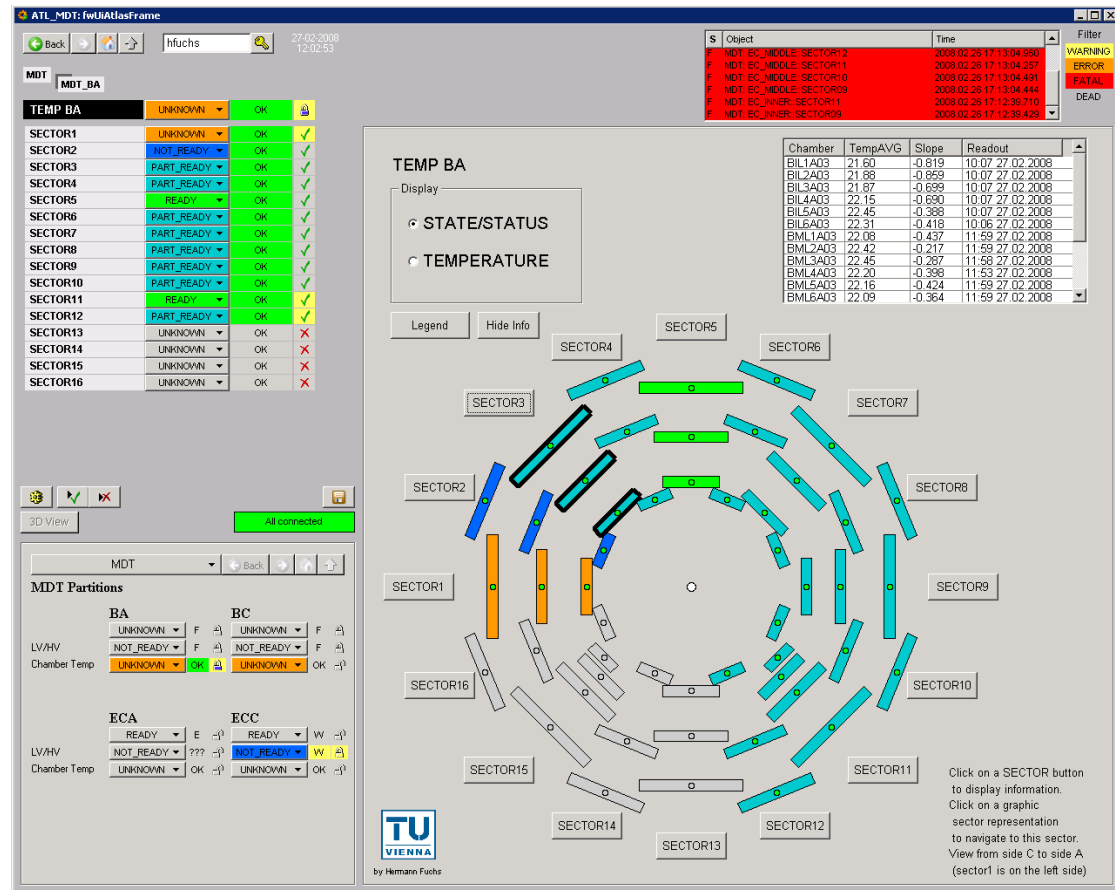


Figure 6.15.: Barrel Partition Panel showing an overview of the FSM STATE/STATUS of the MDT chambers.

Partition Panel (Fig. 6.15 and Fig. 6.16) is similar to the Endcap Wheel Panel described in Chapter 6.9.3. However, some differences exist. The FSM states/status are displayed on a sector basis, due to FSM limitations. The temperatures are displayed per layer averaged over all chambers of each layer.

The sector buttons give access to more detailed information about a sector. Navigating to the corresponding Barrel Sector Panel is possible by clicking.



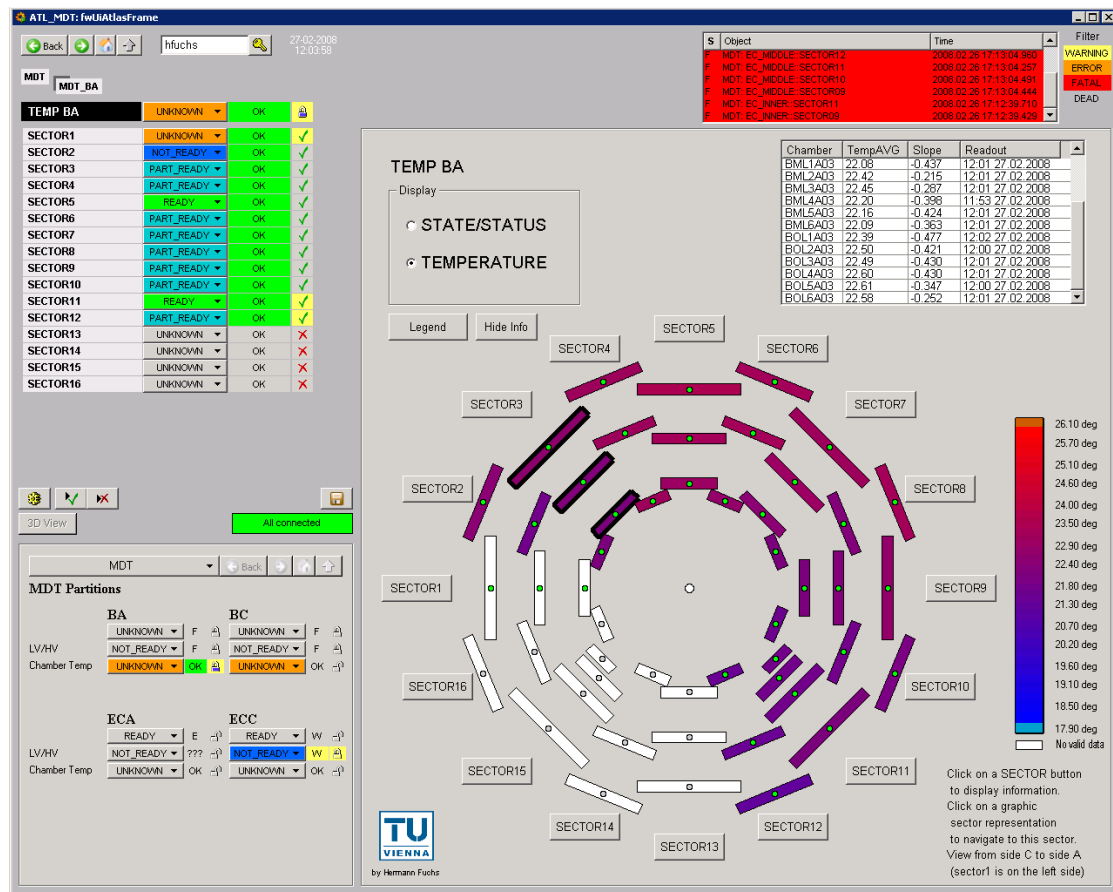


Figure 6.16.: Barrel Partition Panel showing an overview of the temperatures of the MDT chambers.

### **6.9.5. Expert Panels**

An independent set of analysis and monitoring panels has been developed for detector debugging purposes. They can be operated in parallel to the normal FSM panels. Emphasis was placed on quick response and easy use of the panels. The Expert Panels are all accessible from a single expert panel.

#### **MDT Temperature Overview**

The MDT Temperature Overview (MTO) panel (Fig. 6.17) provides an immediate temperature overview. All MDT chambers are logically structured and coloured according to their average temperature. The individual chamber names and precise temperatures are available as tool tips. As you can see in Fig. 6.17 the upper part of the detector (Sectors 2 - 8) are considerably warmer than the lower sectors.

Using this panel it is possible to identify hot spots and other thermal irregularities. Due to requests from Central DCS, a standalone version of this panel has been integrated into the environmental monitoring section of the FSM, providing an easy access to temperature values especially interesting during commissioning and debugging.

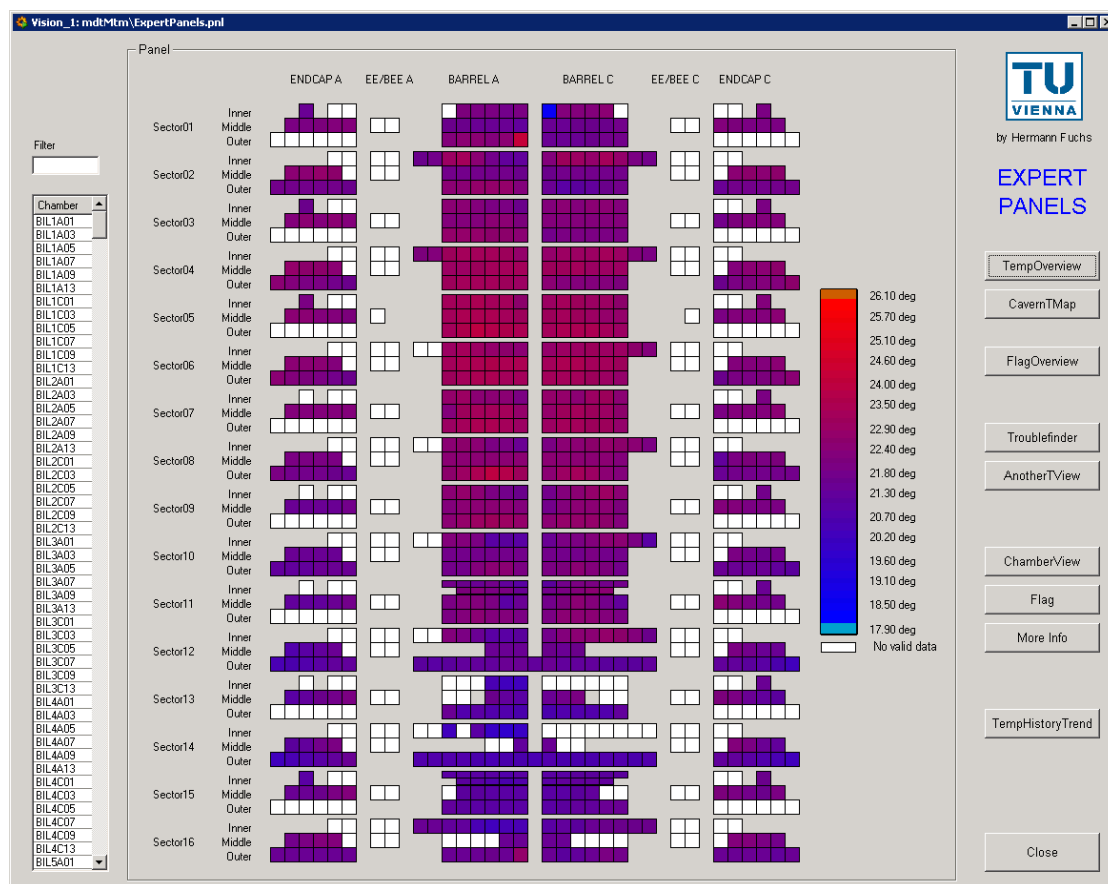


Figure 6.17.: Temperature Overview panel showing a temperature overview of all MDT chambers of the ATLAS Muon Spectrometer

## Cavern Temperature Map

Similar to the MDT Temperature Overview (MTO), the Cavern Temperature Map (CT-Map) (Fig. 6.18) aims at providing a temperature overview. Unlike the MTO the CT-Map does not intend to display all MDT chambers, but focuses on providing an intuitive view of the temperature distribution within the ATLAS experimental cavern.

A disadvantage of the MTO panel is its logical structure, requiring a user to know something about the detectors structure. The CT-Map by taking a horizontal and vertical cross section of the MDT system and displays the MDT chamber according to their position within the experiment, bypasses this disadvantage. A tooltip is available providing chamber name and average chamber temperature for more precise information.

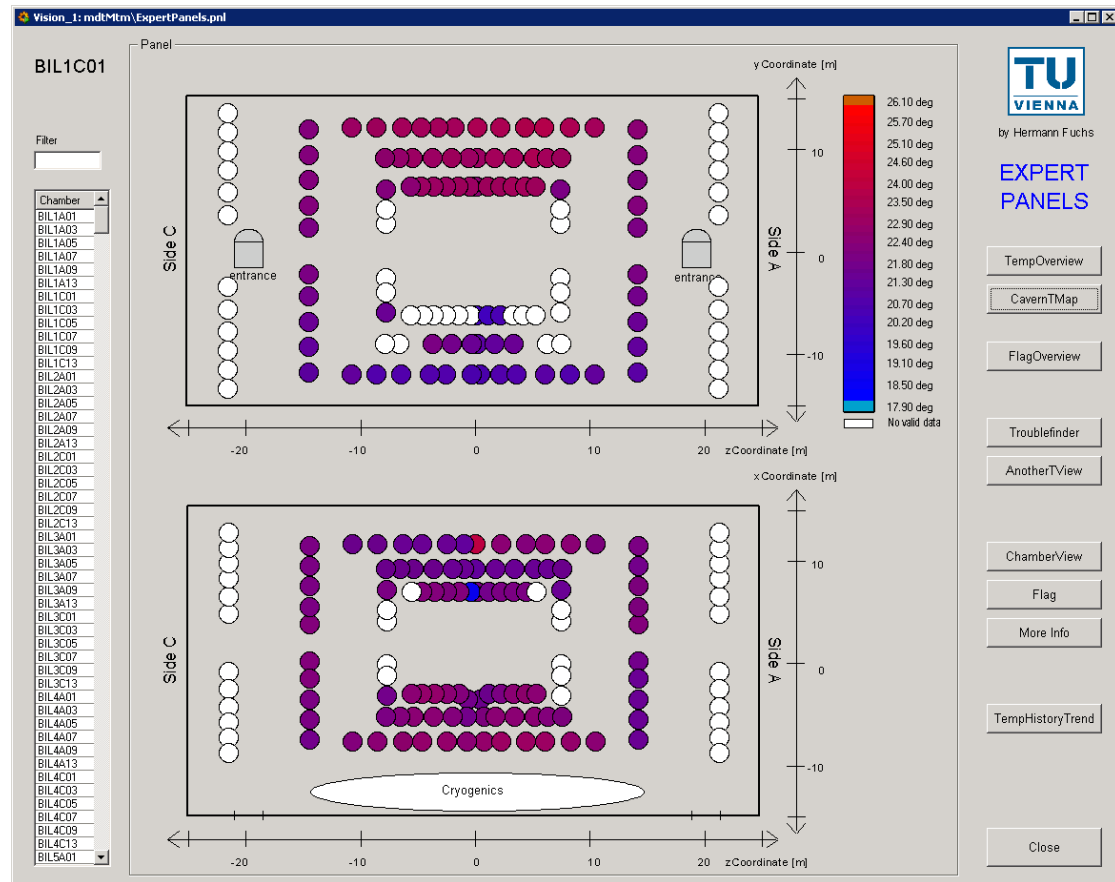


Figure 6.18.: Cavern Temperature Map panel showing two temperature cross sections of the temperature distribution within the ATLAS cavern measured using the MDT temperature sensors.

## Flag Overview

The Flag Overview panel (Fig. 6.19) uses the same logical structure as the MTO panel (Fig. 6.17). It aims at giving a quick overview of the working conditions of the MTM system by displaying the number of not working temperature sensors per chamber.

Because of the large varying number of temperature sensors per MDT chamber (4 - 28), the proportion of malfunctioning temperature sensors is displayed using a colour code, instead of displaying the actual number. A tooltip facilitates the process of identifying chambers while providing the precise percentage of flagged sensors.

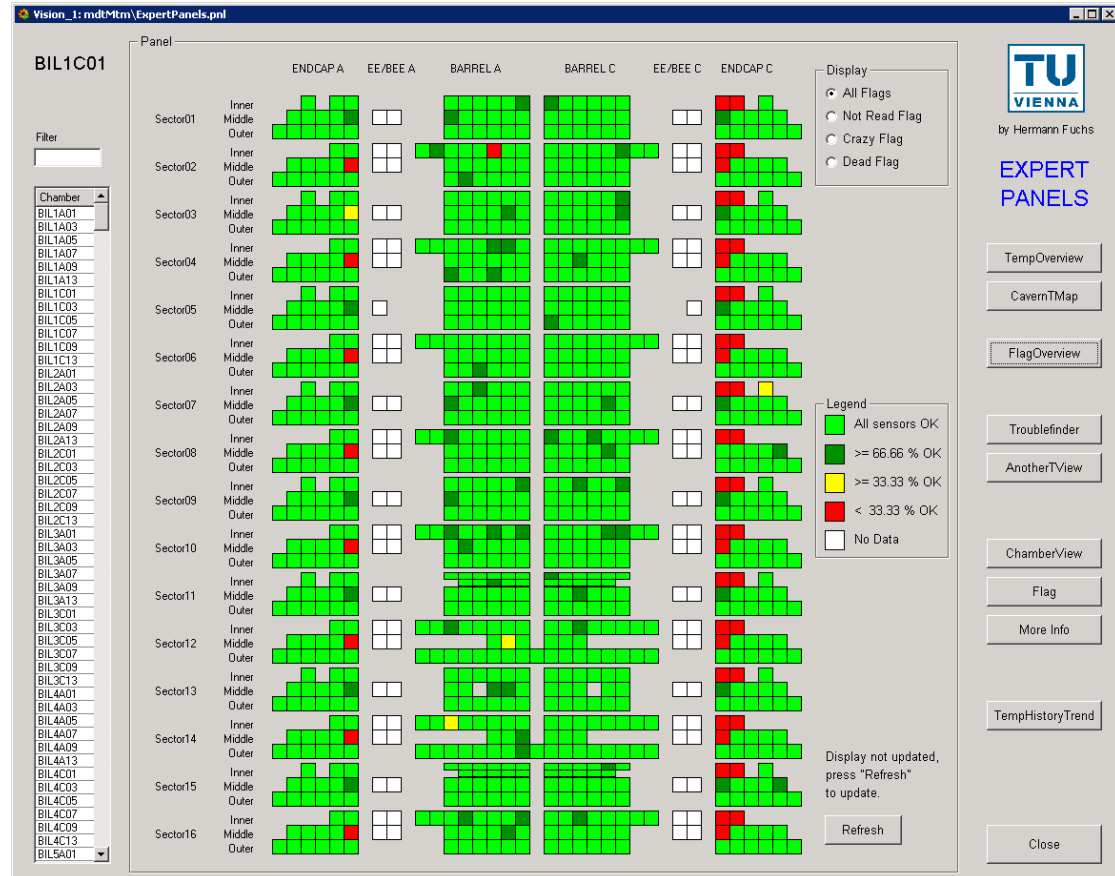


Figure 6.19.: Flag Overview panel showing the percentage of malfunctioning temperature sensors within the MDT system using the same logical structure as the MTO panel.

## Troublefinder

The MTM system consists of more than 12.000 temperature sensors, distributed over 1056 MDT chambers. The sheer number of sensors and chambers makes it very difficult

to find and identify single malfunctioning sensors. While an automated flagging algorithm (see Chapter 6.5.3) will detect the most obvious faults, more subtle malfunctions have yet to be detected manually.

In order to facilitate this detection the Troubfinder (Fig. 6.20) was created. This panel collects and calculates key values for all MDT chambers and displays them in the upper part of the panel. In case of problematic values, these chambers are copied into the problematic chambers table at the bottom of the panel. The values taken into account include minimum temperature, maximum temperature, average temperature and the deviation from the calculated temperature gradient. Furthermore, some general information such as the number of sensors, the number of already flagged sensors and the last readout time are displayed.

It is possible to export both tables for further analysis and reference.

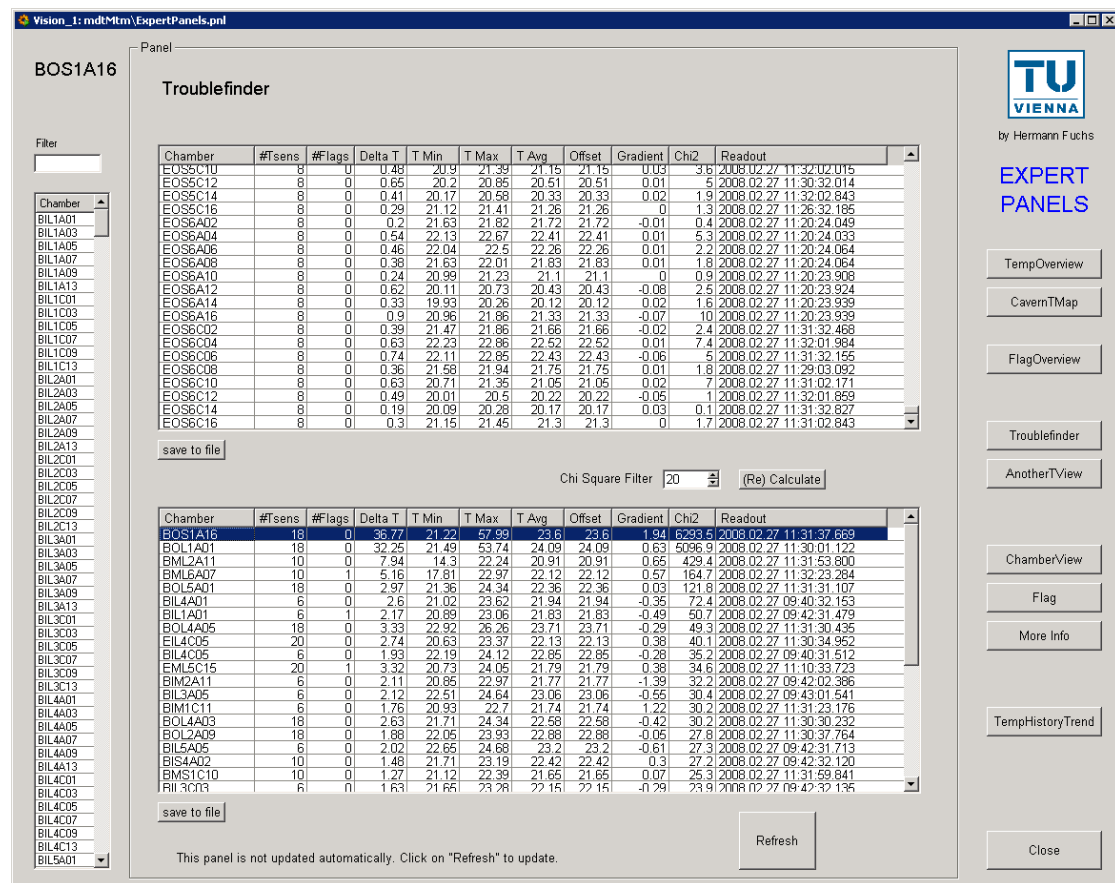


Figure 6.20.: The Troubfinder panel calculates key values for all MDT chambers and identifies potential problematic chambers.

## Archived Data Viewer

Using the Archived Data Viewer (Fig. 6.21) it is possible to view the temperature trend for a given chamber over a user defined time frame.

As a result of the fact that the MTM project is a monitoring system embedded in the ATLAS DCS system, the emphasis lies on current data, which is perfectly adequate for its purpose. However the possibility remains that a temperature trend over a given time frame, as it is provided by this panel, might be required for analysis. Data retrieval from an online monitoring system running in the ATLAS control room is discouraged due to the load on the database servers.

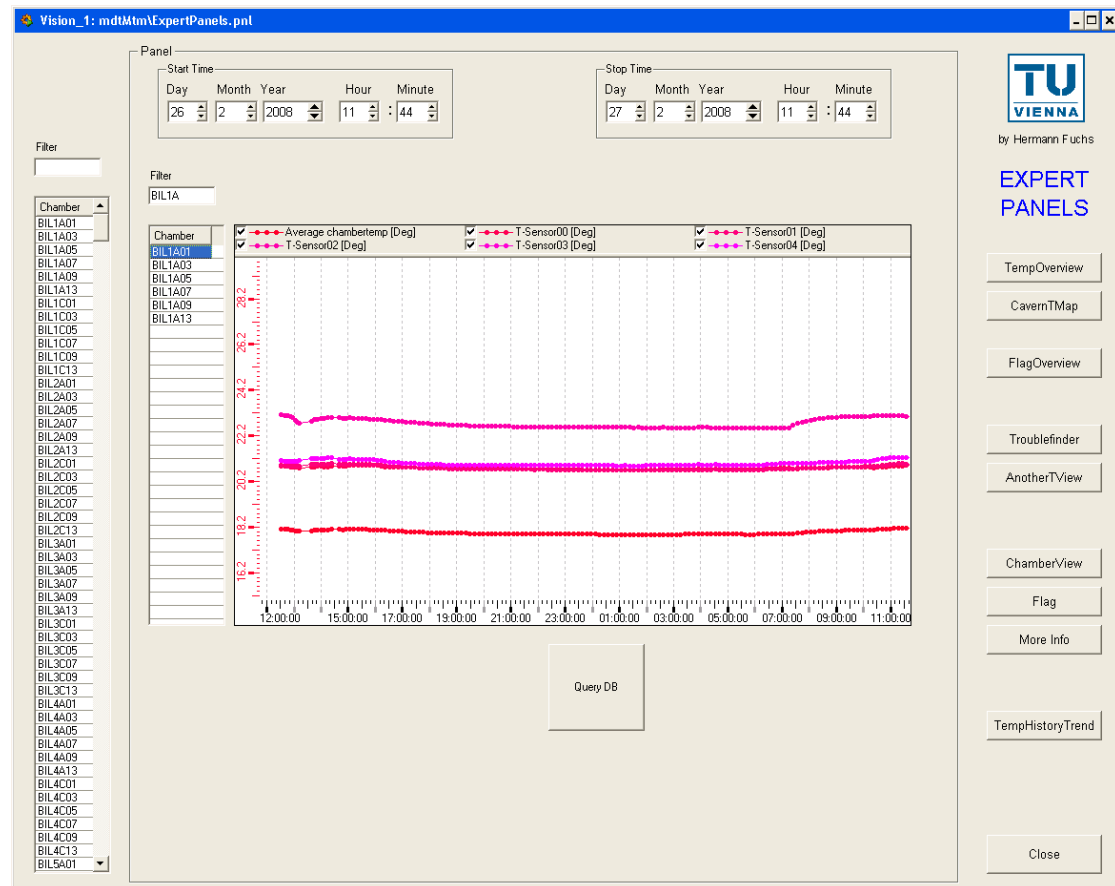


Figure 6.21.: Archived Data Viewer panel displaying archived temperature data per chamber.

## 6.10. Integration

After a development time of eight months, from conception to realisation, the Muon Temperature Monitoring system has been completed.

Although initially not planned, it was decided that the MTM system should run on a dedicated server to improve performance. It was first installed on a temporary server until the final hardware arrived. The installation and set-up of the MTM system on this server, located in the cavern USA 15, was a major milestone.

After completing functional tests, the MTM project successfully passed the Central DCS code review and has been integrated into the ATLAS DCS system on 31 January 2008. Since this time the MTM software has been accessible from the ATLAS control room. Feedback provided by many users helped to fine-tune the 'look and feel' of the system. Furthermore, it turned out that a temperature overview of the whole MDT system was very useful for Central DCS and the commissioning staff for debugging the detector. Therefore a previous expert-only panel, the MDT Temperature Overview panel (Chapter 6.9.5), has been implemented into the infrastructure section of the MDT FSM, proving the usefulness of the MTM system for the whole ATLAS community.



## 7. Summary

The Muon Temperature Monitoring (MTM) project, a part of the ATLAS detector control system (DCS), has been successfully completed. It passed the integration checks on 31 January 2008 and is now available throughout the ATLAS control room.

The MTM project is connected using a PVSS distributed system to readout systems providing the temperature data. After sorting and analysing the data, temperature gradients are exported to COOL and the temperatures of the MDT chambers are displayed using the ATLAS Finite State Machine (FSM) interface. The operator is able to choose between various panels, providing an in-depth overview of the state of the MDT chamber temperature monitoring and of the respective chamber temperatures itself. Additionally, a temperature overview panel is available which provides a quick overview of the temperature distribution within the MDT system.

Expert panels for pinpointing faulty devices and to debug the MDT system are available.

After integrating the MTM system into the ATLAS DCS system a series of tests and comparisons was done to evaluate the temperature behaviour of the ATLAS MDT system. The measurements showed a good agreement between previously simulated temperature behaviour and actual measured temperature distributions using the MTM project.

## A. FSM STATE and STATUS definitions

### A.1. Device Unit

A list of all defined STATES (Tab. A.1) and STATUS (Tab. A.2) conditions can be found below.

Table A.1.: DU STATE conditions used by the MTM project

State	Color	Conditions
READY	FwStateOKPhysics	All sensors <sup>1</sup> are operating <sup>2</sup>
PART_READY	FwStateStandby	More than 1/3 of all sensors <sup>1</sup> are operating <sup>2</sup>
NOT_READY	FwStateAttention3	Less than 1/3 of all sensors <sup>1</sup> are operating <sup>2</sup>
UNKNOWN	FwStateOKNotPhysics	At least one time stamp of one of the temperature values is older than 5 minutes

<sup>a</sup> *All sensors* refers to all sensors which are not declared dead (flag not 1)

<sup>b</sup> *Operating* refers to flag 0

Table A.2.: DU STATUS states used by the MTM project

State	Color	Conditions
OK	FwStateOKPhysics	Less than 1/3 of all operating sensors agree that the temperature is out of range
WARNING	FwStateAttention1	More than 1/3 of all operating sensors agree that the temperature is out of range
ERROR	FwStateAttention2	More than 2/3 of all operating sensors agree that the temperature is out of range
FATAL	FwStateAttention3	Not used

## A.2. Logic Unit - Sector

A list of all defined STATES (Tab. A.3) and STATUS (Tab. A.4) states can be found below.

Table A.3.: STATE conditions used by the LU of type sector of the MTM project

State	Color	Conditions
READY	FwStateOKPhysics	All DUs in READY
PART_READY	FwStateStandby	All DUs in PART_READY or READY
NOT_READY	FwStateAttention3	At least one DU in NOT_READY, but none in UNKNOWN
UNKNOWN	FwStateOKNotPhysics	At least one DU in UNKNWON

Table A.4.: STATUS conditions used by the LU of type sector of the MTM project

State	Color	Conditions
OK	FwStateOKPhysics	All DUs in OK
WARNING	FwStateAttention1	All DUs in WARNING or OK
ERROR	FwStateAttention2	At least one DU in ERROR
FATAL	FwStateAttention3	Not used

## A.3. Logic Unit - Endcap Wheel

The STATE (Tab. A.5) and STATUS (Tab. A.6) evaluations are very similar to the LU sector.

Table A.5.: STATE states used by the LU of type endcap wheel of the MTM project

State	Color	Conditions
READY	FwStateOKPhysics	All sector LUs in READY
PART_READY	FwStateStandby	All sector LUs in READY or PART_READY
NOT_READY	FwStateAttention3	At least one sector LU in NOT_READY, but none in UNKNOWN
UNKNOWN	FwStateOKNotPhysics	At least one sector LU in UNKNWON

Table A.6.: STATUS states used by the LU of type endcap wheel of the MTM project

State	Color	Conditions
OK	FwStateOKPhysics	All sector LUs in OK
WARNING	FwStateAttention1	All sector LUs in WARNING or OK
ERROR	FwStateAttention2	At least one sector LU in ERROR
FATAL	FwStateAttention3	Not used

## A.4. Control Unit - Partition

The full list of STATE (Tab. A.7) and STATUS (Tab. A.7) states can be found below.

Table A.7.: STATE states used by the CU of type partition of the MTM project

State	Color	Conditions
READY	FwStateOKPhysics	All LUs in PART_READY or READY
NOT_READY	FwStateAttention3	At least one LU in NOT_READY, but none in UNKNOWN
UNKNOWN	FwStateOKNotPhysics	At least one LU in UNKNOWN

Table A.8.: STATUS states used by the CU of type partition of the MTM project

State	Color	Conditions
OK	FwStateOKPhysics	All sector LUs in OK
WARNING	FwStateAttention1	All LUs in WARNING or OK
ERROR	FwStateAttention2	At least one LU in ERROR
FATAL	FwStateAttention3	Not used

## B. Alarm Levels

Alerts within the MTM project can be defined in three different groups. Alerts on the normal data point elements (Tab. B.1), summary alerts (Tab. B.2) and archive alerts (Tab. B.3). The tables list all configured alerts with their corresponding alert classes, limits and alert texts.

Table B.1.: Lists all dp alerts, the corresponding limits, alert classes and alert texts

DP element	Range	Alert Text	Alert Class	Alert Description
.FSM.tempsWarning	> 0	T-Sensors in Warning range	_fwWarningNack.	MDT ECA EMS3A14 Temperature Sensors
.FSM.tempsError	> 0	T-Sensors in Error range	_fwWarningNack.	MDT ECA EMS3A14 Temperature Sensors
.FSM.tempsFatal	> 0	T-Sensors in Fatal range	_fwWarningNack.	MDT ECA EMS3A14 Temperature Sensors
.FSM.sensorsPercentOk	<= 33.33	NOT RELIABLE (< 33, 33 % T-sensors working)	_fwFatalNack.	MDT ECA EMS3A14 Chamber Temperature Monitoring
.FSM.percentTempsBad	>= 33.33	BAD CHAMBER TEMP (> 33.33 % T-sensors)	_fwErrorNack.	MDT ECA EMS3A14 Chamber Temperature
	>= 66.66	BAD CHAMBER TEMP (> 66.66 % T-sensors)	_fwFatalNack.	MDT ECA EMS3A14 Chamber Temperature
.FSM.lastReadout	> 600	DATA NOT UPDATED	_fwFatalNack.	MDT ECA EMS3A14 Chamber Temperature Readout
.chamberRead	WRONG	CHAMBER NOT READ	_fwFatalNack.	MDT ECA EMS3A14 Chamber Temperature Readout

Table B.2.: Lists all summary alerts, the corresponding limits and alert texts

DP element	Range	Alert Text	Alert Description
.TempWarning	> 5	T-Sensors in Alert range (> 5 T-sensors)	MDT ECC SUMALERT Tsensor Temperature
.TempError			
.TempFatal			
.NoReadout			
.BadChamberTemperatures	> 5	DATA NOT UPDATED (> 5 chambers)	MDT ECC SUMALERT Chamber Temperature Readout
	> 5	BAD CHAMBER TEMP (> 5 chambers)	MDT ECC SUMALERT Chamber Temperature
.LowNumberOfWorkingSensors	> 5	RELIABILITY IMPAIRED (> 5 chambers)	MDT ECC SUMALERT Chamber Temperature Operational

Table B.3.: Lists all archive alerts, the corresponding limits, alert classes and alert texts

DP element	Range	Alert Text	Alert Class	Alert Description
dbConnection.Connected	WRONG	DISCONNECTED	_fwFatalAck.	MDT MTM RDB Archive Connection



# Bibliography

- [1] K. M. Potter. The Large Hadron Collider (LHC) project of CERN. In *28th International Conference on High-energy Physics, Warsaw, Poland*, pages 1760–1763, 25 - 31 Jul. 1996.
- [2] O. S. Brüning et al. LHC Design Report Volume 1. Technical report, CERN, Geneva, 2004. CERN-2004-003-V1.
- [3] M. Benedikt et al. LHC Design Report Volume 3. Technical report, CERN, Geneva, 2004. CERN-2004-003-V3.
- [4] R. Penrose. *The Road To Reality, a complete guide to the laws of the universe*. Vintage Books, 2004.
- [5] C. W. Fabjan. LHC: Physics, Machine, Experiments. In Arnulfo v. Zepeda, editor, *CAM-94 Physics Meeting, Proceedings of the Conference held in Cancun, Mexico*, volume 342 of *AIP Conference Proceedings*. AIP Press, Sept. 1994.
- [6] W.-M. Yao et al. (Particle Data Group). Review of Particle Physics. *Journal of Physics G*, 33:1+, 2006. <http://pdg.lbl.gov>.
- [7] J. H. Christenson, J. W. Cronin, V. L. Fitch, and R. Turlay. Evidence for the  $2\pi$  Decay of the  $K_2^0$  Meson. *Physical Review Letters*, 13(4):138–140, Jul. 1964.
- [8] L. Wolfenstein. Parametrization of the Kobayashi-Maskawa Matrix. *Physical Review Letters*, 51(21):1945–1947, Nov. 1983.
- [9] ATLAS Collaboration. The ATLAS Experiment at the CERN Large Hadron Collider. Technical report, CERN, Geneva, 2007. submitted to JINST on Dec. 2007.
- [10] M. Della Negra, L. Foà, A. Hervé, and A. Petrilli. *CMS physics: Technical Design Report*. Technical Design Report CMS. CERN, Geneva, 2006. CERN-LHCC-2006-001, CMS-TDR-008-1.
- [11] F. Carminati, P. Foka, P. Giubellino, A. Morsch, G Paic, Jean Pierre Charles Revol, K. Safarik, Y. Schutz, U. A. Wiedemann, H. de Groot, C. W. Fabjan, and L. Riccati. Alice physics performance report. *J. Phys. G*, 30:1517–1763, 2004.
- [12] LHCb Collaboration. *LHCb Technical Proposal*. Tech. Proposal. CERN, Geneva, 1998. CERN LHCC 98-4, LHCC/P4.

- [13] LHCb Collaboration. *LHCb Technical Design Report - Reoptimized Detector Design and Performance*. CERN, Geneva, 2003. CERN/LHCC 2003-030, ISBN 92-9083-209-6.
- [14] G. Bachy. *Co-ordinate axis systems*. ATLAS, CERN, 1211 Geneva 23, Switzerland, 1996. ATLAS Project Document No. ATL-GE-CERN-QAP-0204-01.
- [15] ATLAS Muon Collaboration. ATLAS Muon Spectrometer - Technical Design Report. Technical report, CERN, 1997. CERN/LHCC 97-22.
- [16] ATLAS HLT/DAQ/DCS Group. High-Level Trigger, Data Acquisition and Controls TDR. Technical report, CERN, Geneva, 2003. CERN/LHCC/2003-022.
- [17] J. Wotschack. ATLAS Muon Chamber Construction Parameters for CSC, MDT, and RPC chambers . Technical report, 1211 Geneva 23, Switzerland, 2008. ATL-MUON-PUB-2008-006.
- [18] E. Diehl. Temperature Sensors on Endcap MDT chambers. <http://atlas.web.cern.ch/Atlas/GROUPS/MUON/Logistics/documentation/endcapsensors/endcapsensors.htm>, 2006.
- [19] H. Fuchs. General T-Sensors Naming Scheme Barrel. [https://twiki.cern.ch/twiki/pub/AtlasMdtDcs/MdtTsensorsChamber/General\\_T-Sensor\\_Naming\\_Scheme\\_BARREL.pdf](https://twiki.cern.ch/twiki/pub/AtlasMdtDcs/MdtTsensorsChamber/General_T-Sensor_Naming_Scheme_BARREL.pdf), 2007.
- [20] M. Battistin and A. Romanazzi. 3D Simulation of Temperature and Air Velocity in the MUON Spectrometer. Presented during ATLAS muon week <http://indico.cern.ch/getFile.py/access?contribId=19&sessionId=8&resId=1&materialId=slides&confId=27672>, 2008.
- [21] A. Daneels and W. Salter. The LHC experiments Joint Controls Project. In *ICALEPS, Trieste*, 1999.
- [22] H. Burckhart A. Barriuso Poy, J. Cook, S. Franz, F. Varela Rodriguez, S. Schlenker, S. Filimonov, and S. Khomoutnikov. ATLAS DCS Integration Guidelines. Atlas dcs, CERN, 2007. [https://edms.cern.ch/file/685451/ATLAS\\_DCS\\_Integration\\_Guidelines.pdf](https://edms.cern.ch/file/685451/ATLAS_DCS_Integration_Guidelines.pdf).
- [23] A. Barriuso and S. Schlenker. ATLAS DCS - FSM Integration Guideline. Atlas dcs, CERN, 2007. [https://edms.cern.ch/file/685114/FSM\\_INTEGRATION\\_GUIDELINE.pdf](https://edms.cern.ch/file/685114/FSM_INTEGRATION_GUIDELINE.pdf).
- [24] W. Salter A. Daneels. Selection and evaluation of commercial SCADA systems for the controls of the Cern LHC experiments. In *ICALEPCS'99*, 1999. International Conference on Accelerator and Large Experimental Physics Control Systems 1999, Trieste, Italy.
- [25] C. Gaspar et al. *PVSS Introduction for Newcomers*, 2003. <http://itcobe.web.cern.ch/itcobe/Services/Pvss/Documents/PvssIntro.pdf>.

- [26] ETM. *PVSS 2 - Getting Started - Basics*, 2003.
- [27] L. Del Cano. Extending the Capabilities of SCADA : Device Modelling for the LHC Experiments. In *9th International Conference on Accelerator and Large Experimental Physics Control Systems*, page 255, 13 - 17 Oct 2003.
- [28] A. Barriuso Poy. *Hierarchical Control Of The ATLAS Experiment*. PhD thesis, URV Universitat Rovira i Virgili Departament d'Enginyeria Electrònica, Elèctrica i Automàtica and CERN European Organization for Nuclear Research, Physics Department, 2007.
- [29] P. Aarnio et al. The DELPHI Detector at LEP. *Nuclear Instruments and Methods in Physics Research*, A303:233–276, 1989.
- [30] J. Barlow. Run Control in MODEL: The State Manager. *IEEE Transactions on Nuclear Science*, 36:1549–1553, 1989.
- [31] C. Gaspar and B. J. Franek. SMI++ : object oriented framework for designing control systems for HEP experiments. In *Computer Physics Communications*, volume 110, 1998. International Conference on Computing in High-Energy Physics, Berlin, Germany, 7 - 11 Apr 1997.
- [32] B. Franek (CERN) and C. Gaspar (SLAC). SMI++ Object Oriented Framework for Designing and Implementing Distributed Control Systems. *SLAC-PUB-12067*, page 5, 2004. Presented at 2004 IEEE Nuclear Science Symposium and Medical Imaging Conference (NSS / MIC), Rome, Italy, 16-22 Oct 2004, Submitted to IEEE Trans.Nucl.Sci.
- [33] C. J. Date. *An Introduction to Database Systems*. E. Wesley, eighth edition, 2003.
- [34] C. Dawes and B. Thomas. *Introduction to Oracle9i SQL Study Guide*. OCA/OCP. Sybex, Inc., 2002. ISBN: 0-7821-4062-9.
- [35] H. Fuchs. *Standardized Flags*. CERN, Geneva, 2007. [https://twiki.cern.ch/twiki/pub/AtlasMdtDcs/MdtTsensorsChamber/Standardized\\_flags.pdf](https://twiki.cern.ch/twiki/pub/AtlasMdtDcs/MdtTsensorsChamber/Standardized_flags.pdf).
- [36] H. Fuchs. *Data Model - Flag Tables*. CERN, Geneva, 2007. [https://twiki.cern.ch/twiki/pub/AtlasMdtDcs/MdtTsensorsChamber\\_Database/DataModel\\_FlagTables.pdf](https://twiki.cern.ch/twiki/pub/AtlasMdtDcs/MdtTsensorsChamber_Database/DataModel_FlagTables.pdf).
- [37] H. Fuchs. T-Sensor oracle user tables. [https://twiki.cern.ch/twiki/pub/AtlasMdtDcs/MdtTsensorsChamber\\_Database/DataModel\\_T-Sensor\\_Oracle\\_User\\_Tables.pdf](https://twiki.cern.ch/twiki/pub/AtlasMdtDcs/MdtTsensorsChamber_Database/DataModel_T-Sensor_Oracle_User_Tables.pdf), 2007.

# List of Figures

2.1. Schematic layout of the LHC cryodipole . . . . .	11
2.2. The LHC injector chain [3] . . . . .	12
2.3. Layout of the ATLAS experiment . . . . .	16
2.4. Layout of the CMS experiment . . . . .	17
2.5. Layout of the ALICE experiment . . . . .	19
2.6. Layout of the LHCb experiment . . . . .	20
3.1. Layout of the ATLAS experiment . . . . .	22
3.2. Global ATLAS coordinate system as defined in [14] . . . . .	23
3.3. Layout of the ATLAS inner detector . . . . .	24
3.4. Layout of the ATLAS calorimeter system . . . . .	25
3.5. The eight barrel magnet coils of the ATLAS detector. In the background the calorimeter can be seen before it was inserted into the detector. . . .	27
3.6. Principal components of the DAQ and HLT systems [16] . . . . .	29
4.1. Position and numbering schema of the Monitored Drift Tube (MDT) chambers [15] . . . . .	31
4.2. Layout of the ATLAS Muon Spectrometer. All four chamber types, pre- cision (MDT and CSC) and trigger chambers (RPC and TGC) are shown. . . .	32
4.3. Position and numbering of the 16 ATLAS Muon Spectrometer sectors. The same schema applies to the end-cap section. . . . .	33
4.4. Local MDT chamber coordinate system [15] . . . . .	36
4.5. Schematic layout of a MDT chamber [15] . . . . .	36
4.6. Simplified diagram of the MDT readout electronics [9] . . . . .	37
4.7. MDM box mounted on a MDT chamber . . . . .	38
4.8. Sections of the barrel chambers [18] . . . . .	41
4.9. Position of the end-cap temperature sensors [18] . . . . .	42
4.10. Temperature distribution along a cross section of the ATLAS cavern. The ATLAS experiment is shown within the cavern. [20] . . . . .	45
4.11. Air velocity distribution along a cross section of the ATLAS cavern. The ATLAS experiment is shown within the cavern. [20] . . . . .	46
4.12. Logical view of the temperature distribution throughout the MDT sys- tem during an milestone run of the MDT system (Sectors 3-8 have been powered). Data taken using the MTM project. . . . .	47

4.13. Temperature distribution along the tube axis of a BML chamber in sector 01 (BML5C01) taken with the MTM project using the mounted temperature sensors. The three lines represent sensors mounted on Multilayer 1, Multilayer 2 and the cross-plate respectively. . . . .	48
4.14. Temperature distribution of a BOS chamber in sector 04 (BOS4C04). The upper part shows the position of the temperature sensors on the chamber. The lower part gives the temperature distribution along the tube axis. The three lines represent sensors mounted on Multilayer 1, Multilayer 2 and the cross-plate respectively. . . . .	49
4.15. Temperature distribution of a BML chamber in sector 01 (BML5C01). The upper part shows the position of the temperature sensors on the chamber. The lower part gives the temperature distribution along the tube axis. The three lines represent sensors mounted on Multilayer 1, Multilayer 2 and the cross-plate respectively. . . . .	50
4.16. Temperature distribution of a BMS chamber in sector 04 (BMS1C04). The upper part shows the position of the temperature sensors on the chamber. The lower part gives the temperature distribution along the tube axis. The three lines represent sensors mounted on Multilayer 1, Multilayer 2 and the cross-plate respectively. . . . .	51
5.1. Organization of the ATLAS Back-End DCS system [16] . . . . .	53
5.2. A typical PVSS system . . . . .	56
5.3. Schematical layout of a PVSS scattered system . . . . .	59
5.4. FSM diagram depicting the interaction of states, actions, rules and transitions . . . . .	61
5.5. Diagram showing the interaction of two sub-detector domains with a control domain. Each sub detector domain has various abstract objects. . . .	63
5.6. Screen shot of the ATLAS FSM screen, showing a part of the MTM system. On the left side the FSM informations can be found. The panel on the right and the small panel in the lower left corner show more detailed information using PVSS panels. On the upper right part, all FSM objects which demand investigation are shown. . . . .	65
5.7. Diagram of the ATLAS FSM Architecture [23] . . . . .	66
6.1. Simplified data flow of the MTM project . . . . .	72
6.2. Working schema of the script mdtMtmCollectDataScript.ctl, which collects data from 11 different systems . . . . .	75
6.3. FSM tree structure of the MTM project . . . . .	84
6.4. Main MTM panel for a device unit (chamber), showing as an example the chamber BOS3A04. . . . .	88
6.5. More Info panel for a device unit (chamber), showing as an example the chamber BOS3A04. . . . .	89

6.6. Flag panel of the device unit level, showing as an example the chamber BOS3A04. It enables the user to change and set flags for individual temperature sensors. . . . .	91
6.7. Endcap Sector Panel showing an overview of the FSM STATE/STATUS of the MDT chambers. . . . .	92
6.8. Endcap Sector Panel showing an overview of the temperatures of the MDT chambers. . . . .	93
6.9. Barrel Sector Panel showing an overview of the FSM STATE/STATUS of the MDT chambers. . . . .	94
6.10. Barrel Sector Panel showing an overview of the temperatures of the MDT chambers. . . . .	95
6.11. Endcap Wheel Panel showing an overview of the FSM STATE/STATUS of the MDT chambers. . . . .	96
6.12. Endcap Wheel Panel showing an overview of the temperatures of the MDT chambers. . . . .	97
6.13. Endcap Partition Panel showing an overview of the FSM STATE/STATUS of the MDT chambers. . . . .	98
6.14. Endcap Partition Panel showing an overview of the temperatures of the MDT chambers. . . . .	99
6.15. Barrel Partition Panel showing an overview of the FSM STATE/STATUS of the MDT chambers. . . . .	100
6.16. Barrel Partition Panel showing an overview of the temperatures of the MDT chambers. . . . .	101
6.17. Temperature Overview panel showing a temperature overview of all MDT chambers of the ATLAS Muon Spectrometer . . . . .	103
6.18. Cavern Temperature Map panel showing two temperature cross sections of the temperature distribution within the ATLAS cavern measured using the MDT temperature sensors. . . . .	104
6.19. Flag Overview panel showing the percentage of malfunctioning temperature sensors within the MDT system using the same logical structure as the MTO panel. . . . .	105
6.20. The Troubfinder panel calculates key values for all MDT chambers and identifies potential problematic chambers. . . . .	106
6.21. Archived Data Viewer panel displaying archived temperature data per chamber. . . . .	107

# List of Tables

2.1. LHC beam parameters [2] . . . . .	11
2.2. Classification of fermions and quarks [6] . . . . .	13
2.3. Classification of gauge bosons [6] . . . . .	13
2.4. Fermion masses [6] . . . . .	14
2.5. Design luminosity of the LHC experiments [2] . . . . .	15
3.1. General performance goals of the ATLAS detector [9] . . . . .	23
3.2. Parameters of the ATLAS toroid magnets [9] . . . . .	27
4.1. Typical parameters of MDT barrel chambers [17] . . . . .	34
4.2. Typical parameters of MDT end-cap chambers [17] . . . . .	35
4.3. MDT chamber types and the corresponding temperature sensor types and numbers . . . . .	40
4.4. Naming options for temperature sensors mounted on MDT barrel chambers	43
4.5. Naming options for temperature sensors mounted on MDT end-cap chambers . . . . .	43
5.1. Alert classes defined by the JCOP framework . . . . .	54
5.2. Example explaining the PVSS data point concept using a simplified MDT chamber . . . . .	58
6.1. Systems accessed by Collect data script . . . . .	74
6.2. Contents of a flag [35] . . . . .	79
6.3. Flag states [35] . . . . .	79
6.4. Database tables used for configuration data by the MTM project . . . . .	82
6.5. Chambers in the DAQ partitions, not following the standard classification	83
6.6. Recommandations on the number of FSM elements per PVSS PC [23] . . . . .	86
A.1. DU STATE conditions used by the MTM project . . . . .	110
A.2. DU STATUS states used by the MTM project . . . . .	110
A.3. STATE conditions used by the LU of type sector of the MTM project . . . . .	111
A.4. STATUS conditions used by the LU of type sector of the MTM project . . . . .	111
A.5. STATE states used by the LU of type endcap wheel of the MTM project . . . . .	111
A.6. STATUS states used by the LU of type endcap wheel of the MTM project . . . . .	112
A.7. STATE states used by the CU of type partition of the MTM project . . . . .	112
A.8. STATUS states used by the CU of type partition of the MTM project . . . . .	112
B.1. Lists all dp alerts, the corresponding limits, alert classes and alert texts . . . . .	114

- B.2. Lists all summary alerts, the corresponding limits and alert texts . . . . 115
- B.3. Lists all archive alerts, the corresponding limits, alert classes and alert texts116